MASTER IN BIOCHEMISTRY AND MOLECULAR AND CELL BIOLOGY

Characterization of ageing joint in a large model of musculoskeletal deseases

Bernard, Anaëlle

Award date:
2023

Awarding institution:
University of Namur

Faculté des Sciences

CHARACTERIZATION OF AGEING JOINT IN A LARGE MODEL OF MUSCULOSKELETAL DESEASES

Mémoire présenté pour l'obtention

du grade académique de master 120 en biochimie et biologie moléculaire et cellulaire

Anaëlle BERNARD

Août 2023

Université de Namur
FACULTE DES SCIENCES
Secrétariat du Département de Biologie
Rue de Bruxelles 61 - 5000 NAMUR
Téléphone: + 32(0)81.72.44.18 - Téléfax: + 32(0)81.72.44.20
E-mail: joelle.jonet@unamur.be - http://www.unamur.be

Caractérisation du vieillissement articulaire chez un modèle animal préclinique, le mouton

BERNARD Anaëlle

Résumé

L'arthrose est le trouble articulaire le plus courant se manifestant par des douleurs et des raideurs articulaires. Elle se caractérise par un déséquilibre entre la synthèse et la destruction du cartilage menant à la dégradation de l'ensemble de l'articulation. Le vieillissement et les traumas articulaires sont les deux principaux facteurs de risque d'arthrose.

La synovie et le coussinet adipeux infrapatellaire, deux tissus articulaires semblent jouer un rôle dans l'inflammation articulaire et dans l'initiation et la progression de l'arthrose chez l'homme. Cependant, leur implication exacte dans la pathogenèse de l'arthrose et dans le vieillissement a été peu décrite à ce jour, dans des modèles animaux précliniques de maladies musculosquelettiques. L'objectif de cette étude était de : (1) décrire les changements morphométriques de la synovie et du coussinet adipeux infrapatellaire ovins, avec l'âge et l'arthrose induite, (2) décrire les caractéristiques *in vitro* des synoviocytes de type fibroblastique de moutons jeunes et âgés et leur réponse aux conditions de stress oxydatif et de sénescence.

Dans notre cohorte de moutons, toutes les synoviales ovines avaient un aspect normal macroscopiquement. Certains changements observés au sein du coussinet adipeux, au cours du vieillissement (fibrose et métaplasie cartilagineuse) ont aussi été observés chez certains individus après induction d'arthrose. Les synoviocytes de type fibroblastique cultivés *in vitro*, provenant de spécimens âgés, avaient un taux de croissance plus lent et présentaient un élargissement cellulaire généralement associé à la sénescence. Ces changements ont été associés à d'autres modifications telles que des changements morphologiques du noyau et une activité β-galactosidase associée à la sénescence positive dans les cellules lors de stress oxydatif.

Tous ces résultats soulèvent des questions quant à l'impact clinique réel de ces altérations sur la santé des articulations. Des études futures pourraient explorer davantage les mécanismes moléculaires sous-jacents des changements observés dans la synovie et le coussinet infrapatellaire, ainsi que l'impact potentiel de ces altérations sur le développement de nouvelles stratégies de diagnostic et de traitement pour les pathologies articulaires liées à l'âge.

Mémoire de master 120 en biochimie et biologie moléculaire et cellulaire

Août 2023

Promoteur : F. Hontoir et J.-M. Vandeweerd

Université de Namur
FACULTE DES SCIENCES
Secrétariat du Département de Biologie
Rue de Bruxelles 61 - 5000 NAMUR
Téléphone: + 32(0)81.72.44.18 - Téléfax: + 32(0)81.72.44.20
E-mail: joelle.jonet@unamur.be - http://www.unamur.be

Characterization of ageing joint in a large model of musculoskeletal diseases

BERNARD Anaëlle

Abstract

Osteoarthritis (OA) is the most common joint disorder characterised by joint pain and stiffness. It is featured by an imbalance between the synthesis and destruction of cartilage with joint damage. Aging and joint trauma are the two main risk factors for osteoarthritis.

The synovium and the infrapatellar fat pad two joint tissues that appear to play a key role in joint inflammation and in initiation and progression of osteoarthritis in humans. However, their exact involvement in OA pathogenesis and in ageing has been poorly described to date, in preclinical animal models for musculoskeletal diseases. The aims of this study were: (1) to describe the morphometric changes in the ovine synovium and infrapatellar fat pad, with age and induced osteoarthritis, (2) to describe the *in vitro* characteristics of synovial fibroblasts from young and old sheep and their response to oxidative stress and senescence conditions.

In our cohort of sheep, all ovine synovium were macroscopically normal. Some changes observed within the fat pad, during ageing (fibrosis or chondroid metaplasia) have also been observed in some sheep after induction of osteoarthritis. The fibroblast-like synoviocytes from aged specimens cultured *in vitro* had a slower growth rate and showed a cell enlargement generally associated with age-related senescence. Changes have been associated with other changes such as morphological changes in the nucleus and positive senescence-associated β-galactosidase activity in cells stimulated by oxidative stress.

This result raises questions about the real clinical impact of this alteration on joint health. Future studies could further explore the molecular mechanisms underlying the changes observed in the synovium and infrapatellar pad, as well as the potential impact of these alterations on the development of new diagnostic and treatment strategies for age-related joint pathologies.

Master's thesis in biochemistry, molecular and cellular biology

August 2023

Promoter: F. Hontoir et J-M. Vandeweerd

REMERCIEMENTS

Je voudrais tout d'abord remercier l'ensemble des membres de l'URVI de m'avoir accueillie en tant que mémorante. Je les remercie également pour leurs nombreux conseils prodigués et leur aide ponctuelle au sein du laboratoire tout au long de la réalisation de mon mémoire. Je remercie plus spécifiquement Zoé Blockx qui m'a épaulée dans la prise des photos au microscope confocal.

J'aimerais ensuite dire merci au LABCETI de m'avoir ouvert sa porte et permis d'effectuer mes recherches en histologie. Je citerai plus spécifiquement Valéry Bielarz pour sa patience et ses nombreux services.

J'aimerais souligner aussi l'entraide et le soutien qui ont existé entre tous les mémorants. Tout cela restera à jamais gravé dans ma mémoire.

Plus personnellement, merci à ma famille et mes amis pour leur soutien moral ainsi qu'au professeur d'anglais, Nathalie Vandersmissen, d'avoir accepté de corriger l'orthographe et la grammaire de mon travail.

Enfin et non des moindres, merci à mes promoteurs, Prof. Jean-Michel Vandeweerd et Dr. Fanny Hontoir qui m'ont accordé la chance de découvrir et d'approfondir ce sujet passionnant.
Je tiens sincèrement à te remercier, Fanny, pour ton encadrement jusqu'aux dernières minutes, ta confiance qui m'a permis de me sentir très vite autonome ainsi que ton dévouement à me former, ta bonne humeur permanente et ton humour. Ce fut donc un réel plaisir de travailler avec toi !

ABBREVIATIONS

ADAMTS: a disintegrin and metalloproteinase with thrombospondin motifs

BMP: bone morphogenetic protein

BrdU: bromodeoxyuridine

CCL2: CC-chemokine ligand 2

CD: cluster of differentiation

COL-2: Collagen II

COX2: cyclooxygenase-2

CTRL: control

CXCL13: CXC-chemokine ligand 13

DAMP: damage (or danger) associated molecular patterns

DAPI: 4,6-diamidino-2-phenylindole

DMEM: Dulbecco's Modified Eagle Medium

DPX: Distyrene Plasticizer Xylen

ECM: extracellular matrix

EDTA: ethylenediaminetetraacetic

EdU: ethynyl deoxyuridine

EGF: endothelial growth factor

FCS: foetal calf serum

FLS: fibroblast-like synoviocytes

GM-CSF: granulocyte-macrophage colony- stimulating factor

HU: hydroxyurea

IFN-γ: interferon-γ

IFP : infrapatellar fat pad

IL : interleukin

IL-1Ra: IL-1 receptor antagonist

LIF: leukemia inhibitory factor

LMNB1 : lamin B1

LTB4 : leukotriene B4

MLS: macrophage-like synoviocytes

MMP: matrix metalloproteinase

MRI: magnetic resonance imaging

MSC: mesenchymal stem cell

NAMPT: nicotinamide phosphoribosyl transferase (also called visfatin)

NGF: nerve growth factor

NO: nitric oxide

NOS: nitric oxide synthase

OA: osteoarthritis

PBS: phosphate-buffered saline

PCR: Polymerase Chain reaction

PGE2: prostaglandin E2

PRR: pattern-recognition receptors

PSCs: perivascular stem cells

PTOA: post-traumatic OA model

ROS: reactive oxygen species

SA β-gal: Senescence-Associated beta-galactosidase assay

SASP: senescence-associated secretory phenotype

SF-MSCs: synovial fluid-derived MSCs

TBHP: tert-Butyl hydroperoxide

TIMP: tissue inhibitor of metalloproteinase

TLR: toll-like receptor

TNF: tumor necrosis factor

TNF-α: tumor necrosis factor-alpha

UV : ultraviolet

VCAM-1: vascular cell adhesion molecule 1

VEGF: vascular endothelial growth factor

TABLE OF CONTENTS

Introduction

1. Osteoarthritis, a prevalent disease of the synovial joint

Osteoarthritis (OA) is the most common disorder of synovial joints in humans and animals. It is generally characterized by joint pain and stiffness (Arden and Nevitt, 2006). The aetiology of osteoarthritis involves a combination of factors, including age-related wear and tear, joint trauma, genetic factors, obesity, joint deformity and inflammatory diseases such as rheumatoid arthritis. These factors contribute to the progressive degradation of joint cartilage, leading to pain, joint stiffness and loss of joint function (Arden and Nevitt, 2006). In human, OA mainly affects the knee, hip, and hands (Oliveira *et al*., 1995; Lawrence *et al*., 2008), with knee OA being three time more common than hip or hands OA (Andrianakos *et al*., 2006). In canine as well, knee OA is very prevalent, with up to 20% of dogs affected by knee OA in the USA (Johnston, 1997; Meeson *et al*., 2019).

In human, OA is responsible for a high socioeconomical burden. In France, OA-associated direct costs (hospitalization, physician, medication) have been estimated in 2002 as 1.6 billions Euros (LePen *et al*., 2005). Beside those direct costs are indirect costs (time-off at work, adaptive aids and devices) (Maetzel *et al*., 2004), and social consequences such as: premature retirement or difficulties in participating in social activities. The burden of OA has increased in the last decades (Hawker, 2019). As a chronic disease, it is characterized by a high number of years lived with disability for patients. In Belgium, musculoskeletal disorders are the 2nd cause of healthy life year loss, after mental disorders. Among specific causes, OA is the 6th cause of years lived with disability in Belgium (after depression, low back pain, alcohol use disorders, neck pain) (Sciensano, 2022). Moreover, OA is associated with comorbid conditions such as type-2 diabetes, or cardiovascular impairment (Hawker, 2019). In animals, OA also affects quality of life and performances. Horses suffering from OA may experience lameness, failure to race, and a subsequent early retirement and loss of income for the owner (Santschi, 2008; Schlueter & Orth, 2004). In dogs and cats, OA is responsible for behavioural changes and decreased mobility (Slingerland *et al*, 2011; Lascelles, 2010).

To date, there is no efficient long-term treatment for OA. Main therapeutic strategies aim to reduce catabolism and joint destruction (with anti-inflammatory strategies), to repair tissue (with pro-anabolic therapeutics and tissue repair strategies) and to promote joint function (with pain control, or lubrication medications) (Vincent, 2020; Schulze-Tanzil, 2021; Bland, 2015; Altman *et al.*, 2015; Freitag, 2016). Most of these strategies have only been successful in delaying the surgical, invasive treatment called total joint replacement (Altman *et al.*, 2015; Manen, Nace and Mont, 2012).

2. The synovial joint, a multi-tissue organ

Synovial joints are featured by cartilage layer, covering the bone extremities (subchondral bone), and surrounded by synovial membrane (Zhou *et al*., 2022). Ligaments connect the bones (Figure 1). Beside these tissues, the knee is also featured by menisci and fat pad. Menisci are

shock absorber, shaped to enable congruency between the convexities of the femur and the tibial plate. (Kuyinu *et al*., 2016). The fat pad is basically considered as a space-filler tissue (Davies and White, 1961).

This particular organisation of synovial joint, with multiple tissues, interacting with each other forces to consider the joint as an entire organ, and to investigate the role of each tissue, in health, ageing, and disease. Each tissue is featured by a specific cell and extracellular matrix (ECM) composition, supporting the differences in response to injury and ageing. In the next 5 paragraphs, each tissue is described with an emphasis on its composition, and specificities.

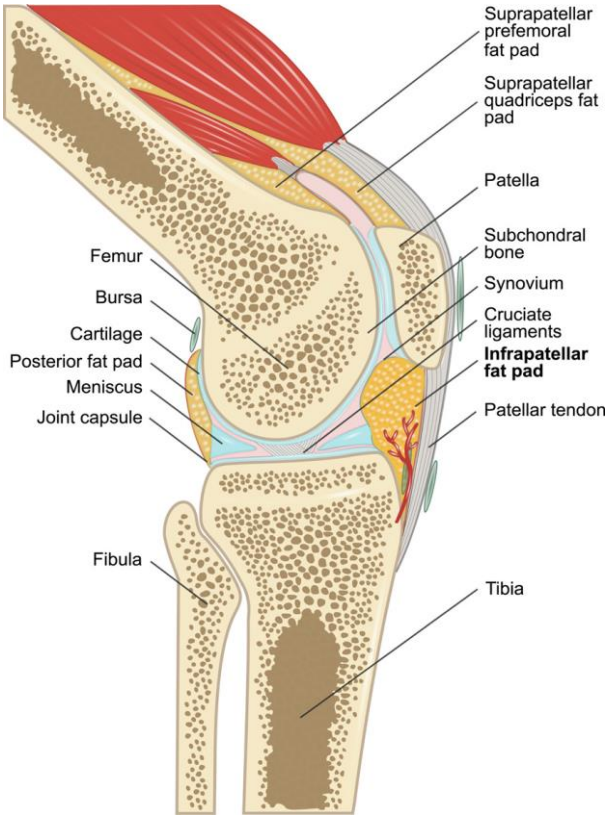

Figure 1 : *Schematic sagittal view of the knee joint. The synovial joint connects bones and includes meniscus, cartilage, subchondral bone, and synovium. Synovial fluid is found in the joints and fills the space between the articular surfaces of the bones. The knee joint is also featured by an important additional tissue displayed in the center: the infrapatellar fat pad between the patellar tendon and the tibia. The knee joint also features two other fat pads: the suprapatellar prefemoral fat pad and the suprapatellar quadriceps fat pad (Zhou et al., 2022).*

2.1. The cartilage, an avascular and aneural translucent layer

Articular cartilage is composed of water (65-80%), collagens (10-20%, mainly type II) and proteoglycans (5-10%, predominantly aggrecan) (Puissant *et al.*, 2006). The latter two are produced by chondrocytes, the sole resident cells (Findlay and Atkins, 2014). It is a smooth tissue that helps reduce wear and friction in the joint. Cartilage is also a shock-absorbing tissue: it reduces the forces transmitted to the underlying subchondral bone (Johnston, 1997; Kuyinu *et al*., 2016). It is not vascularised and not innervated, leading to a limited ability to self-repair and to the absence of pain in case from superficial cartilage damage. Indeed, blood vessels play an essential role in the repair process, bringing nutrients, oxygen and immune cells necessary for healing. Without good vascularisation, cartilage repair responses are ineffective, with

synthesis of fibrotic tissues and/or cartilage with lower biomechanical properties than healthy cartilage, promoting damages to the underlying tissue: the subchondral bone. In addition, cartilage has a low cell density, and chondrocytes are enclosed in spaces called lacunae, preventing them from moving/travel to damaged areas for repair. This makes the cartilage repair process even more difficult (Fellows *et al*., 2016).
Because of these limitations to cartilage repair, external interventions are often necessary to repair damaged tissue and prevent future damage. These interventions can include surgical techniques, cartilage grafts or the use of stem cells to stimulate repair. The aim is to provide cartilage with the help it needs to repair itself properly and thus prevent joint problems from worsening (Fellows *et al*., 2016).

2.2. The Subchondral bone, support and nutrition

The subchondral bone is made of trabeculae (type-I collagen fibres aligned to form walls), organised in multiple directions, and separated by trabecular spaces. This collagen is associated with minerals (Ca, P, Mg, …) providing the stiffness of the subchondral bone. The 3D organisation of the trabeculae allows resistance to stress in multiple planes (Choi *et al*., 1990; Mente & Lewis, 1994). Subchondral bone is highly vascularised and innervated (Suri *et al*., 2007). Together with the synovial fluid, it is involved in the nutrition of cartilage (Johnston, 1997; Wang *et al*., 2013; Kuyinu *et al*., 2016). In opposition to cartilage lesions, lesions of the subchondral bone are known to be painful. Main alterations of the subchondral bone are alteration of bone density such as: sclerosis or osteoporosis.

2.3. The Synovium, the envelope of articular joints

The synovium (also called synovial membrane) constitutes the envelope of articular joints, it creates the separation between the internal joint structures and the musculoskeletal tissues. The synovium is a special tissue derived from a specialised mesoderm called the interzonal mesenchyme (Sun, Chen, and Pei, 2018). It is composed of two layers: the intima (internal layer) and the sub-intima (external layer) (Witherspoon *et al*., 2014).
The sub-intima is composed of fibrous connective tissue, blood vessels, fat cells, fibroblasts (synovial fibroblasts (SF)) and a very small percentage of immune cells in physiological condition. The intima is mainly composed of two types of cells: macrophage-like synoviocytes (MLS) and fibroblast-like synoviocytes (FLS), which play an important role in maintaining the internal homeostasis of the joint. The FLS (type B synoviocytes) secrete the majority of the synovial fluid components: hyaluronic acid and lubricin, both crucial for joint lubrication. These fibroblast-like cells express markers typical of mesenchymal and fibroblastic lineages, such as vimentin, CD90 and intracellular adhesion molecules. However, they can be distinguished from other cells by specific features such as high levels of uridine diphosphoglucose dehydrogenase (UDPGD) (which is linked to hyaluronan production), cadherin 11, receptor tyrosine-protein phosphatase sigma-like protein (R-PTP-sigma) and vascular cell adhesion protein 1 (VCAM-1) what differentiates them from subintimal fibroblasts (Macchi *et al*., 2018; Li *et al*., 2019). Macrophage-like cells (type A synoviocytes) have an immune function: they remove bacteria or particles released into the synovial fluid in case of joint injuries. These macrophages are normally dormant but can be activated during inflammation. (Bhattaram and Chandrasekharan, 2017; Kuyinu *et al*., 2016). They may then play a role in maintaining the balance between pro- and anti-inflammatory cytokine levels in synovial fluid (Macchi *et al*., 2018).

The synovium (the sub-intima and potentially the intima) also host of a small number of mesenchymal stem cells (MSCs) (similar to the MSCs of the infrapatellar fat pad described in section 2.5) the origin of which is not yet fully defined. There are two different views on the origin of synovium-derived MSCs (Li *et al.*, 2019). The first is that MSCs could enter the synovium via blood vessels, as MSCs are generally located around blood vessels and the frequency of MSCs is positively correlated with increased tissue vascularisation (Edwards, 1995; da Silva Meirelles *et al*., 2009). The second hypothesis is that synovial-derived MSCs originate from the synovial intima, as synovial-derived MSCs have a phenotype highly similar to that of B-type synoviocytes, such as the presence of characteristic lamellar bodies (LBs) (Vandenabeele *et al*.) This hypothesis is also associated with the embryonic origin of the synovium in the articular interzone (Greif *et al*., 2020). Moreover, synovial membrane-derived stem cells can be found in synovial fluid. Indeed, synovial fluid-derived MSCs (SF-MSCs) share similar characteristics to synovial-derived MSCs, such as similar morphologies and gene expression profiles, but not with bone marrow MSCs, supporting the hypothesis of the synovial origin of these MSCs. Studies have shown that the number of MSCs in synovial fluid increases significantly in injured or osteoarthritic knees, and that this number increases with disease progression (Jeyaraman *et al*., 2022).

These synovial membrane MSCs have a high capacity for proliferation and differentiation into osteoblasts, adipocytes and chondrocytes *in vitro* (Greif *et al*., 2020). Preclinical studies have assessed their therapeutic potential: synovial-derived MSCs isolated from patients suffering from osteoarthritis and rheumatoid arthritis were successfully re-implanted in patients (using a scaffold-free tissue engineering approach) and showed hyaline-type cartilage repair and better histological scores than untreated groups, 8 weeks after implantation. In addition, other animal studies (such as rabbits, mice, horses, and pigs) have also shown similar promising results. These results indicate that synovial membrane MSCs have a promising chondrogenic potential and reveal themselves to be potential candidates for the treatment of cartilage lesions *in vivo* (Greif *et al.,* 2020).

The synovium is vascularised and innervated, suggesting its involvement in pain feeling in OA (Whiterspoon *et al*., 2014). Most nerves are found around vascular networks in the subintimal layer, but not in the intimal layer of the synovial membrane. In healthy individuals, the intima is around 20 to 40 μm thick, and the subintima is up to 5 mm thick. However, in some areas (such as below the patella, in front of the femur), the synovial membrane appears to be closely connected by its vascular network and nerve innervation to another joint structure: the infrapatellar fat pad (IFP). Together, they form a morpho-functional unit (Macchi *et al.,* 2018).

2.4. The menisci, congruency and shock absorption

Menisci are crescent-shaped, tissues rich in type-I collagen. The collagen fibres of the menisci are aligned and organised. Their extracellular is not mineralised in the normal joint, and is also made of glycoproteins, non-collagenous proteins and water. The menisci are connected to the tibia (and the femur) by short ligaments (Fox *et al*., 2012). The menisci shape enables the congruency between the tibia and the femur. The menisci play the role of shock absorber (Kuyinu *et al*., 2016). Damage to the meniscus can be painful and cause significant functional discomfort. The menisci are innervated, i.e. they have nerve endings that enable them to detect pain. However, meniscus vascularisation and innervation are limited compared to other knee structures. As a result, meniscal lesions are not always painful immediately after they occur.

However, pain can occur if the torn edges of the meniscus displace or irritate other structures in the knee (Greis *et al.*, 2002).

2.5. The Infrapatellar fat pad, a cushion

Like the hip, the elbow, and the ankle, the knee joint also shows a major synovial-fat pad unit: the infrapatellar fat pad (IFP). All its functions and characteristics are shown in Figure 2. The IFP, also known as Hoffa's fat pad in human, is a feature of the knee, together with 2 additional fat pads in this region. These are the suprapatellar fat pad above the patella and the prepatellar fat pad just below the patella, between it and the patellar tendon. These fat pads play a role in protecting and cushioning the surrounding structures of the knee (Jarraya *et al.*, 2018). The IFP is found in the main research mammals: sheep, horse, dog, rabbit, mouse, rat (Barboza *et al.*, 2017; Fuller *et al.*, 2014; Hoegaerts *et al.*, 2005; Kitagawa *et al.*, 2019; Toghraie *et al.*, 2011).

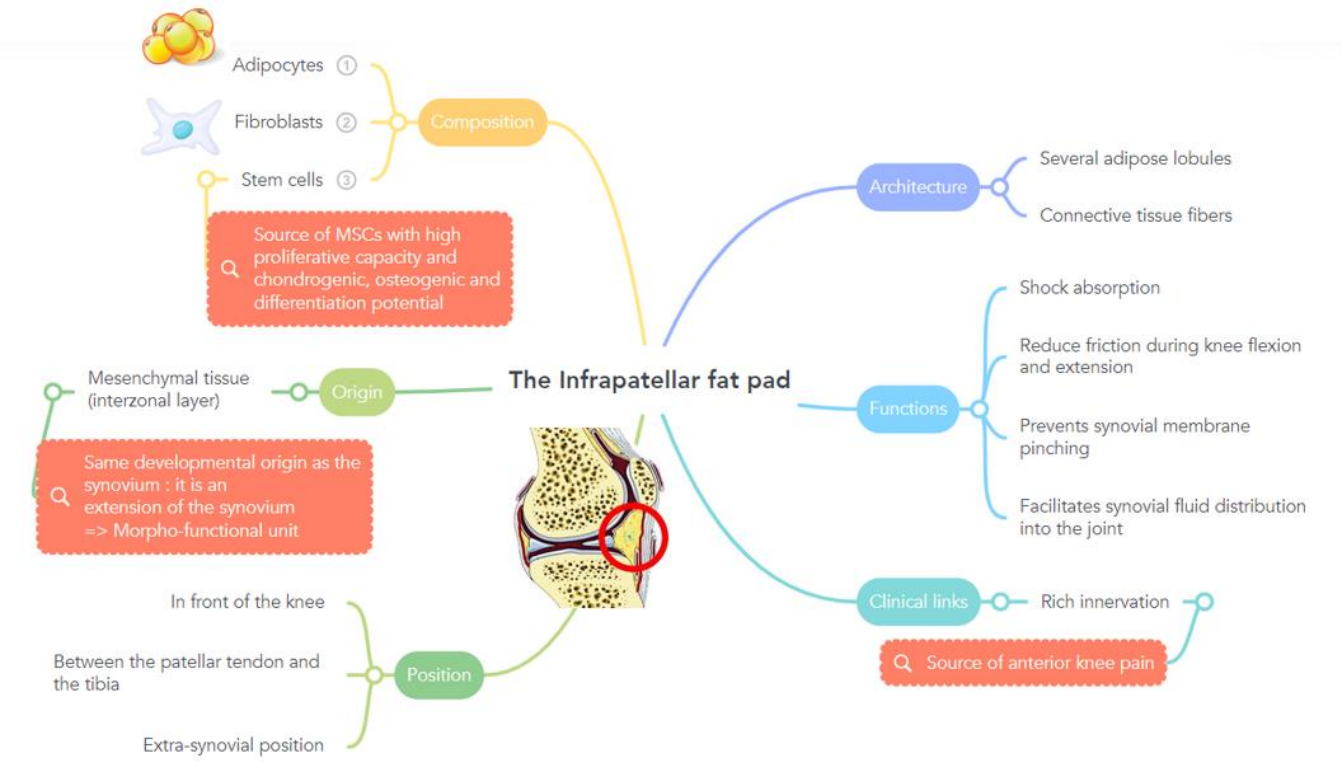

Figure 2 : *Functions and features of the Infrapatellar fat pad. This figure summarizes the main functions, features and controversies (🔍) associated with the infrapatellar fat pad, providing a comprehensive overview of this complex subject.*

The IFP is a vascularised adipose tissue, located in the knee joint extra-synovially (which means that it is covered by a layer of the synovium) (Draghi *et al.*, 2016). It is mainly composed of adipocytes (85 % - 95 %) responsible for the metabolism of the tissue and the endocrine and paracrine functions in the joint. They can secrete large amounts of inflammatory cytokines, interferon, adipokines, and growth factors that may play a signalling role in joint health, as well as articular cartilage degradation and synovial inflammation (Zhou *et al.*, 2022).
The IFP also contains fibroblasts that produce most of the ECM, but also resident monocytes, mast cells, lymphocytes, and macrophages. Macrophages are found in two forms that are balanced in the tissue: a classical M1 form or an alternative M2 form (they are activated and

converted by inflammation). M1 macrophages promote the secretion of pro-inflammatory cytokines and catabolic factors, while differentiated M2 macrophages present anti-inflammatory effects and maintain joint health (Warmink et la., 2019).
Finally, the fat pad shelters a population of stem cells (perivascular stem cells (PSCs), the natural ancestors of MSCs). PSCs are responsible for homeostasis and regeneration *in vivo*. Within these PSCs, two subpopulations have been identified: pericytes (CD31−CD34−CD45−CD146+) which generally reside around small blood vessels such as capillaries, venules and arterioles and adventitial cells (CD31−CD34+CD45−CD146−) which are found around larger arteries and veins. These adventitial cells can produce pericytes. (Hindle *et al.,* 2017.; Greif *et al.,* 2020). Thus, the fat pad is more and more considered as a source of MSCs with significant proliferative capacity, and chondrogenic, osteogenic and differentiation potential (Jiang *et al*., 2019; Francis *et al*., 2020).

Earlier research indicated that adipose tissue (such as subcutaneous adipose tissue) originated from the germinal layer of the mesoderm and that MSCs give rise to common early pre-adipocytes, which could differentiate into mature adipocytes under appropriate stimulation conditions (Gilbert, 2010; Gesta, Tseng and Kahn, 2007). However, more recent studies in animals have revealed that fatty tissue in other anatomical locations, such as the fat pad in the synovial joint, may derive from different embryonic origins (Kouidhi *et al.,* 2015). In the case of the IFP, it shares the same developmental origin as the synovium (Kouidhi *et al*., 2015). As described above, the synovium is derived from dense, flattened mesenchymal tissue between the femur and tibia, known as the interzonal layer produced by the condensation of MSCs, which have been used to model the mesoderm in differentiation within the middle layer. During embryonic development, this region undergoes cavitation, and after a few weeks appears as a triangular space beneath the patella, composed of mesenchymal tissue. The interzonal cells in this newly formed cavity can then contribute to the formation of several joint structures, including the IFP (do Amaral *et al*., 2017). The IFP (adjacent to the synovium) the shows structural and functional similarities with the synovium. There is increasing evidence that the IFP develops as an extension of the synovium. As we have seen, the IFP and synovial membrane share a common origin. As a result of this shared origin, the IFP maintains a close anatomical and functional relationship with the synovial lining of the knee joint (Sun, Chen, and Pei, 2018). These findings suggest that there is close and continuous communication between the IFP, the synovial membrane and the joint capsule (the structure surrounding the knee joint). Some studies even suggest that the IFP and synovium form a single anatomical and functional unit (also known as a morpho-functional unit) (Macchi *et al.*, 2018; Greif *et al*., 2020; Emmi *et al.,* 2022), rather than two separate structures that simply communicate with each other (Ioan-Facsinay *et al.*, 2013; Eymard *et al.,* 2014). This close relationship between synovium and IFP allows molecular regulation of the joint through the release of growth factors and cytokines (Greif *et al*., 2020).

Hoffa's fat pad lies specifically at the front of the knee, between the patellar tendon and the tibial bone. The IFP is made up of several adipose lobules, which are small, distinct units containing adipocytes. These lobules are separated from one another by partitions of connective tissue fibres. These fibres are responsible for the structural support of the fat pad and its connection to the surrounding structures of the knee joint (Clements *et al.,* 2009; Favero *et al.,* 2017). The tissue architecture of the IFP and its composition of adipose tissue with elastic

properties enables it to perform its functions, such as shock absorption when compressed or subjected to stress. It also helps to reduce friction between tendon and bone during knee flexion and extension. In addition, it prevents synovial membrane pinching and facilitates synovial fluid distribution into the joint (Draghi *et al*., 2016; Sun, Chen, and Pei, 2018). A study based on three-dimensional biomechanical numerical models that interpret the actual structural configuration of the tissue was carried out to study fatty tissue under compression and shear forces. To create these models, the researchers took into account the actual characteristics of fat tissue, including the size and structure of adipose lobules. They used finite elements, which are small geometric elements, to represent the virtual tissues in 3D. They then developed different types of numerical models to analyse the different behaviours of fat tissue under compression and shear (Fontanella *et al.*, 2017). This study has demonstrated these unique mechanical properties of the IFP compared to other adipose tissues in the body. They found that these adipose lobules have high volumetric stiffness (volumetric stiffness relates to a material's response to compression and its ability to maintain volume), meaning they can well withstand mechanical stresses and forces. However, IFP adipose lobules also have low iso-volumetric stiffness (iso-volumetric stiffness relates to a material's response to shear forces and its ability to maintain shape without changing volume), which allows them to deform more easily in response to shear loads exerted on the joint (Macchi *et al*., 2018). The IFP therefore plays an essential role in knee function, absorbing shocks, acting as a buffer between the patellar tendon and the tibial bone, and reducing friction. However, due to its rich innervation and sensitivity to nociceptive stimuli, the IFP can also become a source of anterior knee pain. It receives branches of the femoral, common peroneal and saphenous nerves. When subjected to excessive loads, mechanical stress or inflammation, the fat pad can become irritated and cause sensations of discomfort or pain (Draghi *et al.*, 2016).

3. Osteoarthritis, a complex process targeting each joint tissue

For long, OA has been described as an imbalance between the synthesis and destruction of cartilage leading to joint damages, including loss of cartilage, sclerosis of the subchondral bone, decrease in synovial fluid viscosity and inflammation of the synovium with structural histological changes like an increase in inflammatory infiltration, increase in vascularisation, sub-intimal fibrosis, and intima hyperplasia (Greif *et al*., 2020) (Moskowitz *et al*., 2004; Little *et al.*, 2010).

Cartilage and subchondral bone have long been, considered as the most affected tissues in OA. However, all joint tissues are affected by OA (Figure 3) (Arden and Nevitt, 2006; Cope *et al*., 2019; Moskowitz *et al*., 2004), as well as inflammation of the fat pad (Greif et la., 2020).

Furthermore, each tissue can play a role in the initiation of OA (meniscus, cartilage and subchondral bone) and interact with each other in the progression of the disease (Figure 3). In fact, cartilage damage, meniscus damage, synovitis, and bone marrow damage are all risk factors for osteoarthritis (i.e. collagen fragments released by cartilage damage are pro-inflammatory for the synovium, alter the homeostasis of the cartilage matrix and the homeostasis of the subchondral bone) (Goldring and Otero, 2011; Brandt *et al*., 2008; Zhou *et al*., 2022).). This suggests that osteoarthritis is not just a cartilage disease but a disease of the whole joint as an organ. However, the complex interaction between tissues still requires

investigations, to better understand the mechanisms of OA and the exact sequence of events that trigger the onset of the disease (Cope *et al.*, 2019).

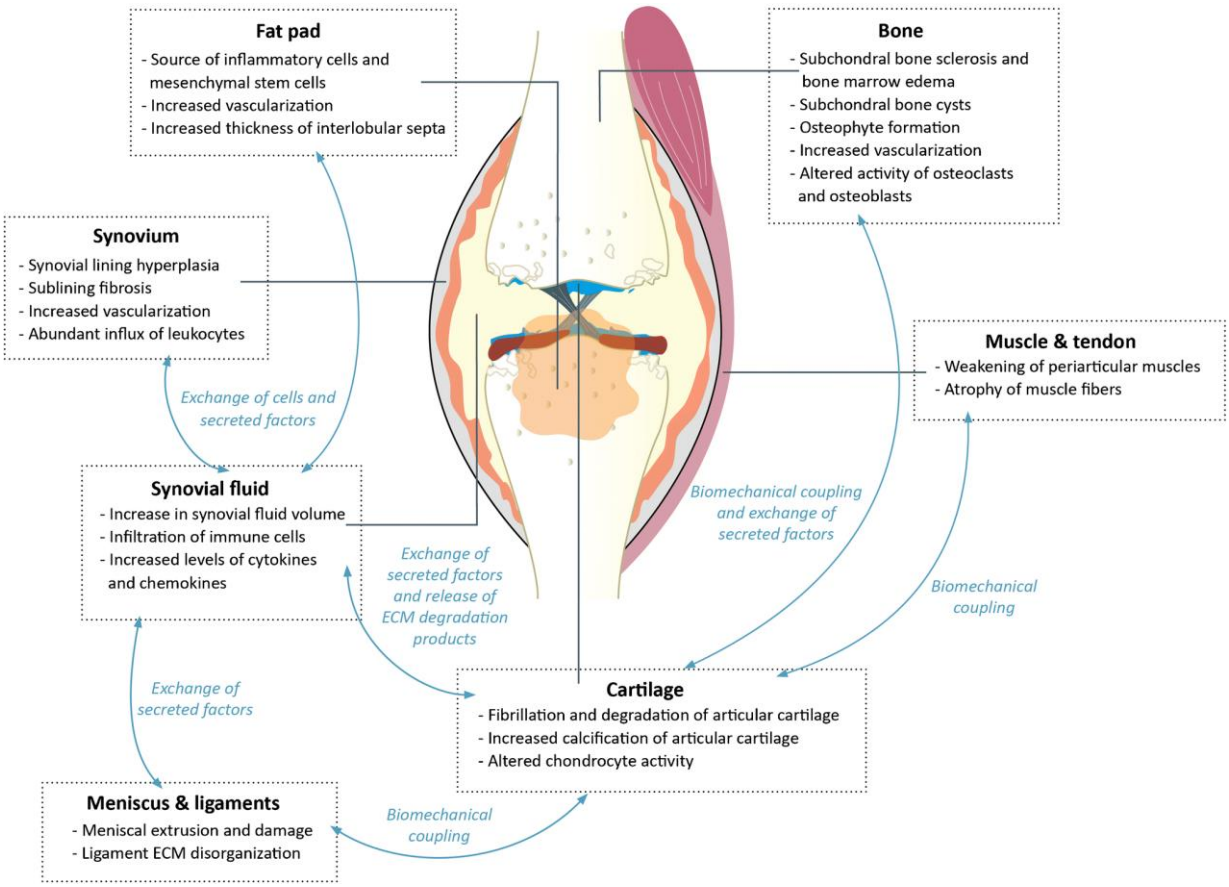

Figure 3 : *A representation of an osteoarthritic knee, including the main contributing tissues, their OA modification, and their interactions. (Mimpen and Snelling, 2019).*

3.1. Cartilage and subchondral bone alterations with osteoarthritis

Cartilage and subchondral bone can suffer from stress and response inadequately. For example, the cartilage does not sustain well excessive mechanical load or shear and is susceptible to age-related degeneration. This can then lead to the development of osteoarthritis. Normal quiescent chondrocytes become activated and undergo a phenotypic change, resulting in fibrillation and degradation of the cartilage matrix (degradation of the damaged ECM then produces damage-associated molecular patterns (DAMPs)), the appearance of chondrocyte clusters, increased calcification of the cartilage and vascular penetration of the subchondral bone. It will then be possible to observe an initial loss of proteoglycans from the upper zone followed by a degradation of the collagen network releasing collagen fragments into the joint space (pro-inflammatory effect on the synovium) (Sharma *et al.*, 2013; Goldring, 2012).

In case of cartilage defect, the subchondral bone will experience increased mechanical load, responding by changing its architecture and have a pro-inflammatory effect in the joint, leading to increased local inflammation. Microarchitectural changes of the subchondral bone may then appear as subchondral sclerosis with thickening of the cortical plate, strong remodelling of the trabeculae, formation of osteophytes that are bony outgrowths that form at the joint margins

(they are the body's attempt to stabilize the joint and compensate for the loss of cartilage) and development of subchondral bone cysts (Donell, 2019; Sharma *et al.*, 2013).

3.2. Meniscal changes with osteoarthritis

Meniscal tears may contribute to joint instability, with alteration of loading pattern along the joint surface, with subsequent cartilage and subchondral bone alterations (Berthiaume *et al.*, 2005; Ozeki *et al.*, 2022). Menisci may be the starting point for OA development, but also the target of an ongoing OA process. Indeed, OA is responsible for change in meniscal metabolism, with for example change in collagen production, leading to a decrease in collagen synthesis. This can weaken the structure of the meniscus and make it less able to withstand mechanical loads in the knee (Katsuragawa *et al.*, 2010; Englund Guermazi and Lohmander, 2009). The pathological changes seen in menisci with ageing and osteoarthritis are similar to those seen in articular cartilage. These include matrix disruption, fibrillation, cell clumping, calcification, and cell death. Increased vascularisation and density of sensory nerves have also been observed in OA menisci. This suggests that the menisci may contribute to the pain associated with knee osteoarthritis.

3.3. The multi-faceted role of the synovium in osteoarthritis: from pain to disease progression

The synovium is more than just a joint wall. Due to its innervation and vascularisation, it is associated with the pain and progression of OA. Inflammation of the synovium (synovitis) can be triggered by the release of cartilage-derived collagen fragments into the joint cavity (Figure 4), as well as meniscus-derived collagen fragments. These fragments induce the production of pro and anti-inflammatory mediators by synoviocytes (shown in Figure 4). The inflammation of the synovium is associated to neo-angiogenesis (stimulated by the proangiogenic vascular endothelial growth factor (VEGF) from macrophage), with infiltration of inflammatory cells (macrophages and T lymphocytes) and sensory nerves growth. Synovitis is a factor involved in clinical pain in OA patients. (Greif *et al.*, 2020; Mathiessen and Conaghan, 2017 ; Berenbaum, 2013; Sanchez-Lopez *et al.*, 2022; Wenham and Conaghan, 2010).

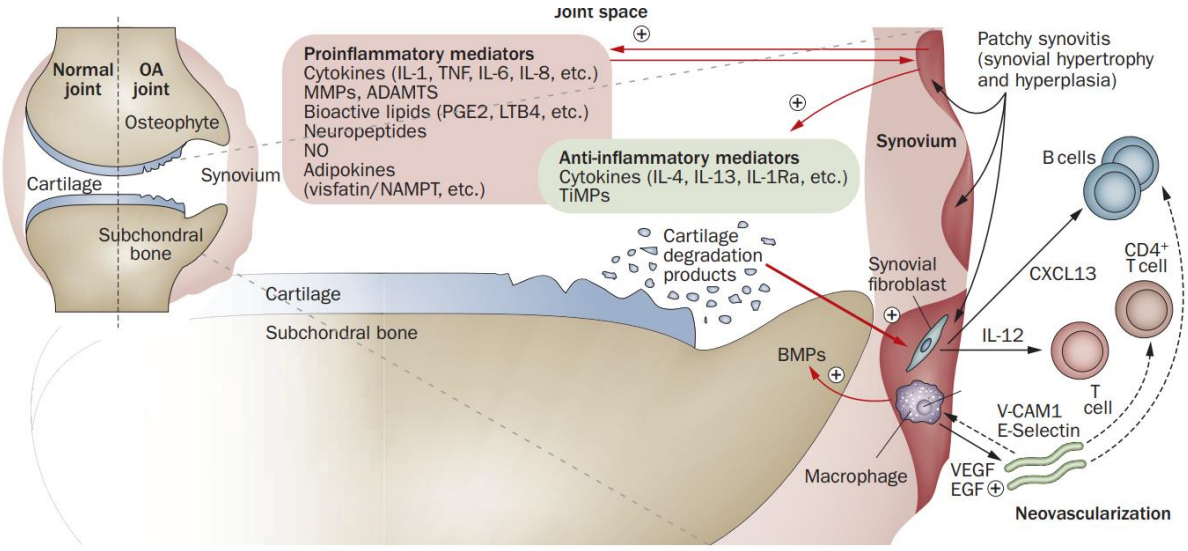

Figure 4 : *Involvement of the synovium in the pathophysiology of osteoarthritis. Cartilage degradation products released into the synovial fluid are phagocytosed by the synovial cells and amplify the synovial inflammation. In*

turn, activated synovial cells in the inflamed synovium produce catabolic and pro-inflammatory mediators that lead to excessive production of proteolytic enzymes responsible for cartilage degradation, creating a positive feedback loop. The inflammatory response is amplified by activated synovial T cells, B cells and infiltrating macrophages. To counteract this inflammatory response, the synovial membrane and cartilage can produce anti-inflammatory cytokines. In addition to these effects on inflammation and cartilage degradation, the inflamed synovium contributes to osteophyte formation via bone morphogenetic proteins (BMPs)(Sellam and Berenbaum, 2010).

Synovitis is also responsible for the progression of OA as the release of pro-inflammatory molecules (such as cytokines, nitric oxide, prostaglandin E2 and neuropeptides) will in turn stimulates the production of metalloproteinases by chondrocytes, leading to cartilage degradation. A vicious cycle then occurs as chondrocytes, producing cytokines and proteolytic enzymes, end up increasing cartilage degradation and promotes synovial inflammation (Mathiessen and Conaghan, 2017; Berenbaum, 2013; Sellam and Berenbaum, 2010).
Many cell types within the joint (chondrocytes, macrophage-like synoviocytes, FLS, vascular endothelial cells) have pattern-recognition receptors (PRRs) capable of responding to DAMPs inducing host immune responses. Although much of the innate immune activation and cytokine production in OA is attributed to the action of macrophage-like synoviocytes, FLS and chondrocytes may also play a role. In fact, FLS have the ability to respond to both inflammatory cytokines and to toll-like receptor (TLR : a family of PRR) ligands (Sokolove and Lepus, 2013).
Finally, osteoarthritic synovial fluid could also be another factor promoting innate immune inflammation in the osteoarthritic joint through its high level of soluble CD14. The presence of CD14 in synovial fluid is mainly due to immune cells (monocytes/macrophages) migrating into the joint cavity in response to inflammation (Lee *et al.*, 2022). Soluble CD14 can increase the fibroblast-like synoviocyte response to TLR ligands. (Sokolove and Lepus, 2013 ; Nair, *et al.* 2012).
In the knee, the synovium also covers the IFP, suggesting an involvement of fat pad in case of synovitis (Zhou *et al*., 2022).

3.4.Infrapatellar fat pad: the good or the bad boy in osteoarthritis?

The IFP may interact with other articular tissues such as cartilage, subchondral bone, and synovial membrane, and thus play a role in the development and progression of knee OA. Its secretory phenotype (release of pro- and anti-inflammatory mediators) may alter joint homeostasis, by promoting joint degradation (IL-1β, TNF-α, IL-6 IL-12 release) (Zeng *et al*., 2020), or by protecting the joint against OA progression (IL-10 and IL-23 secretion) (Han, *et al.* 2014; Jiang *et al*., 2019; Ragab and Serag, 2021; Zhou *et al.*, 2022).
After stimulation by cartilage-derived collagen fragments, the synovium covering the fat pad may induce infiltration of the IFP by lymphocytes, monocytes and granulocytes. These immune cells would interact with local fat pad cells (adipocytes, macrophages, and fibrocytes) and stimulate the secretion of a variety of cytokines and adipokines and thereby contributing to the local inflammatory state (Zeng *et al*., 2020). The increased levels of TNF-α, IL-1β, interferon-γ (IFN-γ), and adipokines, which will then initiate and accelerate signalling cascades in cartilage to promote and maintain its degradation (favouring the imbalance toward catabolism) (Zhou *et al*., 2022). All this then causes the appearance of structural changes in the IFP, at the cellular and histological levels in OA compared to the IFP of healthy subjects. Specific changes observed in the IFP during osteoarthritis included thickening of the interlobular septa, increased

vascularisation, and the presence of inflammatory infiltrates. (Macchi *et al*., 2018). Moreover, the osteoarthritic IFP is characterized by an M1/M2 imbalance, with an increase in M1 macrophages, promoting the secretion of pro-inflammatory cytokines and catabolic factors, that may contribute to the progression of OA (Greif *et al*., 2020).

However, the fat pad has also been suggested to play a beneficial role in joint homeostasis. Indeed, it could enable cartilage and/or bone regeneration through the secretion of hormones and adipose tissue-derived growth factors. IFP secretes leptin, a hormone produced mainly by fat cells, which plays an essential role in regulating metabolism and appetite. When IFP secretes leptin into the knee joint, this hormone acts as a beneficial growth factor for the articular cartilage cells by stimulating the production of proteoglycans and type II collagen in the articular cartilage. by this increase, leptin helps to maintain the health of articular cartilage, preserving its structural integrity and protecting the joint from the pathological processes associated with osteoarthritis. In addition to its direct effect on chondrocytes, leptin can also stimulate the synthesis of growth factors such as insulin-like growth factor-1 (IGF-1) and transforming growth factor-β (TGF-β). These growth factors are involved in cell regeneration, tissue repair and chondrocyte proliferation, which further reinforces the protective role of leptin in the preservation of articular cartilage (Jiang *et al*., 2019). In addition, the presence of PSCs and MSCs within the fat pad, suggest a pro-regenerative role for the fat pad, and a source of stem cells for cartilage regeneration.
One hypothesis by do Amaral *et al*. in 2017 suggests that the pericyte stem cell population of the IFP may be a resident stem cell population of the joint tissue. These cells could then play a role in the regeneration of damaged articular cartilage by migrating into the synovial mucosa and synovial fluid to reach the cartilage. The infrapatellar stem cells, the pericytes being the most naive, would differentiate into synovial membrane stem cells. These could then migrate into the synovial fluid, giving rise to synovial fluid stem cells, which would attempt to heal the damaged cartilage. The high vascularity of the IFP provides a favourable environment for pericyte stem cells to respond to regeneration needs. PSCs present in IFP are known to reside in a perivascular niche around the small blood vessels close to the IFP. This perivascular niche maintains PSCs in an undifferentiated (unspecialised) state. In the event of injury or lesion, the signals in the perivascular niche may change (release of various cytokines), triggering the activation of the stem cells. They then spring into action and begin to differentiate into specialised cells for the repair and regeneration of damaged tissue (do Amaral *et al*., 2017).
In addition, there is growing interest in the therapeutic application of IFP-derived MSCs in tissue repair. Adipose tissue-derived MSCs have previously been identified as a promising source. Although their ability to differentiate into chondrocytes is inferior to that of bone marrow MSCs, they can be harvested less invasively and cheaply using liposuction. This method facilitates the therapeutic application of MSCs derived from adipose tissue, which is on the increase. The elimination of adipose tissue by liposuction offers a dual advantage. On the one hand, the increase in BMI and adipose tissue content is linked to articular cartilage lesions, making the removal of adipose tissue a suitable approach to the treatment of these lesions. Furthermore, adipose tissue is one of the most easily accessible tissues for the extraction of MSCs, which simplifies the procedure for obtaining these cells. Adipose-derived MSCs have been shown to be promising candidates for cell therapy. They can be differentiated into adipose tissue, bone, cartilage and muscle, making them versatile candidates for tissue regeneration. However, obtaining subcutaneous fat through liposuction is not without risk and can be

associated with complications such as skin necrosis, scarring, haematomas, allergic reactions and temporary nerve damage (Vahedi *et al*., 2021).

With regard to the IFP, anatomical location is also an important factor to consider. The IFP is adjacent to the synovial membrane, synovial fluid and articular cartilage, which can influence stem cell differentiation. They can differentiate into: chondrocytes, making them a potential source for cartilage regeneration and treatment of cartilage lesions; osteoblasts, enabling bone regeneration; or adipocytes, contributing to adipose tissue regeneration (Sun, Chen et Pei, 2018; do Amaral *et al*., 2017). Ding *et al*. studied the differentiation of MSCs from IFP and subcutaneous tissue towards chondrocytes and reported that IFP MSCs had a greater capacity for chondrogenic differentiation than mesenchymal cells from body's adipose tissue and bone marrow, suggesting that these cells are more committed to a chondrogenic lineage. This could be explained by the unique anatomical location of the IFP, close to articular cartilage (Almeida, *et al*., 2016; do Amaral *et al.*, 2017; Sun, Chen, and Pei, 2018). Furthermore, the capacity of IFP-derived MSCs to differentiate into a chondrogenic and osteogenic lineage is superior to that of adipose tissue-derived cells. Indeed, the expression of SOX-9, type II collagen and aggrecan genes is higher in IFP-derived MSCs than in adipose tissue-derived MSCs, which may explain their more optimal use for articular cartilage regeneration applications. However, when injected into the body, many MSCs migrate from damaged to healthy tissue and require appropriate support to 'anchor' the MSCs in place. Identifying the optimal cell source and appropriate support material is crucial to the success of stem cell-based regeneration strategies (Vahedi *et al*., 2021).

Animal studies have shown that MSCs derived from IFP have a chondroprotective effect and can also block the secretion of pro-inflammatory mediators, thereby helping to reduce inflammation and prevent cartilage degradation (Zhou *et al*., 2022; Jiang *et al.*, 2019).These MSCs may then be of interest as a protective mediator and as a source of cells for cartilage defect repair (Ioan-Facsinay and Kloppenburg, 2013; Zhou *et al*., 2022). Preclinical studies have shown that MSCs promote cartilage regeneration and reduce inflammation in animal models of osteoarthritis. In clinical trials, intra-articular injection of MSCs improved pain and function in patients suffering from osteoarthritis of the knee (Almeida, *et al*., 2016; do Amaral *et al*., 2017; Sun, Chen, and Pei, 2018).

Finally, in humans, IFP may show alterations at magnetic resonance imaging (MRI). These alterations (oedema, fibrosis, calcification, or ossification) are not consistently associated with knee pain and may be seen in asymptomatic patients. This could be due to individual differences in pain sensitivity or to other factors that influence pain perception. However, abnormalities of the IFP can cause pain if they are significant or if they cause inflammation or compression of the IFP (Draghi *et al.*, 2016). The role of these asymptomatic changes of the IFP in humans is still unclear. Moreover, in clinical context, when performing invasive knee joint surgery, the preservation of the IFP is still controversial due to different views on its role and importance in knee function and pathology (Nisar *et al.*, 2019). There are arguments that this tissue may play a role in joint lubrication and shock absorption, contributing to normal joint function (Draghi *et al.*, 2016; Sun, Chen, and Pei, 2018). In addition, some clinical cases have shown that preserving the IFP can be beneficial in reducing pain and improving post-operative outcomes in some patients (Safran et al., 2003; Zhang *et al.*, 2011; Wang *et al*., 2013). However, other arguments highlight that this tissue may be involved in inflammatory and pathological disorders of the knee, and its presence may increase the risk of post-operative complications, such as

adhesions or reactive synovitis (Rubin and Safran, 2018; Zeng *et al*., 2020). Further studies and research are needed to better understand the role of IFP in knee pathophysiology and to shed light on this controversy in order to improve surgical practice and clinical outcomes.

4. Aetiology of osteoarthritis

The aetiology of osteoarthritis is multifactorial. This degenerative disease generally occurs with age, as well as after mechanical stress (i.e. ligament lesion associated with joint instability), or is associated with genetic or metabolic disorders. The various factors responsible for the development of OA and the various tissues affected by OA give a multifaceted characteristic of this disease, therefore considered as a syndrome rather than a unique disease. This complexity of OA also translates into attempts to classify patients, in order to developed tailored therapeutics (Deveza and Loeser, 2018; Arrigoni *et al.,* 2020; Moskowitz *et al*., 2004; Johnson *et al.,* 2012). This master thesis will only focus on the two main aetiologies of OA: mechanical stress and ageing.

4.1. Mechanical stress

Osteoarthritis may occur as a result of trauma (such as anterior cruciate ligament or meniscus injuries), or mechanical overload (due to obesity, in weightbearing joints). These mechanical stresses activates cyclooxygenase-2 (COX2) and nitric oxide synthase (NOS) pathways (Figure 5) (Griffin and Guilak, 2005).

These pathways activation promotes the establishment of a pro-inflammatory environment (by increasing inflammatory mediators in the joint and ultimately cause progressive degradation of the cartilage matrix, subchondral bone remodelling and extrusion and meniscal tears (Arrigoni *et al.,* 2020; Moskowitz *et al.,* 2004; Johnson *et al.,* 2012; Zhu *et al.,* 2020). This inflammation plays a role in both initiation and progression of OA and is an innate immune response (unlike arthritis).

Inflammation of joint tissue is caused by cytokines, proteases and by the production of inflammatory mediators, and the absence of the lack removal of oxidized proteins, which will increase the concentration of reactive oxygen species (ROS) (Nancy Garrick, 2013). The accumulation of ROS and chronic oxidative stress and promote cellular senescence, particularly chondrocyte senescence secreting IL-6 (a cytokine) and IL-8 (a chemokine). This can lead to a loss of the ability to maintain and repair the cartilage ECM (Figure 5) (Berenbaum, 2013; Yunus, Nordin, and Kamal, 2020). Moreover, oxidative stress is increasingly considered to be one of the main factors responsible for the pathogenesis of osteoarthritis. Under physiological conditions, reactive oxygen species (ROS) and reactive nitrogen species (RNS) are eliminated by the antioxidant defence system. These ROS can cause damage to various joint components, including collagen, proteoglycans and hyaluronic acid if they are not eliminated (Karan *et al,* 2003).

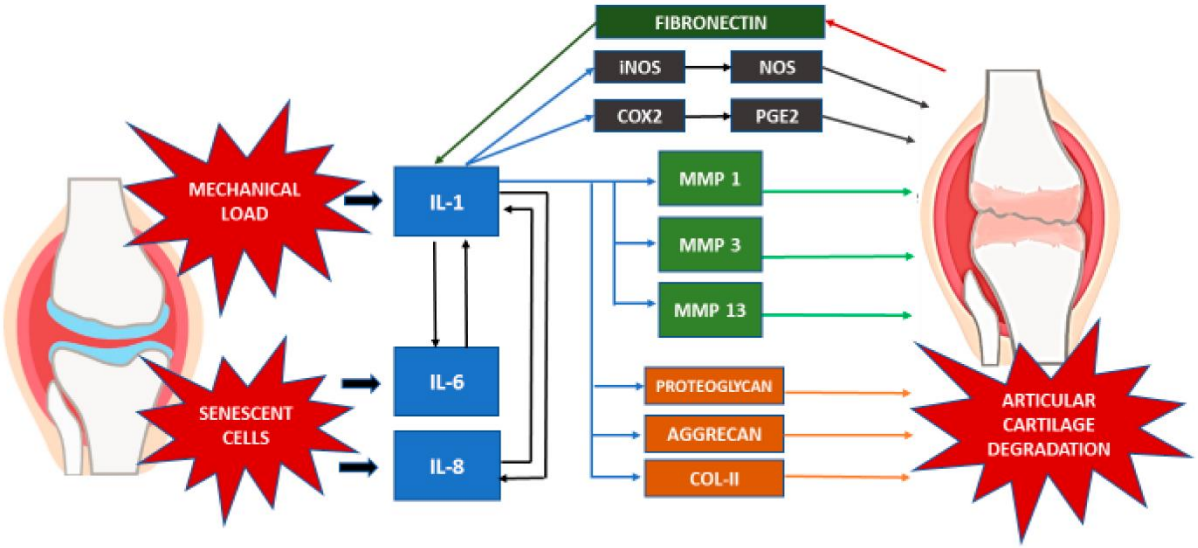

Figure 5 : *Mechanical stress and Senescence promotes inflammatory mediators in articular cartilage, resulting in cartilage degradation and development of osteoarthritis (Yunus, Nordin, and Kamal, 2020).*

The effect of mechanical stress on cartilage, subchondral bone and meniscus has been extensively described over the last 5 years. However, the effect of mechanical stress on other joint components (such as the fat pad) still need to be documented, as well as its impact on OA progression (Zhu *et al.*, 2020; Chang *et al.*, 2019; Yunus, Nordin, and Kamal, 2020; Chen *et al.*, 2020).

4.2.Ageing

Ageing is one of the strongest predictors of osteoarthritis. It is an inevitable process that causes many diseases in both humans and animals. The exact mechanisms behind the increase in prevalence and incidence of OA with age are still poorly understood, although it is suggested that age-related cellular changes such as senescence (Loeser *et al.*, 2009), combined with exposure to risk factors (age-related sarcopenia, increased bone turnover), lead to a reduction in the joint's ability to adapt to biomechanical challenges (Rezuș *et al.*, 2019).

Over time, cartilage, which covers the bony ends of joints, becomes progressively thinner due to wear and tear and micro-lesions accumulated over the years (Chevalier, 2004; Hügle *et al.*, 2012). Histologically, this is associated with an irregular appearance of the collagen fibres, thinning of the calcified layer, irregularities in the demarcation zone between the calcified layer and the deep layer and a decrease in the number of chondrocytes, particularly in the superficial layer of ageing cartilage. The focal lesions of ageing cartilage are histologically similar to the initial lesions of osteoarthritis. They are located on the surface of the cartilage and extend downwards (Chevalier, 2004).

Furthermore, ageing is often associated with a loss of muscle mass, which can weaken the muscular support of the joints, thereby increasing stress on the joint structures. This can be accompanied by the ageing of other tissues associated with cartilage, manifested by biochemical changes, particularly in cruciate ligaments, calcification of menisci and, above all, changes in the biomechanical properties and density of subchondral bone (Chevalier, 2004). Ageing leads to a reduction in regenerative capacity, as evidenced by the reduction in stem cells in connective tissue in the elderly, resulting in a catabolic state with a loss of connective tissue homeostasis. The mechanical properties of connective tissue, such as strength and elasticity,

can then be altered with age, affecting the ability of joints to absorb forces and shocks. In addition, chronic inflammation can increase with age, contributing to the degradation of cartilage and joint tissues. The exact cause for the inflammatory state in osteoarthritic joints is not fully understood. Overuse may activate osteoblasts and mast cells, subsequently attracting other immune cells from the innate or adaptive immune system. On the other hand, ageing may reduce the ability of the immune system to resolve inflammation in general (Hügle *et al*., 2012). These age-related joint changes are considered normal to a certain extent and are part of the ageing process. However, in some people these changes may be exacerbated by factors such as obesity, repeated joint trauma or certain inflammatory diseases, leading to more rapid progression of osteoarthritis (Chevalier, 2004; Hügle *et al.*, 2012).

Then there's the cellular senescence, which is associated with age. Senescence can be divided into two main categories: replicative and secretory senescence (Zhang *et al.*, 2020).
Senescence is associated with irreversible cell cycle arrest, and morphological and functional changes in the cell. Morphological differences that can be observed during staging such as increased but irregular cell size, increased amount of lysosomes, dysfunctional mitochondrial accumulation, enlarged endoplasmic reticulum, increased vacuole, SASP secretion and many changes in the architecture of the nuclear presented in Figure 6. These features can be significant tools to identify senescent cells and determine the senescence process. (Zhang *et al.*, 2020) Senescence is caused by telomere shortening related to vigorous cell proliferation (Berenbaum, 2013).

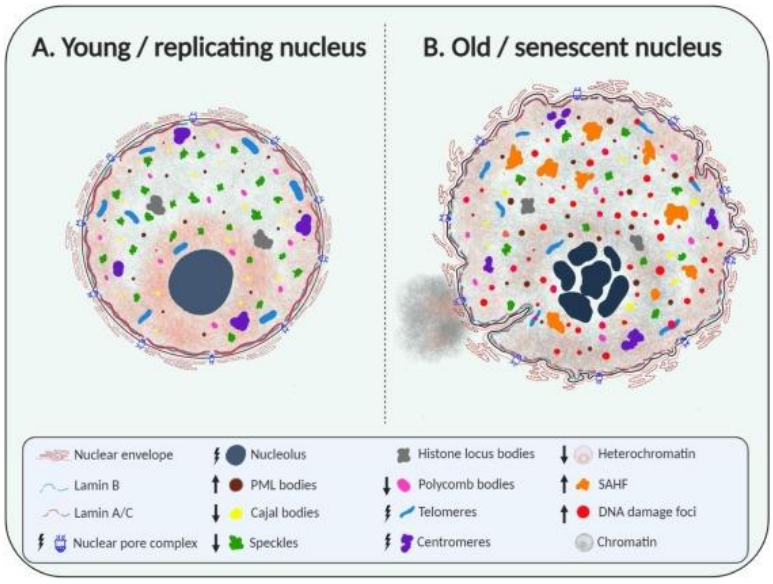

Figure 6 : *Age/senescence-related changes at nuclear level.*
A schematic diagram that shows changes in the nuclei during senescence.
depicts increase in number.
depicts decrease in number.
depicts damage to components. (Pathak, Soujanya and Mishra, 2021)

Secretory senescence is associated with the secretion of factors that constitute the pro-inflammatory secretory phenotype also called the senescence-associated secretory phenotype

(SASP). This SASP could be caused by oxidative stress generated by inflammation (Berenbaum, 2013). It is highly likely that the biological changes that occur with age (loss of ability for cells to divide, loss of tissue repair capacity and production of pro-inflammatory molecules known as the SASP) are responsible for the increased prevalence for OA in the elderly (Johnson *et al*., 2012). As a result of these changes, ageing joint tissue may become less resilient and less able to effectively withstand the mechanical forces applied during daily activities. This can lead to an accumulation of stress on the joint tissues, increasing the risk of damage and deterioration. In addition, tissue repair, particularly in cartilage, becomes less effective with age, leading to a reduced ability to restore tissue structure and function after injury or microtrauma. This can lead to progressive cartilage degradation, contributing to the development of osteoarthritis (Kraemer and Goldring, 2005; McGarvey *et al*., 2011).
Inflammation plays an important biological role in the aging process. In ageing a low-grade pro-inflammatory state is present. This low-grade pro-inflammatory state of ageing is also called Inflammaging. Inflammaging is systemic, chronic, and asymptomatic but sometimes systemic inflammaging can lead to cartilage destruction, pain, disability, and an impaired quality of life. Thus, in OA, which increases with age, there is a strong correlation between inflammaging, the presence of inflammasomes, autophagy, and chondrosenescence (all age-dependent deterioration of chondrocytes) (Rezuș *et al.*, 2019; Leonardi *et al.*, 2018).

The effect of age and senescence has been studied for cartilage (Price *et al.*, 2002; Martin and Buckwalter, 2002; Chen *et al.*, 2019) but is poorly described in tissues such as the synovium or the fat pad, the latter having controversial roles for the joint and in OA initiation and progression (Figure 7). For example, we still don't know whether these structures might accumulate changes, with age, that would initiate age-related OA.
It would therefore be interesting to study how synovial and fat pad cells evolve with age. This would include assessing senescence, analysing differences in gene expression, epigenetic modifications and alterations in cellular metabolism. Understanding how the synovium and fat pad respond to mechanical stress and how these responses may be modified by age. This would involve studies on the viscosity, elasticity and lubrication properties of these tissues. And studying how they interact with cartilage, ligaments and other joint structures. These interactions could play a crucial role in the initiation and progression of osteoarthritis. It could also be interesting to study the inflammatory markers present in the synovium and fat pad, and how their expression changes with age. This could help to assess the role of inflammation in age-related joint degeneration. It may also be of interest to examine the composition and structure of synovial and fat pad tissues (using histology, for example) to determine how it changes with age. This could reveal potential degenerative changes that could contribute to osteoarthritis.
These in-depth studies could then enable us to gain a better understanding of the mechanisms involved in the ageing of joint tissues, in particular the synovium and the fat pad, and their potential link to the initiation and progression of age-related osteoarthritis.

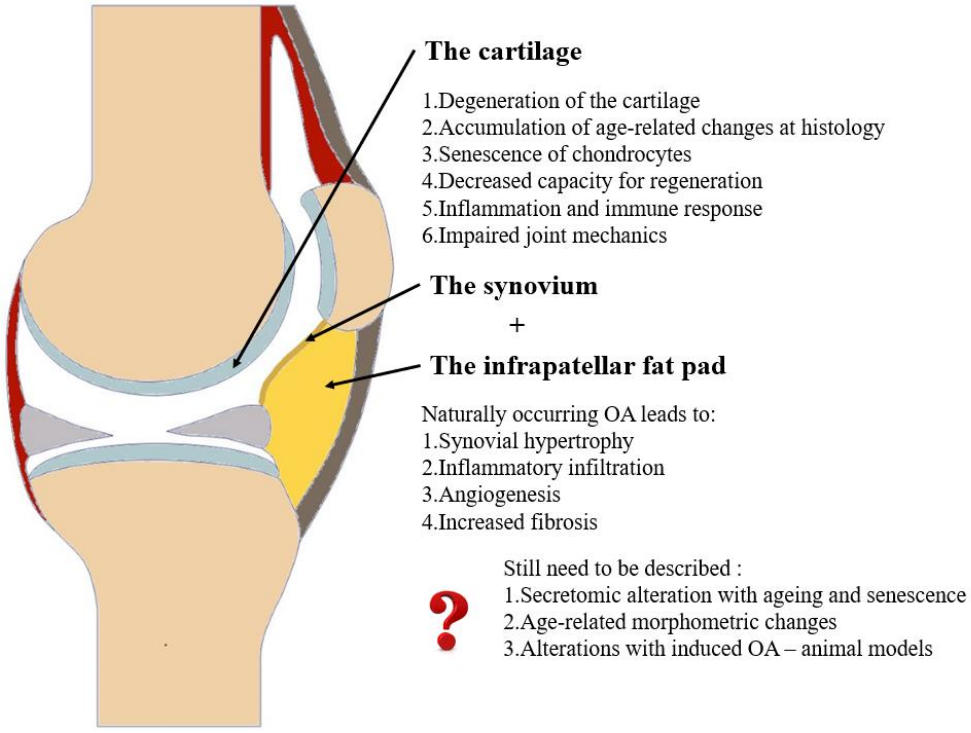

Figure 7 : *Effect of ageing and OA Initiation in the Knee Joint. This figure illustrates the key structures of the knee joint, including the synovium, fat pad and articular cartilage, and shows the known age-related changes that potentially contribute to the initiation and progression of age-related osteoarthritis. This figure also highlights research questions raised about the effect of age on less studied components such as the synovium and infrapatellar fat pad.*

5. Studying osteoarthritis

Although significant advances have been made in our understanding of AO and joint ageing, there are still many unanswered questions. To further our knowledge of the pathophysiology of OA and joint ageing, it is essential to understand in detail the cells that make up joint tissues, and the associated biological and molecular mechanisms, which can be explored through *in vitro* studies. However, it is equally important to understand the complex interactions that occur between different joint tissues, which requires *in vivo* models. By combining *in vitro* and *in vivo* approaches, we will be able to gain a better understanding of the underlying mechanisms of OA and joint ageing.

Understanding OA initiation and progression therefore requires *in vitro* and *in vivo* models. Despite the development of 'joint-on-a-chip' systems, to date there is no *in vitro* model to mimic the interaction between all the tissue of the joint, within a biomechanical environment (Jorgensen and Simon, 2021; Piluso *et al.*, 2019; Little and Smith, 2008).

Animal models of OA mainly focus on the stifle (knee joint). Small animal models (mouse, rat, rabbit and guinea pig) are useful and can be submitted to genetic manipulation. The advantages of smaller model organisms include relatively low cost, ease of handling and maintenance. They are often used as the first models for developing therapeutic interventions and initial drug-screening studies. On the other hand, samples from small animal models are more difficult to obtain and in smaller quantities, the sizes of the tissues are very different from those found in

humans and the induction of osteoarthritis by surgery is much more complicated (Little and Smith, 2008).
Large animal models (dog, goat, sheep, and horse) have a lot of anatomical similarities to humans. This is one of the major advantages of large model organisms. This allows better study of the pathological process of osteoarthritis, develop more clinically relevant characteristics and are necessary to test the efficacy of drugs prior to clinical trials. in the anatomical similarities with humans include the size of the joint and the thickness of articular cartilage. Other advantages of large animal models are the prevalence of natural primary and secondary osteoarthritis, the feasibility of arthroscopic intervention and diagnostic imaging such as MRI (Draghi *et al*., 2016; Gahier, M. *et al*. (2020). Often, the disadvantages of large animal models are primarily related to cost, handling difficulties, longer ageing time, slower progression of OA, and ethical considerations (Kuyinu *et al.,* 2016; Samvelyan *et al.*, 2021). Therefore, large animal models plays a key role in translation from fundamentals findings to human, and are used as preclinical models. One of these, the sheep, is known to develop cartilage damage with age (Vandeweerd *et al*., 2013). In sheep, it is possible to make surgically induced osteoarthritis models. Surgery can include: the unilateral radial meniscal tear, unilateral medial meniscectomy, unilateral anterior (or cranial) cruciate ligament transection or the combination of several of these methods (Little *et al.*, 2010). After that, it is possible to take various samples such as tissue samples, cells, synovial fluid, blood or to take repeated samples. In our study, we will use a large animal model: the sheep. We will use sheep with meniscectomy (= PTOA = post-traumatic OA model).

6. Objectives

Although cartilage and bone changes with OA and ageing have been described in the litterature, investigations are still required to understand the pathophysiology of the synovium and fat pad. The growing interest on synovium and fat pad in the OA field, and the strong association between ageing and OA leads to the hypothesis that synovium and fat pad show alterations with ageing. Reports on age-related changes of the fat pad and of the synovium in animal models (rabbit, or dogs) are sparse (Sagİroglu, 2012; Jilani and Ghadially, 1986; Clockaerts *et al*., 2010). In the sheep, there are no reports of age-related changes of these two tissues. As the sheep is a main preclinical model for therapeutics trials, it is essential to document the alteration of the joint with ageing and post traumatic OA. This could highlight cross-species mechanisms, therapeutic targets, or biomarkers.

The aims of this master thesis were:

(1) to describe the morphometric changes in the ovine synovium and infrapatellar fat pad, with age and induced osteoarthritis. This would allow us to see if changes in the aged synovium and fat pad are observable at histology and to compare them to the already relatively well-known changes in the osteoarthritic synovium.

(2) to describe the *in vitro* characteristics of synovial fibroblasts from young and old sheep and their response to oxidative stress and senescence conditions. This would allow us to see whether, as in chondrocytes, oxidative stress or inflammation can influence the

senescence of FLS and to see whether FLS from young and old sheep changes its cellular phenotype with age.

Materials and Methods

1. Animals, joint collection and macroscopic evaluation

Sixteen healthy ewes (n = 16) (7 young adults, and 9 old adults, age cut-off 7 years) were euthanised to assess the age-related changes in the synovium and fat pad.
Resection of the cranial part of the medial meniscus and transection of the cranial cruciate ligament were performed in 16 other ewes (n = 16) whilst skin incision only (sham surgery) was performed in 4 ewes (n = 4). Synovial fluid was collected at baseline. Animals were euthanised at different time points, i.e. 4 (n = 4), 6 (n = 8) and 28-weeks (n = 4).
All the animals came from the Ovine research Centre of the University of Namur, and free of musculoskeletal diseases.
After euthanasia, hindlimbs were collected and identified. Synovial fluid was collected, soft tissues (skin, subcutaneous fat, and muscles) were removed, and the joint were processed for histological sampling, and synovium was collected for cell isolation.

2. Histological sampling and processing

The knee joints were opened. Visual assessment of the synovium, the fat pad, as well as all relevant features of joint status (for example: cartilage surface) was performed by an experienced veterinarian. Synovium and IFP were collected and, following the recommendations of the Osteoarthritis and Cartilage Society International (OARSI), samples were fixed in 4% buffer formalin solution (Little *et al*., 2010) for 24-48 hours before being stored in 70% ethanol until processed. Paraffin inclusion was performed in Tissue-Tek VIP automates. Paraffin embedding was performed manually on a HistoStar workstation. After trimming, blocks were immersed in CellSoft (CellPath) and ice-cooled. Sections were cut (6-µm thick) and spread on Superfrost + slides. The overnight drying (46-48°C) was followed by staining.
Synovium staining included only Hematoxylin Eosin Saffran staining, to perform gold standard evaluations, following OARSI guidelines. The IFP assessment included multiple staining, to assess tissue organisation (HES) and to highlight the previously described alterations, observed in human knee MRI (Draghi *et al*., 2016) such as calcification (Toluidine Blue), ossification (Alizarine Red) or fibrosis (Picrosirius red).

2.1.Hematoxylin Eosin Saffran staining (HES)

Slices were stained on an Histostain workstation, and mounted with DPX mounting medium (#317616, Sigma). Sections were observed under a light microscope.
Synovial assessment followed the OARSI guidelines for microscopic scoring (Little *et al*., 2010), and included the evaluation of: intimal hyperplasia (0-3), inflammatory cell infiltration of the subintima (0-3), sub-intimal fibrosis (0-3), and vascularity (0-3) (Table 1).
In the absence of guidelines for fat pad histological assessment, the synovial scoring guidelines were partially adapted to the fat pad. The intima lining the fat pad, the infiltration of inflammatory cells in the fat pad and the vascularity of the fat pad were scored following the

intimal hyperplasia scoring (0-3), inflammatory cells infiltration of the subintima (0-3) and vascularity (0-3), respectively. The interstitial fibrosis of the fat pad was scored as follows: 0 for absence of interstitial fibrosis, 1 for 10 to 20 % interstitial fibrosis, 2 for 20 to 40% interstitial fibrosis, 3 for 40 to 60% interstitial fibrosis, 4 for 60 to 80% interstitial fibrosis, 5 for 80 to 100% interstitial fibrosis.

Table 1 : *Glossary for histological assessment of synovium in the sheep (Little et al., 2010)*

Intima hyperplasia (0 – 3)	
0	Normal: one cell deep only
1	Mild, focal (2-4 cells deep, and < 20% area)
2	Mild diffuse (2-4 cells deep, and > 20% area) OR moderate focal (5 or more cells deep, and < 20% area)
3	Moderate diffuse (5 or more cells deep, and > 20% area)
Inflammatory cell (lymphocytic/ plasmocytic infiltration) (0 – 3)	
0	Normal: occasional cell
1	Mild: focal infiltration, no lymphoid aggregates
2	Moderate: diffuse infiltration, no lymphoid aggregates
3	Marked: discreet lymphoid aggregates
Sub-intimal fibrosis (loose connective tissue areas only) (0 – 3)	
0	None
1	Light, focal (<20% area) collagen staining
2	Heavy focal (<20% area) or slight diffuse collagen staining
3	Heavy diffuse collagenous staining
Vascularity (0 – 3)	
0	0 – 2 vascular elements per 100x field
1	3 - 4 vascular elements per 100x field
2	5 - 8 vascular elements per 100x field
3	More than 8 vascular elements per 100x field
Aggregate score (0 – 12) = sum of the scores obtained for the four criteria above	

2.2. Toluidine Blue O/ Fast Green staining

After deparaffinization, the slices were stained in 0.04% w/v toluidine blue O (pH 4) for 10 minutes at room temperature. After a brief wash in tap water, the sections were incubated in 0.1% w/v aqueous fast green FCF for 2 minutes and washed briefly in tap water. The sections were dehydrated in isopropanol and cleared with toluol, before mounted with DPX mounting medium (#317616, Sigma) and observed with a light microscope (Olympus).
Toluidine Blue (cationic dye) displays a purple metachromatic colour when fixed to the negative charges of sulphated groups of the glycosaminoglycans, such as those of the cartilage matrix proteoglycans. Fast green was the counterstain (Sridharan and Shankar, 2012).

2.3. Safranin O/ Fast Green staining

After deparaffinization, sections were stained in 1.5% aqueous safranine solution for 40 minutes followed by 30 seconds in alcoholic fast green solution (0.02%). After dehydration in ethanol and toluol, the slides were mounted with DPX mounting medium (#317616, Sigma) and observed with a light microscope (Olympus).
The safranin O reacts with the chondroitin 6-sulphate and keratan sulphate and has a high specificity to glycosaminoglycans (Kiviranta, *et al*., 1985). This stain colours the cartilage in red in proportion to its proteoglycan content, and the counterstain (Fast Green) stains the collagen in green).

2.4. Alizarine red staining

Sections were deparaffinized, hydrated, rinsed in distilled water, and stained in 2% alizarin red S solution (pH 4.2) for 2 minutes and dipped successively in acetone and acetone-toluene. Finally, the section was cleared in toluene and mounted with DPX mounting medium (#317616, Sigma). The samples were then observed under a light microscope (Olympus).
Alizarin red stains calcium deposits a red-orange colour and can reveal ossification areas (Bertoni *et al.*, 2009).

2.5. Picrosirius red staining

For the picrosirius red staining, the sections were deparaffinized in a series of xylene and ethanol baths. Then, the tissue was predigested for 1 hour at 37° with bovine testicular hyaluronidase (1000 U/ml) in buffer A. The slides were washed with running tap water before the staining by 0.1% Sirius red F3BA in saturated aqueous picric acid for 2 hours. The sections were dehydrated in methanol and cleared with toluol. Finally, the slides were mounted with DPX mounting medium (#317616, Sigma) and observed with a light microscope and polarized light microscope.
Picrosirius red dye stained the collagen bundles in red under a light microscope as it specifically bonds the basic groups of collagens. Under polarized light microscopy, Picrosirius red stain increases the natural birefringence of collagen which allows observing the architecture of organised collagen fibres (orange/red) against a black non-refringent non-organised collagenous structure (Junqueira *et al*., 1979).

3. Primary fibroblast-like synoviocyte experiments

To understand the effect of ageing on synovium, primary FLS were isolated and stimulating them with oxidative stress conditions, inflammation and senescence-induction to see if, as in chondrocytes, oxidative stress or inflammation can influence the senescence of FLS and to see if FLS from young and old sheep react differently to these stresses.

3.1. Isolation of primary synovial fibroblasts and cell expansion

The limbs were cleaned under a hood for sterile handling. After dissection and joint opening, the synovial membrane was visually inspected, collected with a scalpel blade and rinsed with sterile NaCl. The synovium was incubated in DMEM-F12-HEPES medium with 1% Primocin (ant-pm Invivogen), 2mg/ml collagenase II (1148090 sigma) overnight at 37°C with 5% CO2.

The solution was then filtered through a 70-µm cell strainer, centrifuged at 1100rpm for 10 minutes at 4°C. The supernatant was removed and the FLS pellet was resuspended in DMEM/F12 complete culture medium (containing 10% foetal calf serum (FCS), 1% non-essential amino acids, 1% Glutamax and 1% Primocin). Fibroblast-like synoviocytes were then cultured in T75 flasks. The medium was changed after 24 hours, and then three times a week until confluence. Cells were either split for further expansion and experiments or cryopreserved for further experiments. Passages were recorded to use cells between passages 1 and 4, as recommended in previously published protocols (Neumann *et al*., 2010).

At confluence, cells were collected with trypsin + EDTA 0,05 % (25300054 Thermo Fisher) and split 1:2 into T-75 flasks for cell expansion.

3.2. Optimization of protocols for oxidative stress condition and induced senescence

Investigation of senescence in joint pathophysiology is relatively recent (Goldring, Jones, and Hunter, 2005). This master thesis initially aimed to set the protocol for induction of senescence in synovial fibroblasts, testing different doses and timepoints.

In a preliminary experiment, cells were seeded at 15 000 cells/cm² in 12-well plates and stimulated with 25µM or 50µM of tert-butylhydroperoxide (TBHP) for 24 hours; 50µM, 100µM or 2000µM of hydroxyurea (HU) for 24 hours and 3 days.

We finally decided to treat our cells with 25µM TBHP and 200µM HU for 24 hours. As we will see in section 4 of the results, a concentration of 50µM TBHP caused too much reduction in the number of cells in the well and the concentration of 200µM HU was the one that induced the most senescence in our FLS.
Non-treated and HU-treated cells were seeded at 15 000 cells/cm² in 12-well plates and cells treated with TBHP were seeded at 20 000 cells/cm² because TBHP induced a reduction in the number of cells in our wells.

After 24 hours (Day 1), cells were stimulated with one of the following medium:

Condition	Medium
normal joint status	DMEM-F12 medium with 1% FCS and 5% normal synovial fluid collected from healthy sheep
oxidative stress condition	culture medium with 25µM tert-butylhydroperoxide (TBHP), 1% FCS
OA inflammatory condition	culture medium with 1% FCS and 5% inflammatory synovial fluid (synovial fluid collected from sheep after induction of post-traumatic OA
cell senescence induction	culture medium with 1% FCS and 200 µM hydroxyurea

During incubation steps, cells were maintained in a humidified environment at 37°C, 5% CO2.

Cells were observed before and after stimulation under microscope to assess change in cell morphology. Light microscope pictures were taken at several stages: before, during and after stimulation.

After 24-hour stimulation (Day 2), the stimulation medium was removed and replaced with DMEM/F12 complete culture medium for 4 days. During these 4 days, the culture medium was changed every 2 days. The sequence of the different stimulation events is shown in Figure 8.

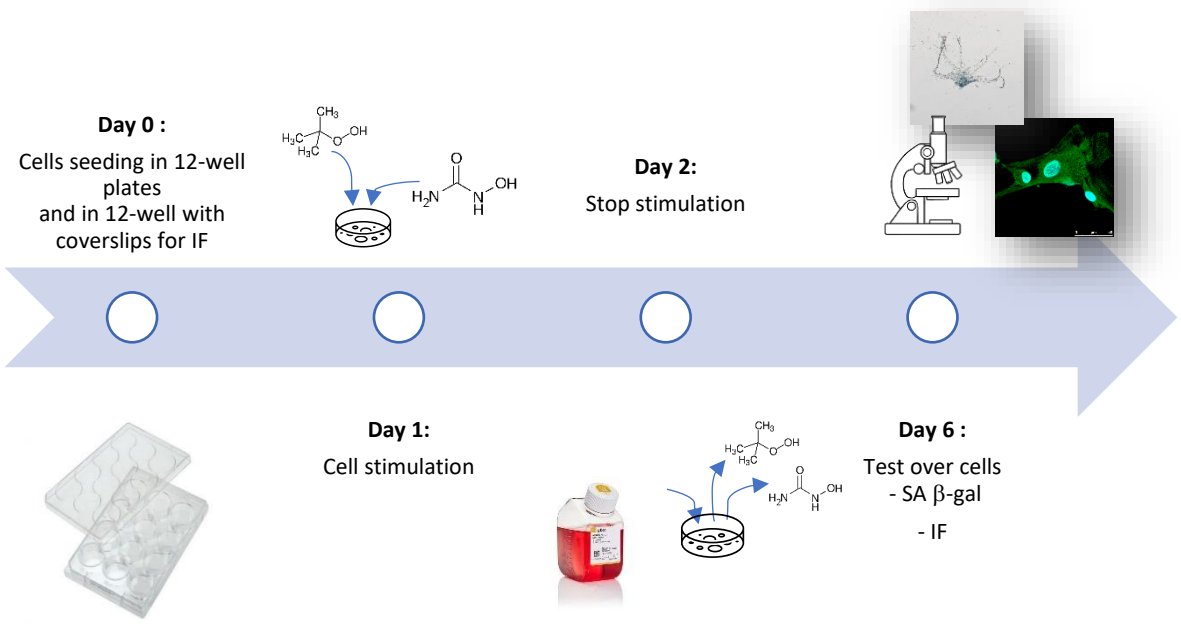

Figure 8 : *Representation of the temporality of cell stimulation events. Day 0 represents the day of passage of the cells in the 12-well plate, and day 6: the last day of cell culture equivalent to the day of stimulated cell assays such as Senescence-Associated beta-galactosidase (SA-b-gal) or immunofluorescence (IF).*

3.3.Immunocytochemistry for cadherin-11

In vitro experiments on FLS recommend the use of cells between passages 1 and 4 (Zimmermann *et al*., 2000; Lee *et al*., 2008; Aupperle *et al*., 1999). Our experiments include FLS from young adults and old animals at passage 2 or 3. Cell origin (i.e. old animals) and passages may lead to an accumulation of genetic and phenotypic changes in FLS and contribute to a loss of their original phenotype (Zimmermann *et al*., 2000). To check the persistence of FLS phenotype, cells were marked with antibody against cadherin-11, a specific adhesion molecule that plays a key role in the homotypic aggregation of FLS *in vitro* and *in vivo* (Bartok and Firestein, 2010).

Cells were growth on coverslips coated with FBS, in 12-well plates. After 24-h stimulation and 5 days (this experiment was carried out after 5 days and not 4 because it was performed the day after the SA β-gal test) with DMEM/F12 complete culture medium, the medium was removed, the cells were washed three times with PBS and then fixed in methanol 100% for 5 min. Fixed cells were washed three times with PBS and permeabilized with a solution of PBS, glycine (0.3M), Tween-20 (10%) and donkey serum (10%) for 1 hour. Permeabilised cells were washed three times with PBS. The coverslips (with the cells) were removed from the 12-well plates and incubations were performed in a humidified chamber (made with moist paper towel and

parafilm). Cells were incubated 24 hours at 4°C with 36µL of primary antibodies anti-cadherin 11 (Abcam, #ab223087, 1:200). Then, cells were washed three times with PBS and incubated 1 h with Alexa fluor 488 donkey anti-rabbit IgG conjugate (Abcam, GE3446005-1, 1:1000) and 4,6-diamidino-2-phenylindole (DAPI) (1:10000) for nuclei labelling. Cells were washed three times with PBS. Coverslips were then mounted with Fluoromont G on a Superforst slide (J1800AMNZ). Staining was observed with Broadband Confocal TCS SP5 (Leica), with settings: presence of green fluorescence associated with cadherine-11. Nuclei were stained blue with DAPI and evaluated for morphology and size (area). Cells with particular nuclei morphology (such as deformities with, for example, enlargement, elongation or the appearance of protrusion or invaginations) were counted (for 100 cells per well) and nuclei area were measured with ImageJ (for 50 cells per well).

3.4. Senescence-Associated beta-galactosidase assay (SA β-gal)

After 24-hour stimulation and 5 days with DMEM/F12 complete culture medium, the medium was removed, the cells were washed and then fixed with a solution of PBS pH 7,4 with 2% formaldehyde and 0.2% glutaraldehyde (1 mL/well) for 5 minutes. After two PBS pH 7,4 washes, cells were incubated with a staining solution (1 mL/well) containing 40mM citric acid/Na phosphate buffer pH 6, 5mM K4[Fe(CN)6]3H2O, 5mM K3[Fe(CN)6], 150mM sodium chloride, 2mM magnesium chloride and 1mg/ml X-gal in distilled water at 37°C without CO2 overnight. The next day, the cells were washed twice with PBS pH 7,4 and once with methanol. The cells were allowed to dry before counting the number of cells stained in blue (for 300 cells per well).

4. Statistical analysis

Quantitative data (such as age) and qualitative data (such as scores) were compared between young and old animals using the t-test and the Mann-Whitney test, respectively. Spearman correlation coefficient was calculated to assess the correlation between parameters (i.e., age and scoring of synovium/fat pad, or visual assessment and histological scoring for the synovium and the fat pad).

Multiple variable regression was applied considering the total score for fat pad, and for synovium, as a dependent continuous variable. The model included all data and considered the following independent variables: age (continuous data), type of intervention (no surgery, sham operated, post-traumatic OA). This model enabled assessment of the statistical significance of individual effects (P value).

All statistical analyses were performed with GraphPad Prism 9.4.1.

Results

1. Macroscopic changes of synovium and fat pad

1.1. Synovium and fat pad show slight visual changes with ageing

Macroscopic assessment of synovium from old sheep (9.7+/- 1.4 years old) and young adult sheep (4.2 +/-0.7 years old) showed slight changes, with normal synovium in 4/7 old sheep and 5/7 young adults. Abnormal findings were slight focal increase in vascularity, thickness and change in coloration (OARSI score 1). (Figure 9)

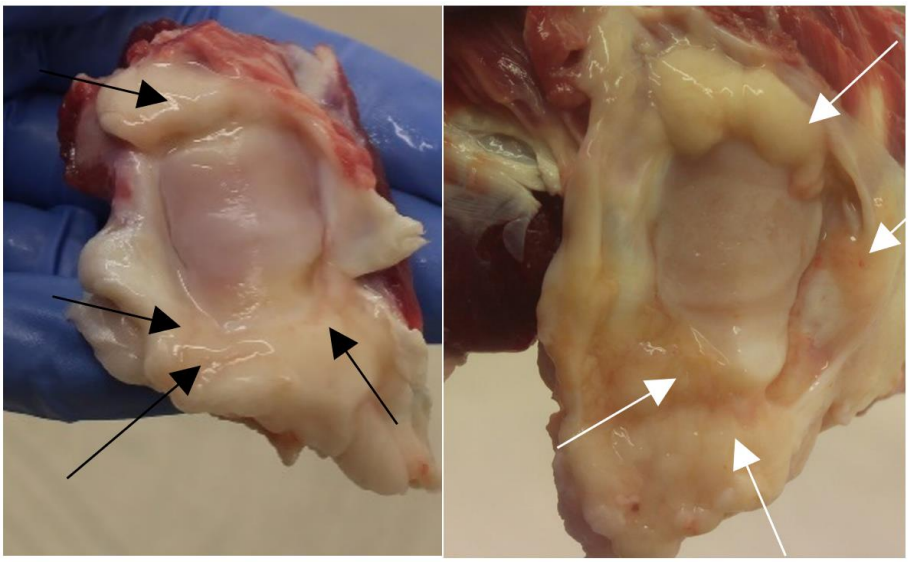

***Figure 9** : Pictures of normal synovium, around the patella with normal, opal white, semi-translucent (black arrows). Synovium with focal change in coloration, thickening and slight focal increase in vascularity.*

Fat pad was pale, white to yellowish, without obvious vascularisation in 3/7 old sheep and 6/7 young adults and 4/7 old sheep and 1/7 young adults' fat pad showed focal increase in vascularity, visible as a focal pink appearance of the fat pad. (Figure 10)

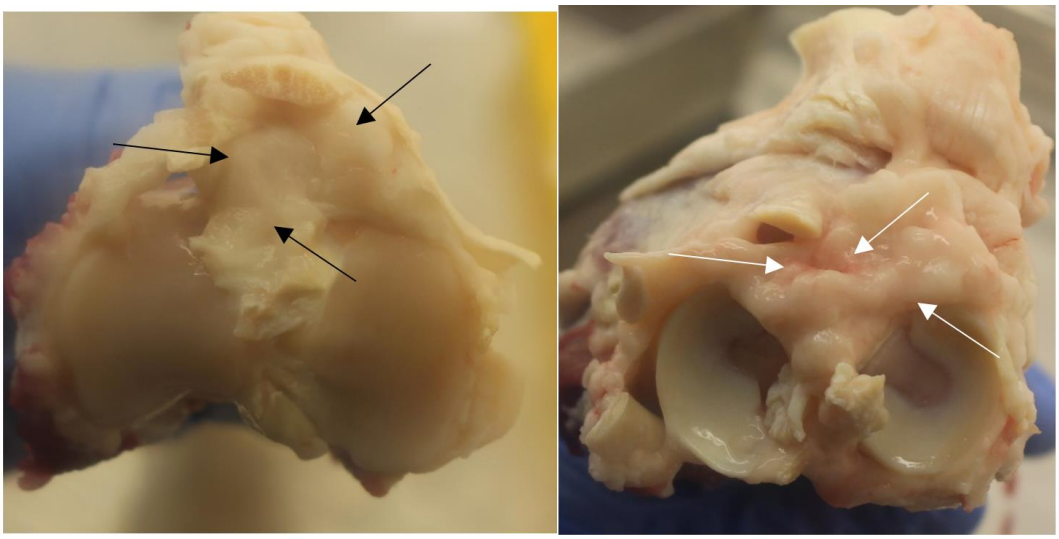

Figure 10 *: On the left: the fat pad is normal and shows a homogeneous pale white to yellowish colour (black arrows). On the right: The fat pad shows a slight focal increase in vascularity, as revealed by the pink – reddish colour (white arrows).*

1.2. Synovium and fat pad show moderate alterations with induced osteoarthritis

Post-traumatic osteoarthritis (PTOA) induced by partial medial meniscectomy and cranial cruciate ligament transection, led to moderate alterations of synovium and fat pad.

At an earlier timepoint (4 weeks post-PTOA surgery) changes were moderate to severe synovial discoloration, fibrillation, thickening and hypervascularity (mean visual score: 4; range: 3-5), and mild to marked discoloration and increased vascularity for the fat pad (mean visual score: 3; range: 2-4) (Figure 11 B).

Six weeks after surgery, synovium showed less severe changes with moderate to marked diffuse discoloration, fibrillation and hypervascularity (mean visual score: 3; range: 3-4), while corresponding fat pad showed slighter changes mild to moderate discoloration, with increased vascularity (mean visual score: 2; range: 2-3) (Figure 11 C).

Sham surgery led to slighter changes with mild to moderate discoloration of synovium and fat pad (mean visual score: 3; range: 2-3, for each tissue), six weeks after sham surgery (Figure 11 A).

The longer timepoint (28 weeks post-PTOAsurgery) showed mild to severe alterations of the synovium (mean visual score: 4, range: 2 to 5), and similar alterations of the fat pad (mean visual score: 3.5, range: 2 to 4).

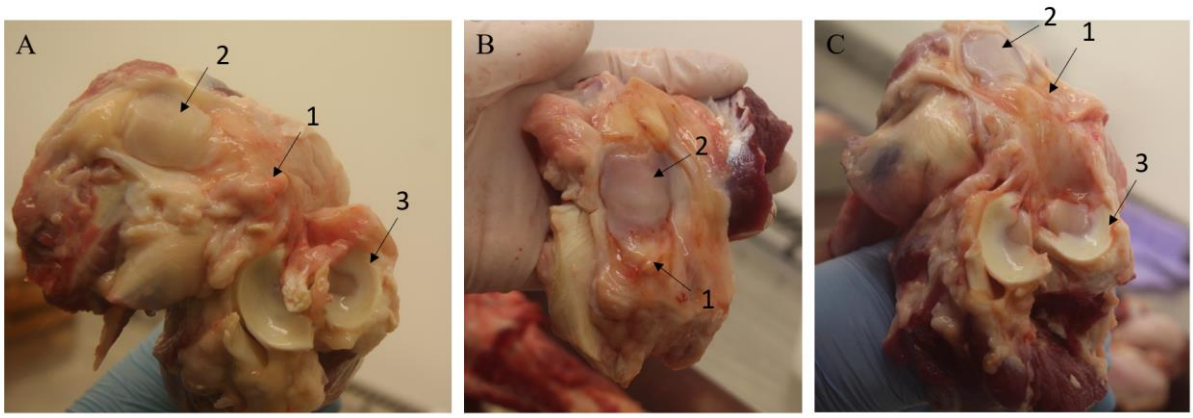

***Figure 11** : Post-traumatic osteoarthritis (PTOA) induced and Sham surgery. (A) Fat pad, patella and meniscus of sham operated sheep (left limb) 6 weeks after surgery (B) Patella and fat pad (below) of a sheep 4 weeks after partial medial meniscectomy with cranial cruciate ligament resection. (C) Fat pad, patella and meniscus of a sheep 6 weeks after partial medial meniscectomy and cranial cruciate ligament resection. The medial meniscus (right) is cut, the cranial part is missing = partial medial meniscectomy. Arrow: 1= Fat pad, 2=Patella and 3= meniscus.*

2. Histological assessment of synovium and fat pad

2.1.Synovium and fat pad changes with age were slight to moderate

Mild alterations were observed at histology. For example, some samples showed mild focal intimal hyperplasia, or focal inflammatory cells infiltration (Figure 12). At histology, fat pad showed mild diffuse (to moderate, localised) intimal hyperplasia, as well as moderate interstitial fibrosis (<40%).

Difference between young and old specimens for synovium and for fat pad were not significant (Table 3). Correlation between age and histology scorings for fat pad and synovium was not significant for this set of 14 sheep (Table 2).

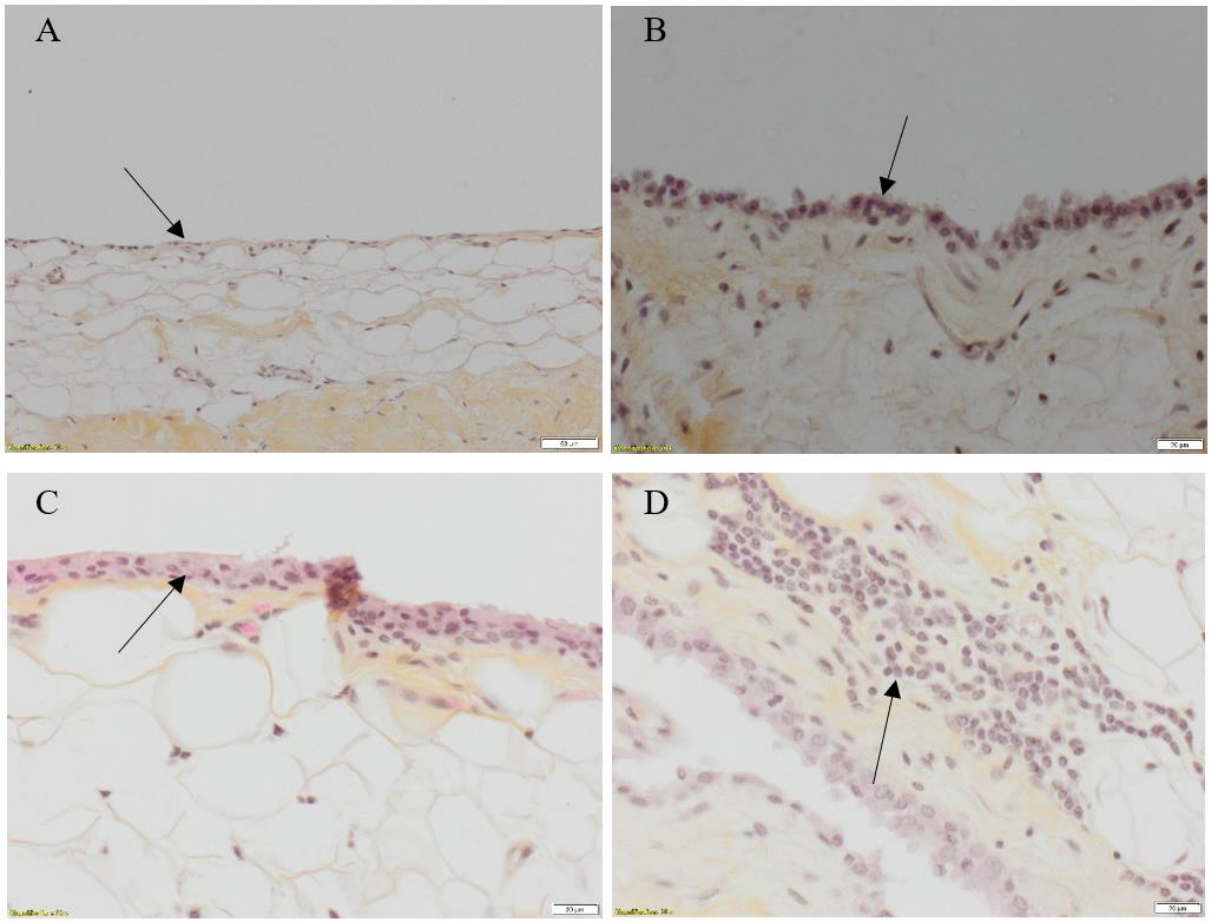

Figure 12 : *Representative Hematoxylin Eosin Saffron stained sections of synovium (A,B) and fat pad (C,D) from sheep. (A) This young specimen showed a score-0 synovial intima (arrow) without cell invasion of the subintima and normal vascularity. (B) Synovial intima showed a mild diffuse hyperplasia (arrows) (score 2) (C) Example of mild diffuse intimal hyperplasia (arrows) of old sheep fat pad (score 2) (D) This old-sheep fat pad shows a focal cellular infiltration and an interstitial fibrosis (score 1) (arrows).*

Table 2 *: Spearman coefficient and associated P values for correlation between age and scorings at histology*

Correlation between age and…	Spearman r	P value
... Synovial Intimal hyperplasia	0,013	0,482
... Synovial Inflammatory cell infiltration	-0,330	0,123
... Synovial Sub-intima fibrosis	0,205	0,240
... Synovial Vascularity	-0,205	0,275
... Synovial Total Score	-0,118	0,342
... Synovial visual score	0,312	0,141
... Fat pad Intimal hyperplasia	-0,144	0,322
... Fat pad - Inflammatory cell infiltration	0,226	0,228
... Fat pad Interstitial fibrosis	0,432	0,077

... Fat pad Vascularity	-0,352	0,231
... Fat pad Total Score	0,193	0,265
... Fat pad visual score	0,397	0,082

Table 3 : *Characteristics of the young adults and old specimens. Data are given as mean +/- standard deviation for continuous data, and median (minimum-maximum) for scoring*

Characteristics	Young adults (N=7)	Old animals (N=7)	P value
Age (years old)	4.2 +/-0.7	9.7+/- 1.4	<0.0001
Synovium – intimal hyperplasia	1 (0-3)	1 (0-2)	0.38
Synovium – inflammatory cells infiltration	1 (0-2)	0 (0-2)	0.24
Synovium – subintimal fibrosis	1 (0-2)	1 (1-2)	0.50
Synovium – vascularity	0 (0-1)	0 (0-1)	0.50
Synovium Total Score	3 (0-7)	2 (1-6)	0.30
Fat pad – intimal hyperplasia	0 (0-1)	0 (0-2)	0.43
Fat pad – inflammatory cells infiltration	0 (0-1)	1 (0-1)	0.22
Fat pad – interstitial fibrosis	0 (0-1)	1 (0-2)	0.10
Fat pad – vascularity	0 (0-0)	0 (0-1)	0.54
Fat pad Total Score	1 (0-1)	2 (0-4)	0.10

Interstitial fibrosis of the fat pad was visible in 2 out of 7 young adults, and 5 out of 7 old adults. In the young animals, this fibrosis was visible as an organised collagen deposition (aligned fibres), whereas in the old animals, the deposition showed a different organisation with metaplasia of the fat tissue into a dense conjunctive tissue cartilage-like structure with lacunae filled with cells (Figure 13). This metaplasia was found in 4 old adults.

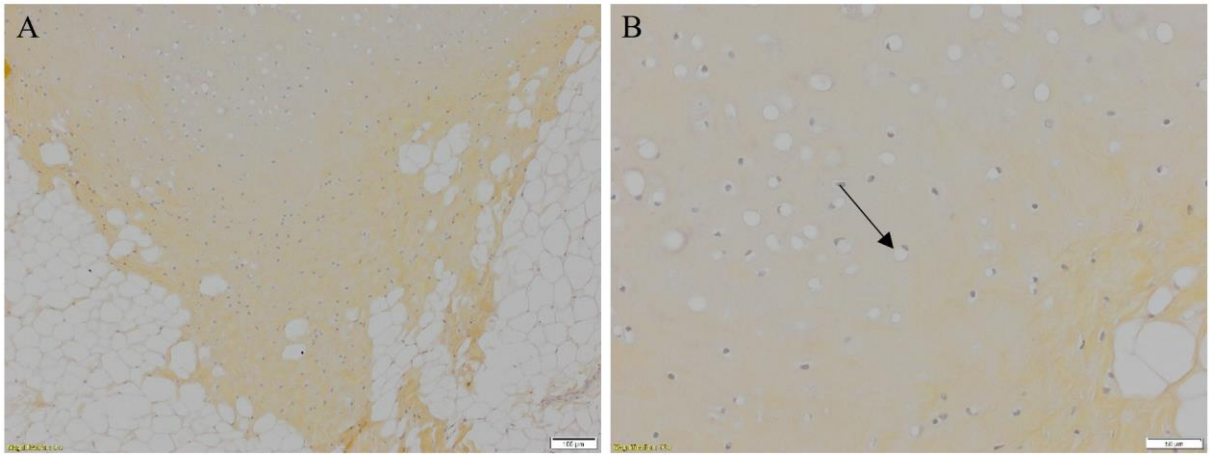

Figure 13 : *Representative Hematoxylin Eosin Saffron stained sections of fat pad from old sheep. This specimen showed an interstitial fibrosis with a particular collagen deposition (A) with lacunae (arrows) (B).*

2.2. Synovium and fat pad showed moderate to severe changes upon surgery

Six weeks after induction of post-traumatic osteoarthritis, the total synovial score on histology ranged from 4 to 11 (mean = 8). Changes were more severe 4 weeks after induction (mean: 11, range: 9-12) and less severe in sham operated synovia (mean: 7, range 3 to 9).

Multivariate analysis revealed that score for synovial assessment, at histology, was influenced by the type of intervention (non-operated controlateral, sham surgery, PTOA induction; P=0.02).

Examples of histological synovial scores are shown in the Figure 14.

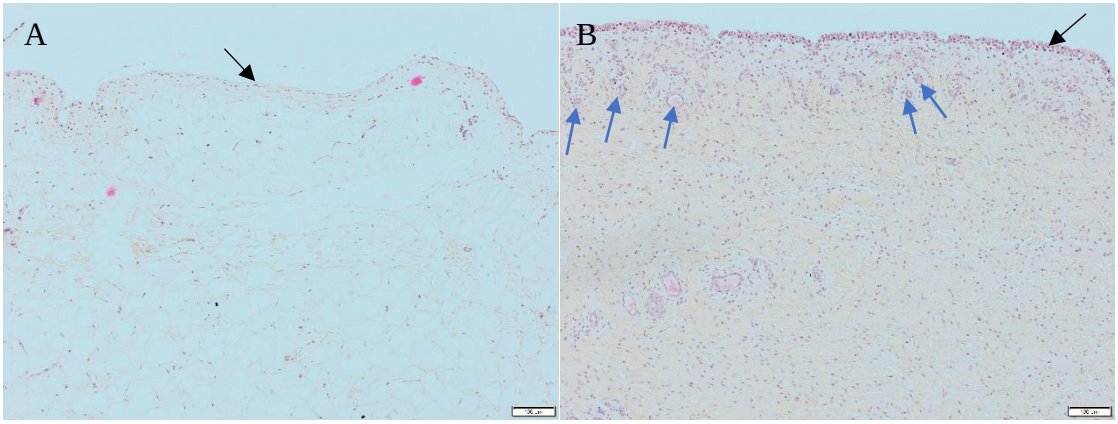

Figure 14 : *Representative Hematoxylin Eosin Saffron stained sections of synovium from sheep who had a meniscectomy and cruciate ligament transection. (A) This specimen showed a score-0 synovial intima (black arrow) without cell invasion of the subintima and normal vascularity. (B) Synovial intima showed moderate diffuse hyperplasia (black arrows) (score 3), a diffuse cellular infiltration (score 2), an interstitial fibrosis (score 3) and vascularisation (score 2) (blue arrows).*

Scoring of fat pad at histology was influenced by the type of intervention (P=0.003). Histological changes of fad pad included interstitial fibrosis (10 of 16 operated sheep, and 2 out of 4 sham sheep). Chondroid metaplasia was found in 6 operated sheep. Examples of histological fat pad scores are shown in the Figure 15.

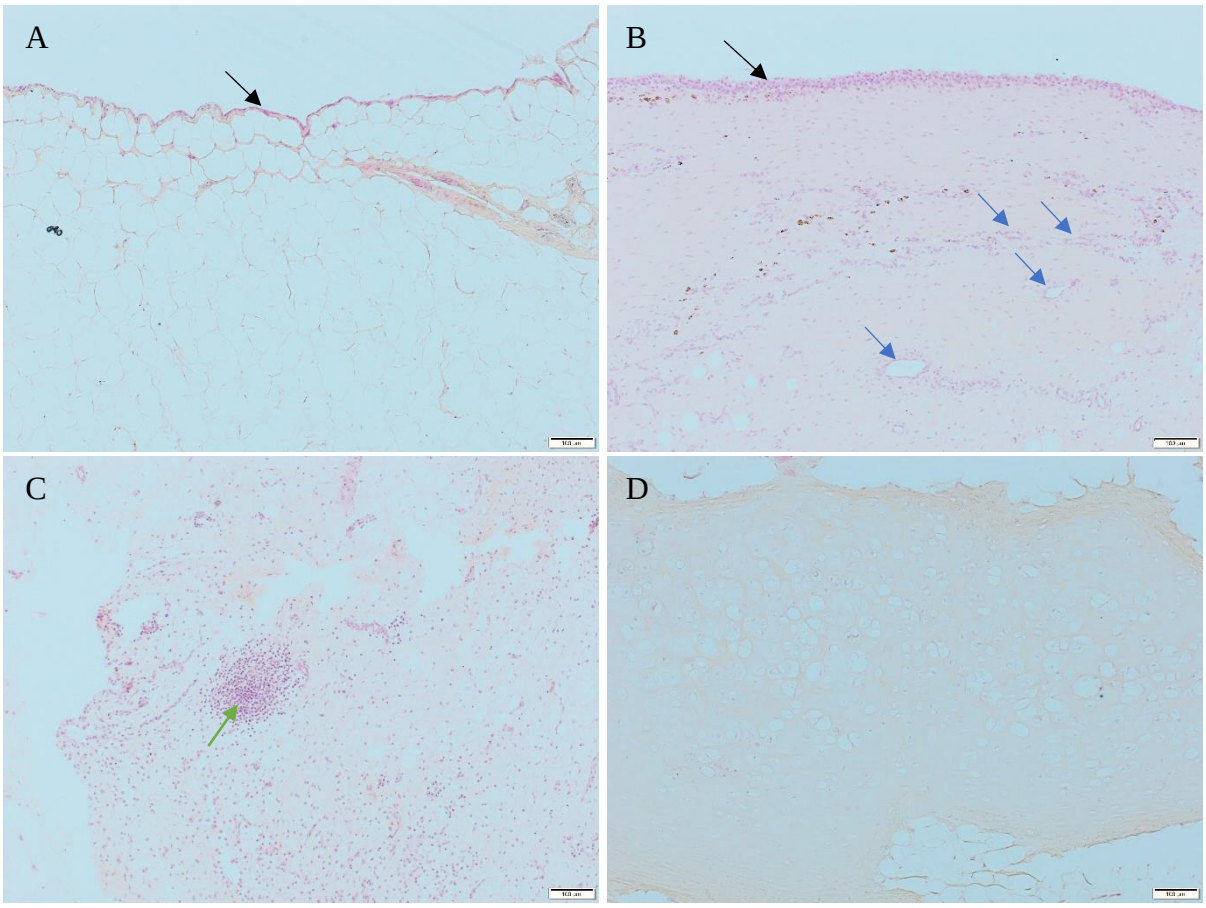

Figure 15 : *Representative Hematoxylin Eosin Saffron-stained sections of fat pad from sheep who had a meniscectomy and cruciate ligament transection. (A) This fat pad showed an Aggregate score 0 with a normal intima (black arrow) without cell invasion of the subintima and normal vascularity. (B) Example of moderate diffuse intimal hyperplasia (black arrows) of fat pad (score 3) and a vascularisation (blue arrows) (score 3) (C) This sheep fat pad shows a focal cellular infiltration (score 3) (green arrows). (D) This specimen showed an interstitial fibrosis with a cartilage-like collagen organisation.*

2.3. Histochemical stainings allowed to characterise the interstitial alterations of the fat pad with ageing and PTOA

2.3.1. Toluidine-blue O Fast-Green staining

Fat pad from old healthy sheep showed a slight toluidine blue uptake for 4 olds sheeps.

Toluidine Blue / Fast Green staining only slightly marked the areas of adipose tissue metaplasia in dark blue/purple of old sheep fat pad (Figure 16).

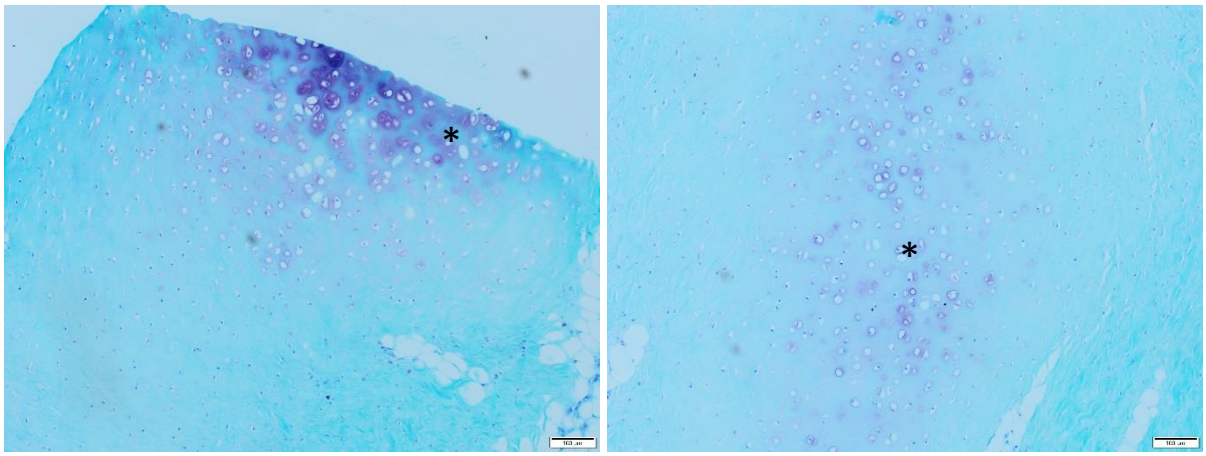

Figure 16 *: Representative Toluidine Blue / Fast Green Stain stained sections of fat pad from old sheep. This specimen showed this particular collagen deposition with lacunae stained slightly dark blue/purple (*)*

Chondroide metaplasia of the osteoarthritic fat pad stain with Toluidine Blue / Fast Green staining appeared in dark blue/purple but darker than metaplasia of the old sheep (Figure 17; Figure 16). This various toluidine blue uptake suggests different degree of metaplasia and proteoglycan deposition. Metaplasia was visible in 7 of 16 operated sheep, and 0 of 4 sham sheep. All observed metaplasia was stained with toluidine blue. 6 sheep showed metaplasia 6 weeks after surgery and 1 after 4 weeks surgery.

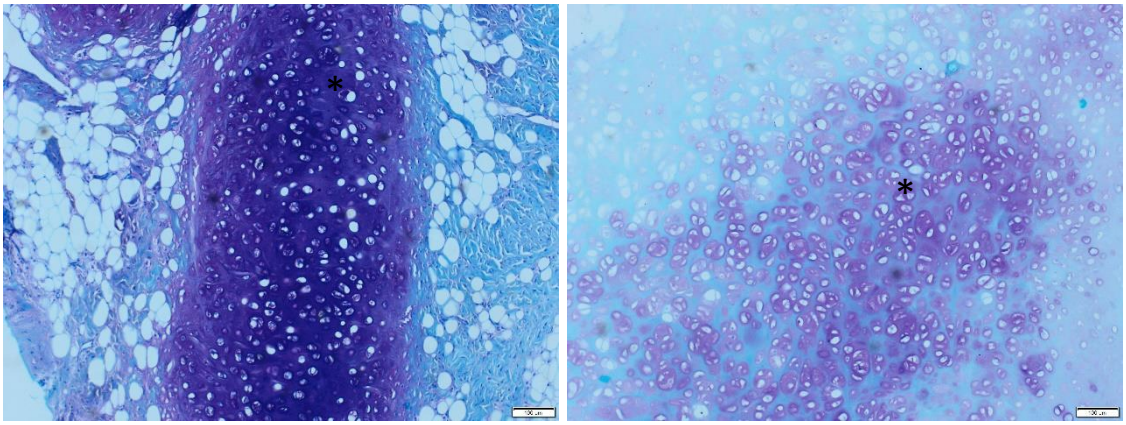

Figure 17 *: Representative Toluidine Blue / Fast Green Stain stained sections of fat pad from sheep that had undergone resection of the cranial part of the medial meniscus and transection of the cranial cruciate ligament whilst only skin incision. This specimen showed a metaplasia darker stained in dark blue/purple (*)*

2.3.2. Alizarin Red staining

No calcium deposits were found in alizarin red stained sections.

2.3.3. Safranin O- Fast green staining

Fat pad metaplasia areas showed a reddish pattern (Safranin O uptake) over a light green background (Fast Green counterstain). The Safranin appeared to accumulate at the border of the lacunae, suggesting that proteoglycans are produced by cells entrapped in lacunae (Figure 18).

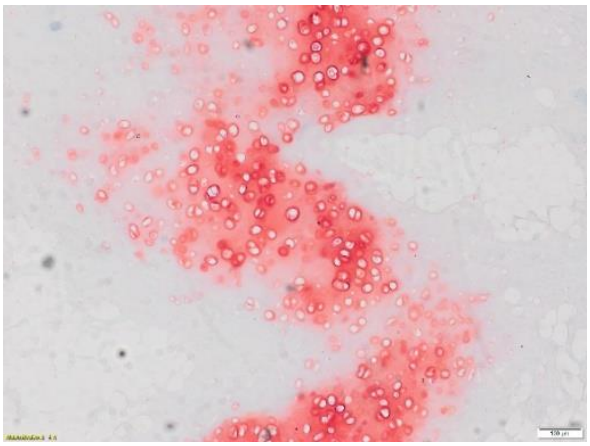

***Figure 18** : Representative Safranin O/ Fast Green Stain stained sections of fat pad from old sheep. This specimen shows this particular collagen deposition stained in red.*

2.3.4. Picrosirius red stained sections under polarized light microscope

Adipose tissue of the fat pad was featured by small amount of interstitial fibres (white arrow) (Figure 19).

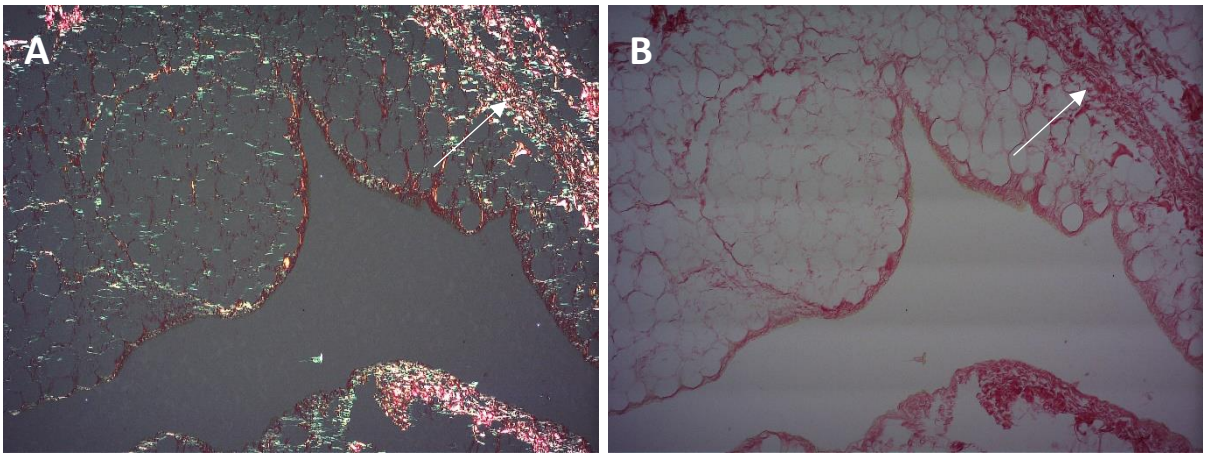

***Figure 19 :** Representative picrosirius red stained sections of normal fat pad from old sheep (A) under polarized light microscopy and (B) under classical light optical microscope. The small number of interstitial fibers showed a heterogeneous birefringence pattern.*

The general appearance of the collagen fibres in fibrous areas of the fat pad appeared to be mostly disorganised presenting a slightly heterogeneous birefringence pattern (Figure 20).

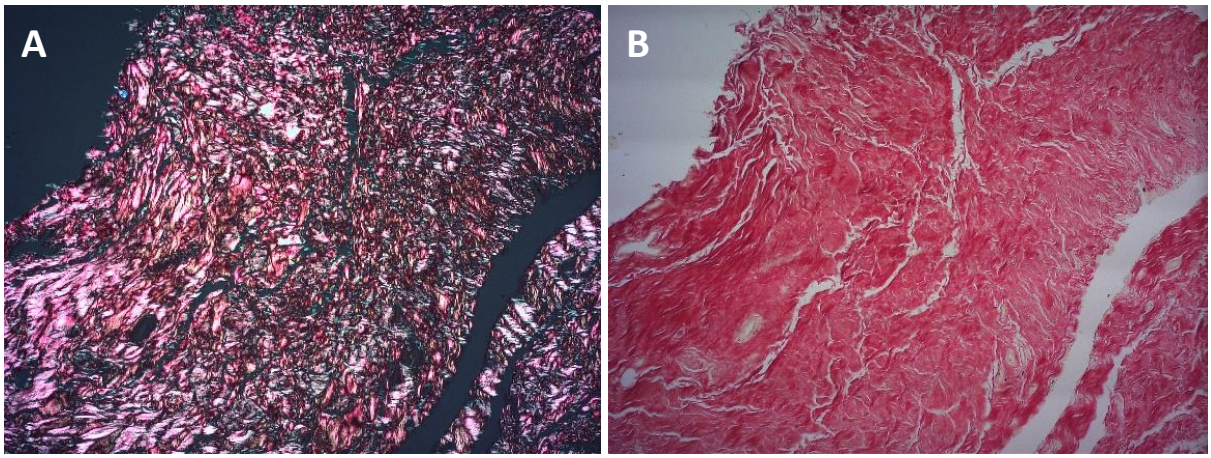

Figure 20 *: Representative picrosirius red stained sections of fat pad from old sheep (A) under polarized light microscopy and (B) under classical light optical microscope. Collagen fibres showed with a slightly heterogeneous birefringence pattern.*

In contrast, in areas of chondroid metaplasia, collagen fibres were more aligned to each other, forming walls that were perpendicular to each other. This was observed as different colour depending on the orientation of aligned fibres (i.e. vertical-red or horizontal-blue) (Figure 21).

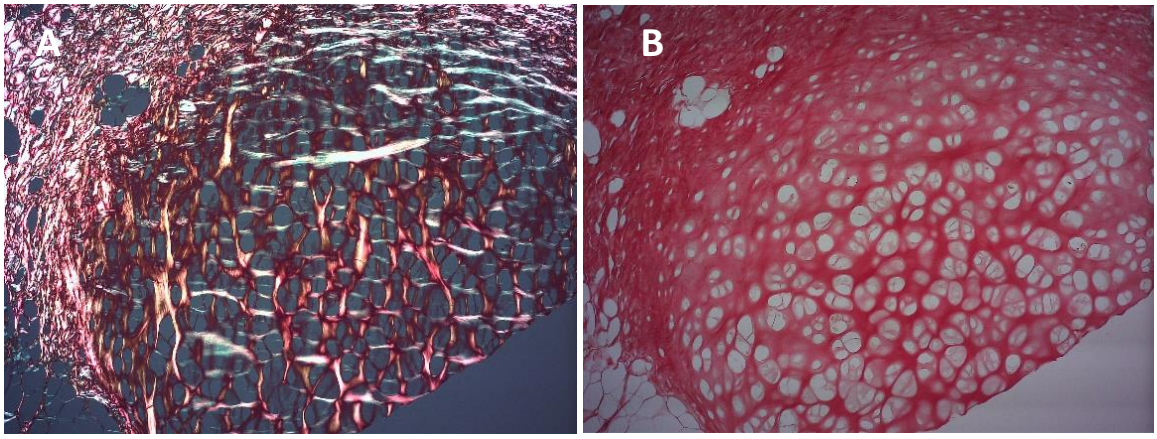

Figure 21 *: Representative picrosirius red stained sections of fat pad with a specific collagen deposition from old sheep (A) under polarized light microscopy and (B) under classical light optical microscope. Collagen fibres in areas of chondroid metaplasia showed a more homogeneous birefringence pattern with a structured organisation.*

3. Cell proliferation after thawing and morphology

After cryopreservation and thawing (one million cells in a T75 flask), synovial fibroblasts from young adult specimen (N=4) needed 4 days to grow and reach confluence, whereas synovial fibroblasts from old specimens (N=3) needed 7 days. Cell morphology was similar between young adult and old specimen (Figure 22).

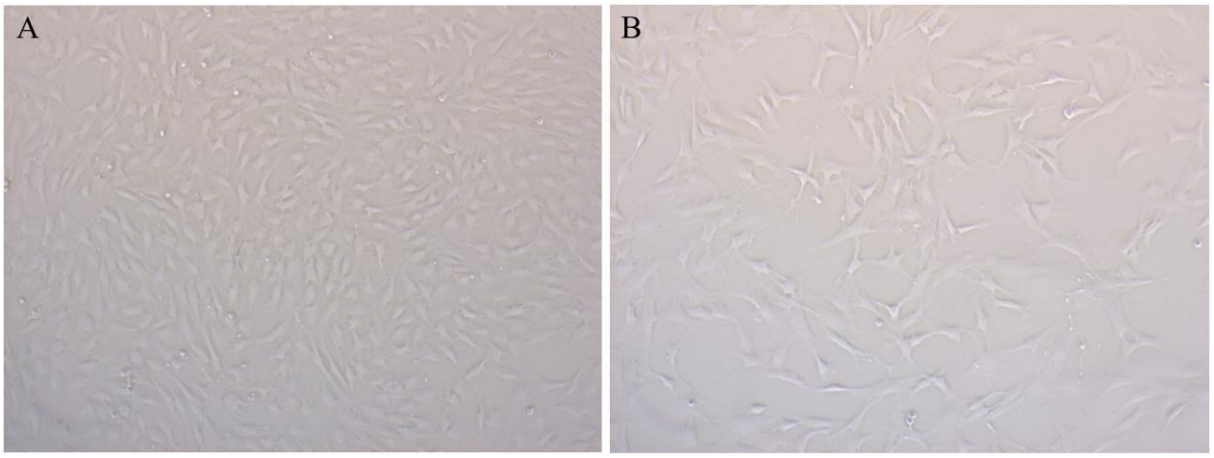

***Figure 22** : Synovial fibroblasts 4 days after thawing and cultured in T75 flasks. (A) Confluence of young sheep cells. (B) On day 4, old sheep synovial fibroblasts were not confluent.*

4. Optimization of protocols for oxidative stress condition and induced senescence

We wanted to test different concentrations, durations of stimulation and number of cells per plate for the tests because we had no experience with the induction of senescence in FLS.

During our tests, when cells were cultured after 24 hours stimulation with 50µM and 25µM TBHP, the cells were found in lower numbers after 4 days of culture compared to control cells (Figure 23) or cells stimulated with HU. The impact of TBHP on cell proliferation was too strongin stimulation with 50µM TBHP (and led to the impossibility to get reliable data with for example SA β-gal staining), so we chose a dose of 25µM for subsequent experiments.
In addition, this difference was more pronounced in FLS from old sheep than from young sheep (Figure 23).

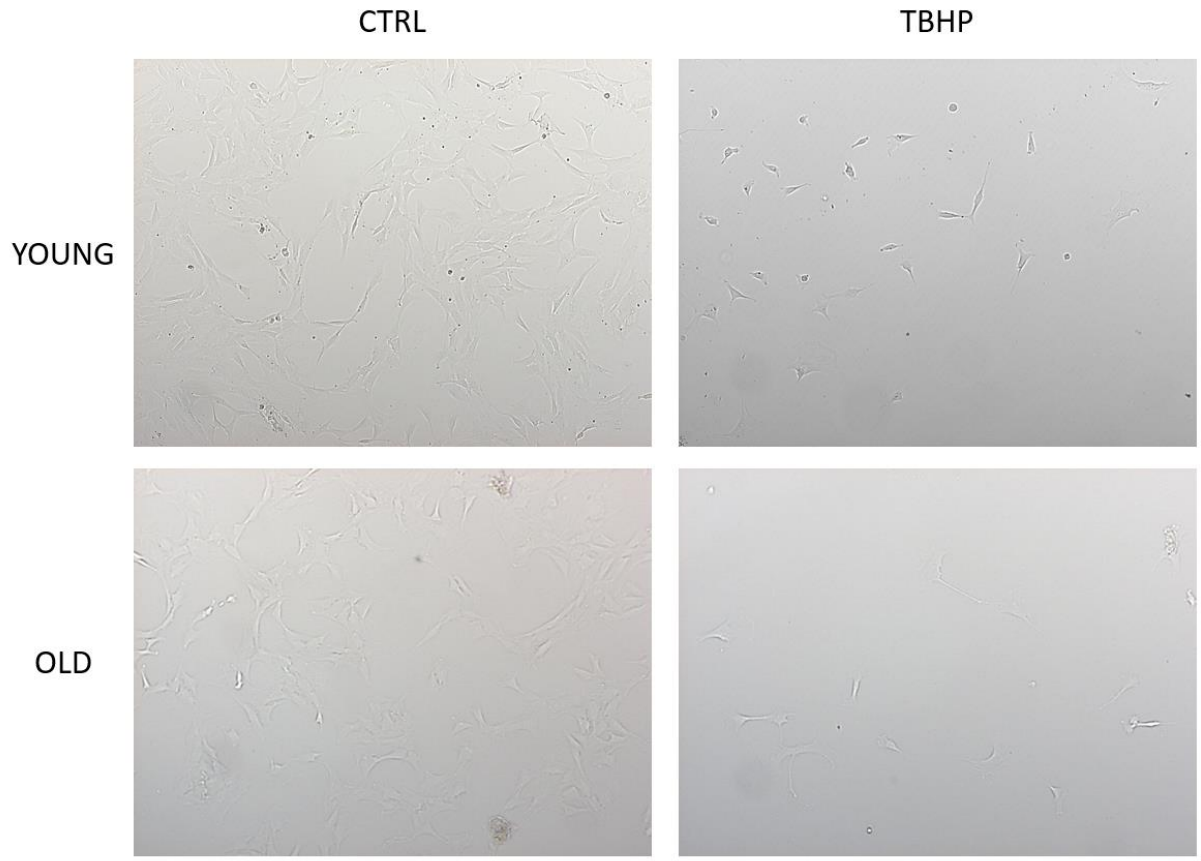

Figure 23 : *Synovial fibroblasts 4 days after stimulation for the condition of oxidative stress (TBHP) with 25µM of TBHP and without stimulation (CTRL). Cells were seeded at 15 000 cells/cm² in 12-well plates. Cells were sub-Confluence for young and old sheep. Cells numbers were in lower after TBHP stimulation especially in older sheep.*

When the cells were stimulated with a concentration of 50µM HU, an average of 9.6% of SA β-gal positive cells were observed after 24 hours of stimulation and 5% after 3 days. With a concentration of 100µM, 17.9% of SA β-gal positive cells were observed after 24h of stimulation and 11.2% after 3 days. Finally, with a concentration of 200µM, 53.2% of SA β-gal gal cells were positive after 24h of stimulation and 48.8% after 3 days (Figure 24).

Stimulation at a concentration of 200µM for 24h induced a slightly more than 50% of SA β-gal positive cells which seems relatively interesting for the "senescence induction" condition. We therefore used this concentration and incubation time for our following experiments.

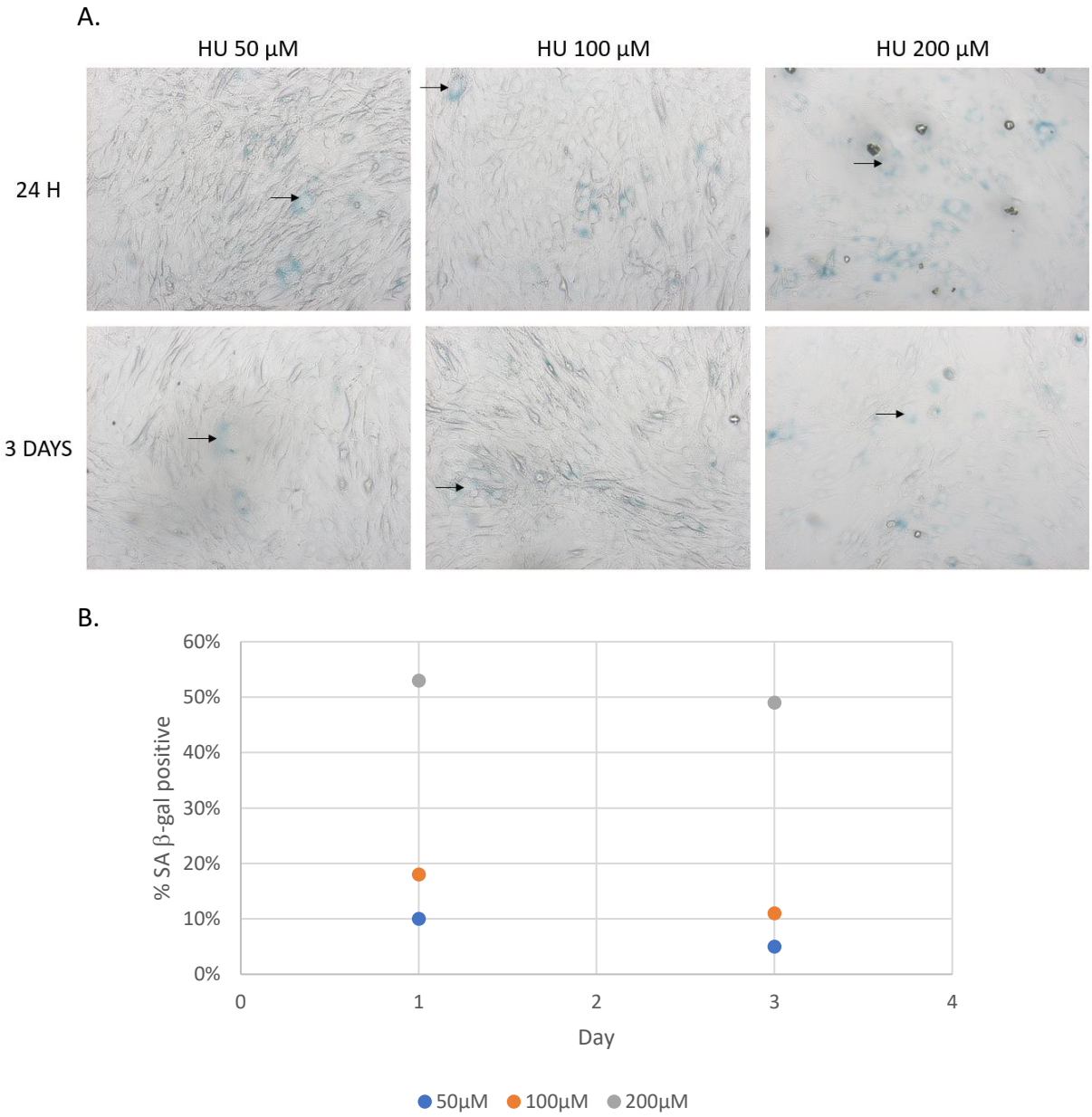

Figure 24 *: (A) SA-βgal staining (in blue) of fibroblast-like synoviocytes stimulated with different concentration of hydroxyurea (HU): 50µM, 100µM and 200µM. Cells were stimulated with hydroxyurea for 24 hours (24 H) or 3 days (3 DAYS). (B)* Percentage of SA-βgal positive cells, determined by counting 300 cells/well, 3 wells per condition.

So, the most appropriate concentrations for our tests were: 25µM TBHP and 200µM HU.

The stimulation time was finally set to 24 hours because no major differences were really noticed between 24 hours and 3 days of stimulation.

Finally, due to the decrease in cells under TBHP conditions, untreated and HU-treated cells were seeded at 15,000 cells/cm² in 12-well plates and TBHP-treated cells were seeded at 20,000 cells/cm².

Cell morphology before and after stimulation was similar between the young adult and the old specimen. Before stimulation, the FLS showed a typical fibroblast morphology that is rather spindle-shaped, flattened, and elongated (Figure 25 C). After stimulation with TBHP or HU, the FLS showed an enlarged and irregular morphology extending over long pseudopodia (Figure 25 A, B).

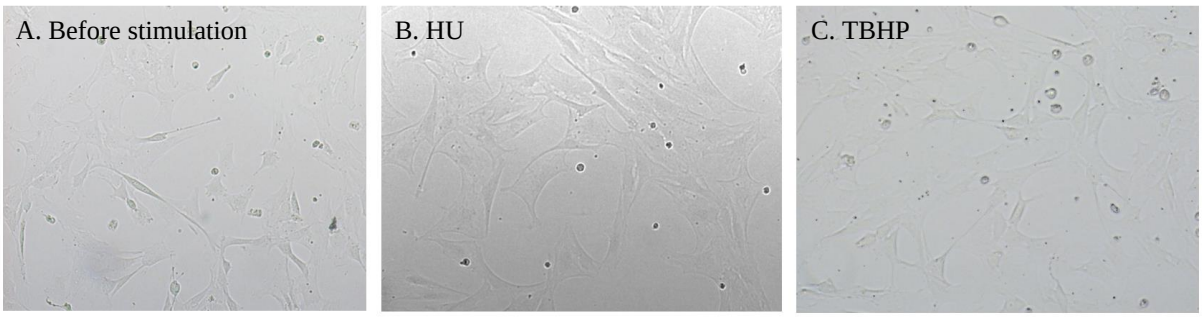

***Figure 25** : Fibroblast-like synoviocytes (A) before stimulation cultured in 12-well plates with DMEM-F12 complete culture medium. Fibroblast-like synoviocytes cultured in 12-well plates and stimulated (B) with culture medium with 1% FCS and 50µM hydroxyurea (HU) during 3days and (C) with culture medium with 25µM tert-butylhydroperoxide (TBHP), 1% foetal calf serum (FCS) for 24hours.*

5. In vitro cadherin-11 expression of fibroblast-like synoviocytes

Immunofluorescence analysis showed the expression of cadherin 11 in FLS derived from synovia from all young (N=3) (Figure 26) and old (N=3) sheep (Figure 27) regardless of the stimulation condition. Cadherin 11 did not accumulate at cell-cell contact.

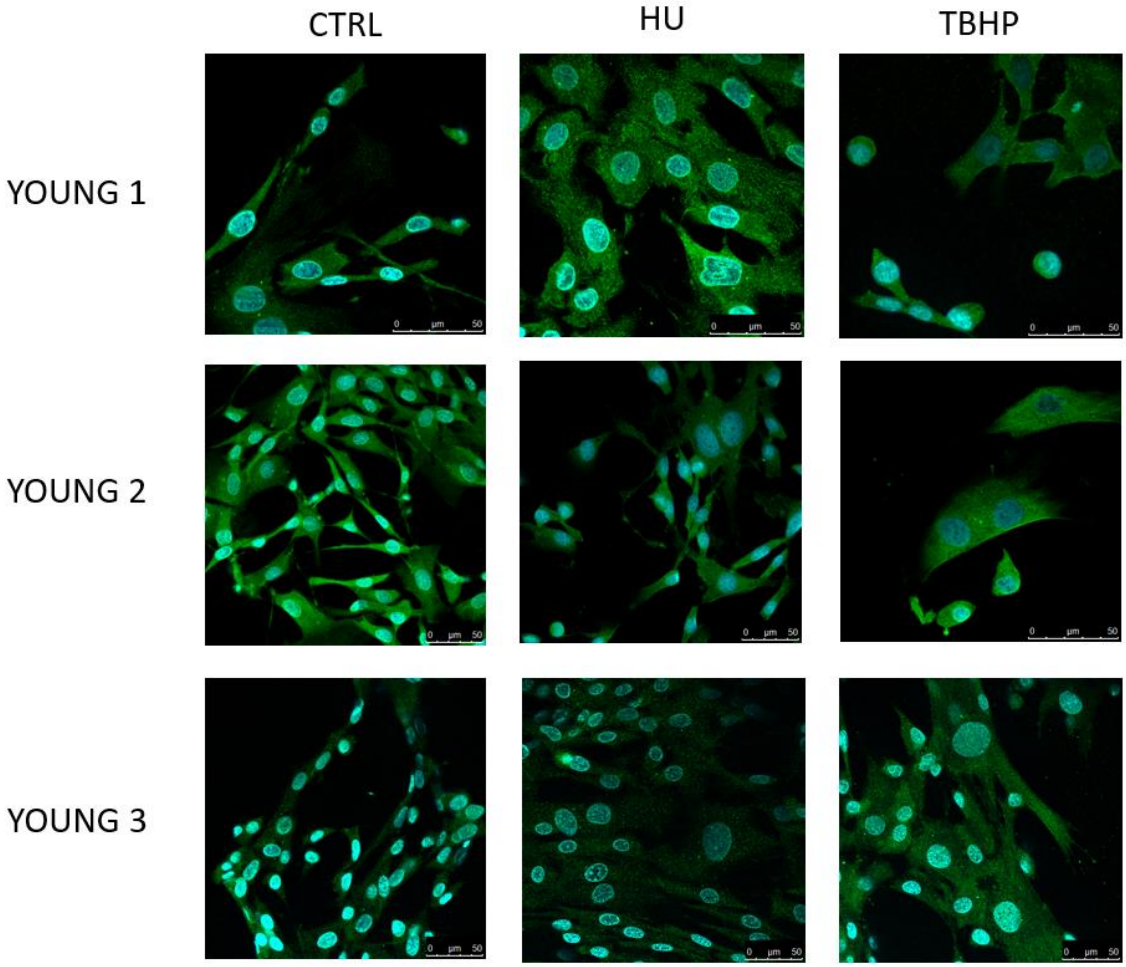

Figure 26 *: Confocal micrographs of cadherin-11 expression for each stimulation condition (CTRL: culture medium, HU: senescence induction condition and TBHP: oxidative stress condition) in 3 young sheep. cadherin-11 is immunostained (green fluorescence) and nuclei are counterstained with DAPI (blue).*

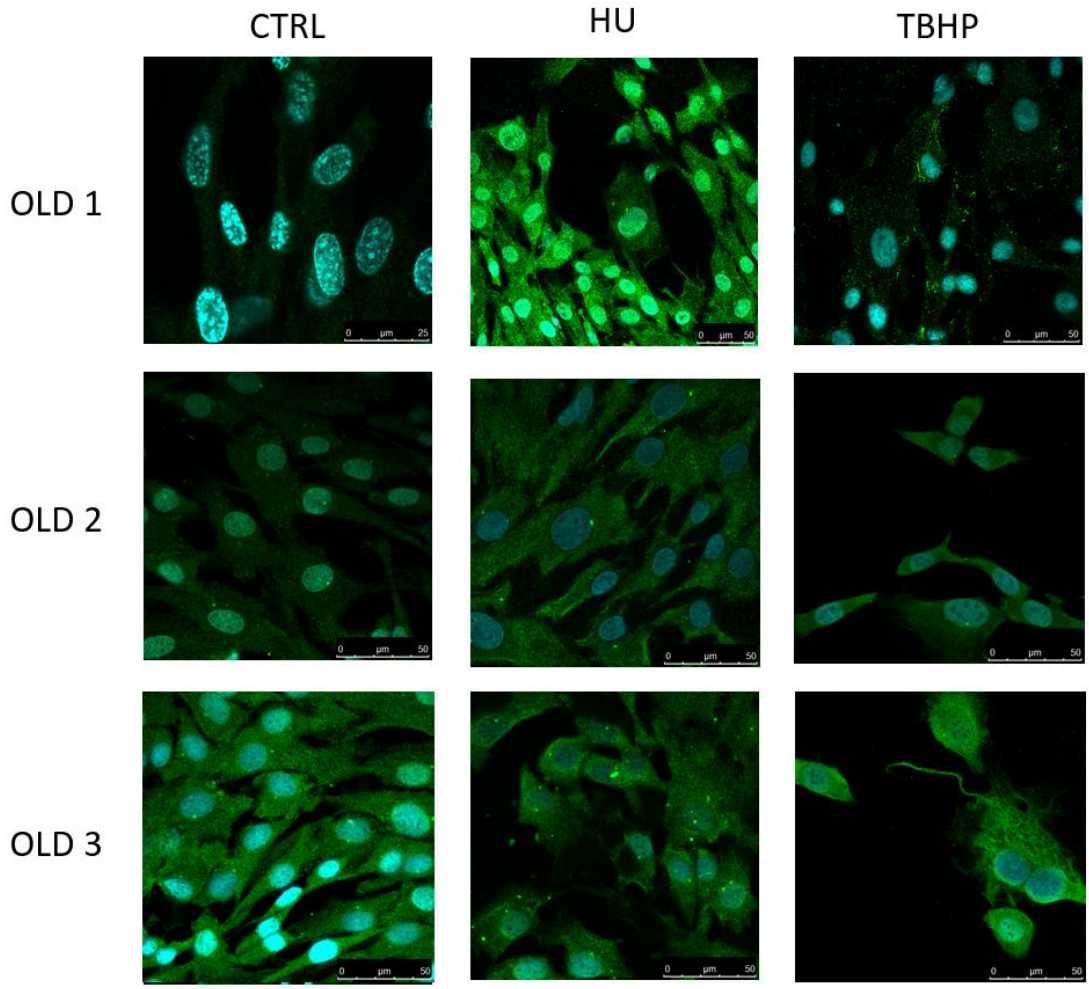

***Figure 27** : Confocal micrographs of cadherin-11 expression representative of 1 replicate for each stimulation condition (CTRL: culture medium, HU: senescence induction condition and TBHP: oxidative stress condition) in 3 old sheep. cadherin-11is immunostained (green fluorescence) and nuclei are counterstained with DAPI (blue).*

6. Nuclei morphology

When the cells were observed by immunofluorescence, we observed the presence of large DAPI-labelled nuclei in the HU and TBHP stimulation conditions. 61% of the cells from young sheep appears to have a larger nucleus in HU condition and 47% in TBHP condition. For the cells from old sheep, 57% have a larger nucleus in HU condition and 30% in TBHP condition (Figure 28). These large nuclei were approximately 1.5 to 2 times larger than the smaller nuclei found in greater proportions in the control conditions without stimulation (Figure 28 A, B, C). The average size of the nuclei is shown in Figure 28 F.

Some nuclei in the HU and TBHP conditions showed protrusion (Figure 28 B : yellow arrow) and others showed focal invagination (Figure 28 C, D : yellow arrow).

Some cells stimulated with TBHP showed a nucleus that appeared to be vacuolated (Figure 28 E: yellow arrow). 4% of the cells from young sheep had nuclei with this morphology and 2.4% of the cells from old sheep had nuclei with this morphology.

In addition, DAPI intensity appears decreased in many nuclei in the HU and TBHP conditions (Figure 26, Figure 27).

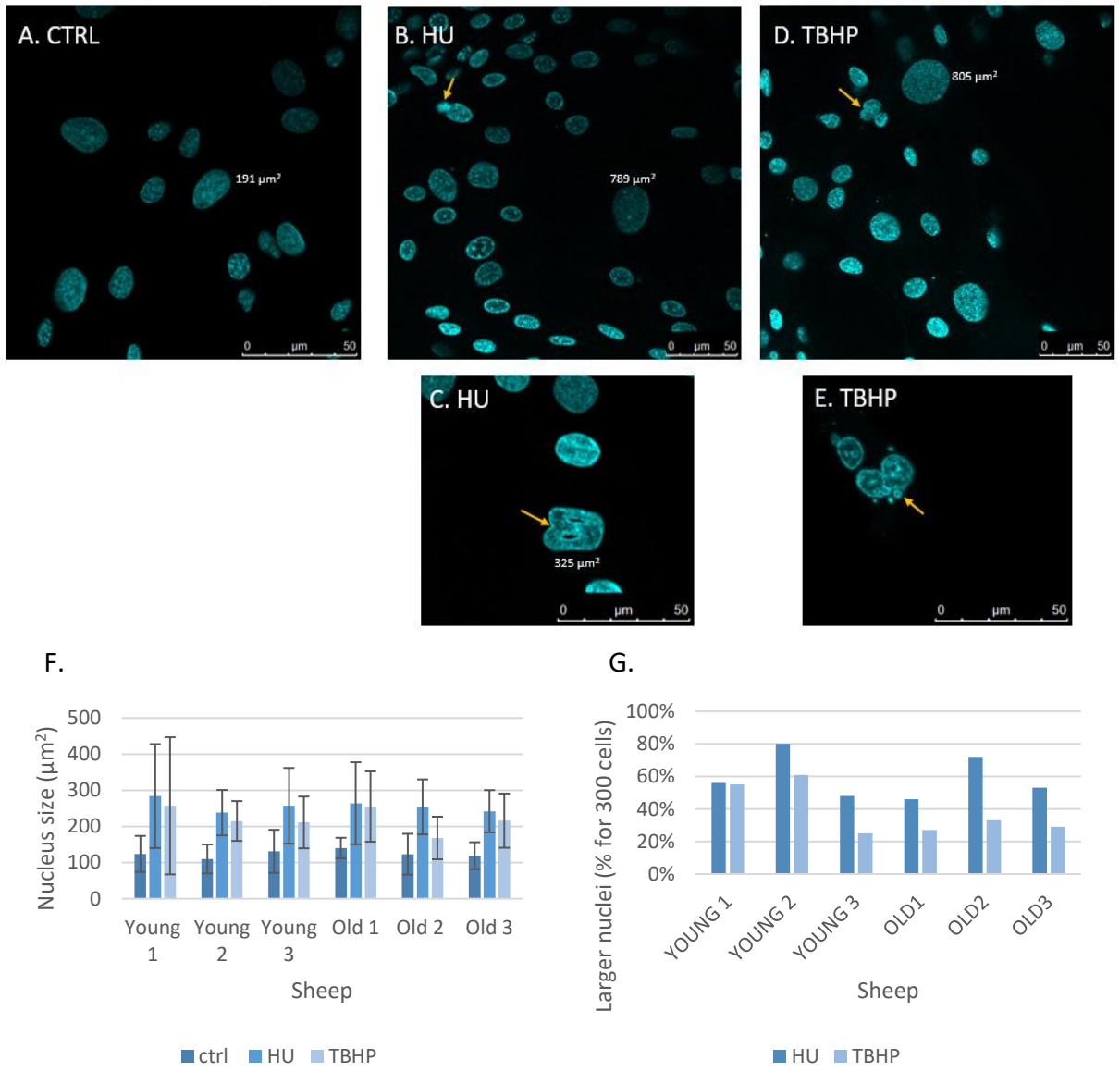

Figure 28 : *Confocal micrographs representative of morphological changes in nucleus for each stimulation condition: (A) CTRL: no stimulation condition, (B, C) HU: senescence induction condition and (D, E) TBHP: oxidative stress condition, observed in 3 young and 3 old sheep. Nuclei are stained with DAPI (in blue). (F) Average nuclear area of FLS collected from 6 sheep in each condition, determined by measuring 100 nuclei/well, 3 wells per condition with ImageJ. (G) Percentage of larger nuclei, determined by counting 100 cells/well, 3 wells per condition. The nuclei defined as larger have an area greater than the mean area of the nuclei in the control condition + tow standard deviation (215 µm2).*

7. Senescence-associated beta-galactosidase

Then, the SA β-gal staining tests were performed on 6 sheep: 3 young adults and 3 old sheep under conditions simulating a normal joint state, simulating an oxidative stress state and under HU senescence induction. Only two sheep: one young and one old were tested tests, under the condition of an inflammatory state of osteoarthritis. The three young sheep had a ratio of positive SA β-gal cells of 0.2% in average in the normal condition, 12,5% in the simulated oxidative stress condition and 40% in the senescence condition. The sheep tested in the simulated inflammatory OA condition presented 12% cells positive for the SA β-gal. For the three old-specimen, their ratio of SA β-gal positive cells in normal condition was in average 2%, 23% in oxidative stress condition and 49% under HU senescence induction. The old sheep tested in simulated inflammatory OA condition presented 2%. Representative FLS images after SAβ-gal staining are shown in Figure 29.

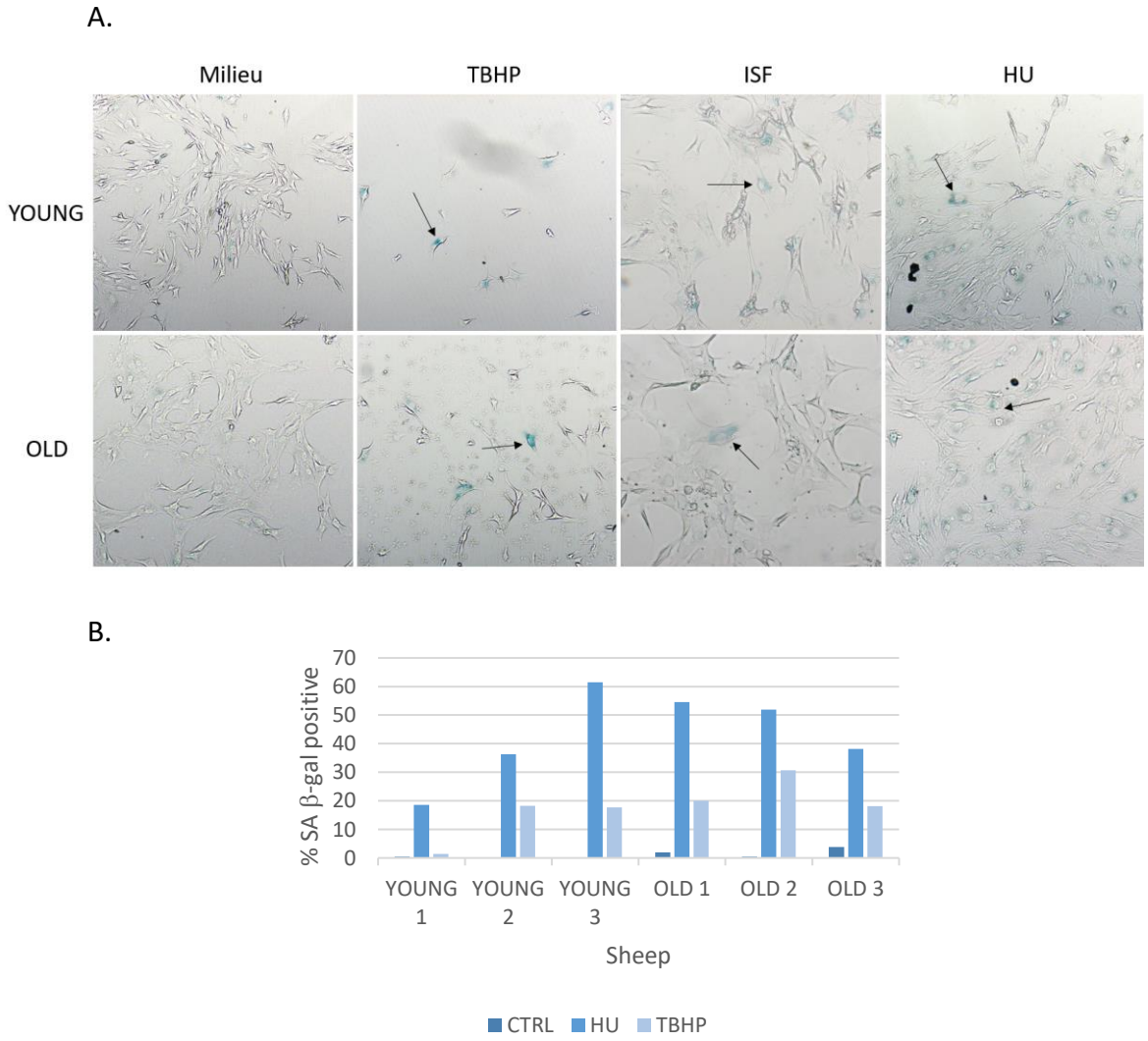

Figure 29 *: (A) SA-βgal staining (in blue) of fibroblast-like synoviocytes from young sheep (YOUNG) and old sheep (OLD) cultured 24 hours in normal condition with DMEM-F12 medium (Milieu), stimulated with culture medium with 25µM tert-butylhydroperoxide (TBHP), stimulated with culture medium with 5% inflammatory synovial fluid for 24 hours (ISF) and stimulated with culture medium with 200µM of hydroxyurea (HU). (B)* Percentage of SA-βgal positive cells, determined by counting 300 cells/well, 3 wells per condition.

Discussion and perspectives

OA is an age-related disease. Age is associated with chronic inflammation (inflammaging) (Rezuș *et al*., 2019). Cellular senescence can be promoted by this chronic oxidative stress or by inflammation. We therefore wanted to see how aging alters joint biology in a preclinical animal model, and more specifically how the synovium and IFP behave in knee osteoarthritis.

Our first objective was to characterise the ageing joint by observing the fat pad and synovium alterations between young and old sheep and comparing them to OA-induced specimens. In the present study, the description of the characteristics of the synovium in ovines, describe only small changes in vascularity and thickness at visual inspection (with alteration of synovium colour) for some old specimens and a normal visual appearance in a majority of young adults. This was not associated with an increase in vascularity at microscopy. Some studies have reported the age-related changes of the synovium in humans or in animal models of musculoskeletal diseases (Fukui *et al*., 1998; Manninen *et al.,* 2002; Pasquali-Ronchetti *et al.,* 1992). As we have observed macroscopically in our sheep study, those reports mentioned that, in humans, there is an increase in the number of blood vessels in the synovial membrane with age, which is associated with an increase in membrane thickness. This is due to an increase in the number of cells and the amount of ECM. In these studies, an increase in inflammatory cell infiltration could also be observed (Fukui *et al.,* 1998; Manninen *et al.,* 2002; Pasquali-Ronchetti *et al.,* 1992).

Interestingly, one of these studies (Pasquali-Ronchetti *et al.,* 1992) found that the increase in vascularisation was more pronounced in the subintima of the synovial membrane. This increased vascularisation may be associated with an inflammatory response, as new blood vessels could allow more immune cells and inflammatory substances to enter the region, thereby contributing to the progression of inflammation and degradation of joint tissue (Walsh and Pearson, 2001) As the sub-intima is the layer of the synovial membrane closest to the surrounding tissue, it may be more exposed to inflammatory factors and growth signals from the surrounding connective tissue. As a result, this region may be more intensely and extensively vascularised than the intima, which lies at the direct interface with the joint cavity (Levick and McDonald, 1995).

Animal studies have also shown similar results. For example, there is a significant increase in synovial vascularisation and inflammatory cell infiltration in the synovium of aged rats compared to younger rats (Nishioka, Inoue and Ueki, 2003). Another study investigating structural changes in the synovium of rabbits and dogs with age found that the synovium of older animals was thicker and more vascularised than that of younger animals. They also found that the synovium of older animals contained more inflammatory cells than that of younger animals. These results suggest that the synovial membrane becomes more inflammatory and less functional with age (Sagİroglu, 2012; Jilani and Ghadially, 1986). Indeed, inflammation can lead to changes in the composition of synovial fluid, making it less effective at protecting and lubricating the joints and leading to deterioration of the synovial tissue itself, which can alter its mechanical properties (Khan and Radin, 2004). In some aged sheep, we were also able to see, microscopically, a focal infiltration of inflammatory cells. These results are potentially important as they suggest that ageing may play a role in structural and inflammatory changes in the synovial membrane. An inflamed synovial membrane could have a negative effect on the joint because, as we know, the release of pro-inflammatory molecules from the synovium can

have an impact on the progression of osteoarthritis, which can lead to the deterioration of the joint tissues, particularly the cartilage, and then to joint problems associated with ageing (Mathiessen and Conaghan, 2017).

On the other hand, some of our results highlight the importance of changes in the synovium following major joint injury in sheep. This proves that the sheep is a relevant study model for understanding the synovial response to joint injury. Indeed, moderate to severe changes in synovium were observed in sheep at 4, 6 and 28 weeks after meniscectomy and cruciate ligament transection. These results are comparable to those obtained in rats after transection of the anterior cruciate ligament, which showed higher synovium scores in rats 30 and 60 days after surgery compared to controls (Barbosa *et al*., 2020). And as for our sheep, the changes and therefore the synovial score were more severe at shorter timepoints (30 days after surgery for rats and 4 weeks after surgery for sheep). In both rats and sheep, this was associated with an increase in the number of inflammatory cells.

The results in sheep suggest that age-related changes in the synovium may be less pronounced than in other species, although slight changes may be observed. Age-related changes are also less marked than those observed in synovium following arthritic joint injury.

Beside synovium, I also investigated the fat pad, which is increasingly being considered as a player in OA (Clockaerts *et al.,* 2010). In 2010, the Osteoarthritis Research Society International published guidelines for assessment of the joint tissues in animal models in OA (Little *et al.,* 2010, McIlwraith *et al.,* 2010). However, due to the absence of interest in the fat pad at this time, no guidelines have been proposed for the IFP evaluation. We therefore adapted the visual and histological scoring scales provided for synovium evaluation. Indeed, the OARSI Sub-intimal fibrosis scale of the synovial membrane only takes into account a heavy focal (<20% of the sample) or heavy diffuse collagenous staining (score 2 or 3), that was not enough to describe the various fibrosis conditions visible in the large fat pad sample collected from sheep. We therefore converted the subjective scoring for interstitial fibrosis into a ratio on the whole section (fat/fibrous tissue ratio) enabling a better description of fibrous tissue occupation of 40, 60 or 80% of the tissue surface.

As with osteoarthritic synovium, changes in the fat pad with age and osteoarthritis were observed at histology. The IFP in almost all young sheep was normal both macroscopically and histologically. In older sheep a slight focal increase in vascularity was observed macroscopically and interstitial fibrosis at histology. Sheep that underwent meniscectomy and cruciate ligament transection showed mild to moderate macroscopic changes in the fat pad

.

As in ovines, fibrosis of the fat pad tissue has previously been shown in humans at histology (Fontanella *et al.,* 2018; Chang *et al.,* 2018) and MRI. The fibroses may be a tissue response to chronic inflammation and present in osteoarthritis patients undergoing total knee replacement. This microarchitectural modification may lead to an alteration of the biomechanical properties of the fat pad, as well as the secretory properties. Indeed, as described above, the fatty tissue is known to have a shock absorption capacity when it is anatomically associated with the skeleton (Zwick *et al.,* 2018), whereas fibrous tissues are less shock absorbing (Gaugler *et al.,* 2015). This change could therefore affect its ability to absorb shock and thus promoting joint damage

(Clements *et al.,* 2009; Favero *et al*., 2017). This is the case in osteoarthritis where the biomechanical properties of the IFP undergo notable changes. These changes then result in a loss of the IFP's ability to respond appropriately to the mechanical loads exerted on the knee joint (Macchi *et al*., 2018). We can then also assume that fibrosis of the fat pad could also lead to an alteration in its ability to ensure friction-free sliding between the tendon and the bone during knee flexion. In the current study, the ovine fat pad showed a slight tendency towards fibrosis of the interstitial tissue with ageing. I hypothesise that this fibrosis could then have decrease the suggested protective properties of the fat pad, thus increasing the risk of osteoarthritis and joint damage in elderly individuals. In addition, it would be relevant to compare the population and activity of MSCs between the fat pads of young and elderly subjects, as well as between the fat pads of healthy subjects and those with osteoarthritis. This assessment could help determine whether fibrosis leads to a significant reduction in MSCs in the fat pad, which could compromise its ability to regenerate and perform protective functions. Studies have already shown that the MSC population in various tissues, including adipose tissue, tends to decline with age. Similarly, in IFP, there may be a decrease in the number of MSCs in older people compared with younger subjects (Stolzing *et al.,* 2008). To characterise more precisely the MSC present in the fat pad, it may be relevant to use a marker specific for perivascular stemness. MSCs tend to be located close to blood vessels in different tissues. One perivascular stemness marker that would be interesting to test on histological sections of IFP is CD146. It is widely used to identify perivascular MSCs in various tissues, including adipose tissue. Its expression on these specific stem cells distinguishes them from other MSC populations present in adipose tissue such as adventitial cells (CD146) (Hindle *et al.,* 2017). By assaying CD146 on IFP histological sections, it would be possible to specifically visualise perivascular MSCs in the tissue. This would then allow us to characterise their spatial distribution, abundance in the context of age and osteoarthritis. The use of antibodies specific for CD146 for experiments involving sheep tissue can present particular challenges. Sheep are not as commonly studied as other laboratory animals such as mice or rats. Consequently, there may be a limited supply of specific antibodies suitable for this species. As no specific antibodies were available to identify ovine PSCs, Hindle et al. determined whether antibodies raised against another species (such as anti-human antibodies) would cross-react with ovine cells. Immunohistochemistry demonstrated that anti-human CD146 antibodies cross-reacted with ovine tissue and that the antigens had a perivascular localization (Hindle et al., 2016).

One of the most striking age-related changes observed in the fat pad of sheep in our study consisted mainly of fibrosis and/or chondroid metaplasia of the adipose tissue. This chondroid metaplasia was also present in PTOA. Several studies in humans and horses have previously demonstrated the presence of areas of cartilage metaplasia in the IFP similar to those observed in our study (Gigis and Gigis, 2012; Kim *et al*, 2022; Fjordbakk and Marques-Smith, 2023). In most cases, this cartilage metaplasia was associated with a case of lipoma (benign tumour of the fat cells of Hoffa's fat pad). The formation of chondroid and bone metaplasia within lipomas is relatively rare. Gigis and Gigis in 2012 pointed out that metaplasia is generally associated with the development of additional functional problems and pain compression syndromes in the patient's knee joint. According to a study by Katzer in 1989, chondroid or bone metaplastic transformations in lipomas could be explained by the relationship of local trauma with a particular reactivity of the mesenchyme, which could be influenced by the close location of the joint capsules. This proximity could lead to a specific disposition of the mesenchyme to produce

a chondroid substance, enabling cartilage maturation. Mechanical stresses, trophic disturbances (e.g. changes in vascularisation within the lipoma, which could influence mesenchyme cell metabolism and affect the supply of nutrients and oxygen to the cells, leading to changes in their behaviour and differentiation), frequent contact with joint components and even as yet unknown factors may represent the causes of metaplastic transformations (Katzer, 1989).

The age-related appearance of metaplasia in the IFP could therefore be associated with additional functional problems and pain syndrome in the knee joint. The appearance of this chondroid metaplasia could then, as Katzer observed in lipoma in 1989, be the result of a combination of factors, in particular mechanical stress (which may result from physical activity or daily joint use), trophic disturbances and frequent contact with neighbouring joint components encouraging the production of chondroid substances and allowing cartilage maturation. These factors could act together to influence the reactivity of the mesenchymal tissue of the fat pad, leading to changes in its behaviour and cellular differentiation. However, further research is needed to better understand the underlying mechanisms of these changes and their impact on overall joint health in sheep and possibly in other species, including humans. On histology, we were also able to highlight that the operated sheep by resection of the cranial part of the medial meniscus and transection of the cranial cruciate ligament showed chondroid metaplasia with a more marked toluidine blue deposition of glycosaminoglycans. This suggested that different degrees of metaplasia characterised by different proteoglycan deposits could exist. This could then allow to assess the degree of metaplasia suggesting that the older sheep had a lower degree of metaplasia than the operated sheep. Documenting fat pad alterations in healthy, ageing and diseased knee joint is essential since it is nowadays considered as a biologically active tissue, within the knee joint and no longer just as a simple filling structure (Clockaerts *et al*., 2010).

Our final aim was to see whether, as in chondrocytes, oxidative stress or inflammation can influence the senescence of fibroblast-type synoviocytes, and to see whether fibroblast-type synoviocytes from young and old sheep responded differently to these stresses. Inflammation is a key process in OA. Inflammation can cause oxidative damage, can promote cellular senescence and plays a role in altering cellular signalling pathways by disrupting the response to growth factors in chondrocytes (Loeser, 2011). It is therefore interesting to see if, as with chondrocytes, the increase in inflammation and oxidative stress can increase the senescence of FLS to see how the synovium of young and old animals reacts to these stresses. *In vitro* investigations of synovial fibroblasts extracted from ovine young adults and old specimens showed a similar cell morphology before stimulation, although the time to reach confluence was longer in old specimen-derived synovial fibroblasts. Basically, this observation was not included in the parameters to be evaluated. It was an observation made during the experiment, which is why no precise measurements were taken. For this, proliferation tests would have to be carried out. To assess the proliferation of synovial cells in this study, we could use a cell proliferation test commonly used in cell research: the MTT (3-[4,5-dimethylthiazol-2-yl]-2,5-diphenyltetrazolium bromide) test (Liu *et al*., 1997). The MTT assay is a colorimetric test that measures cell viability and proliferation according to the capacity of cells to convert MTT salt into an insoluble violet product. To do this, the synoviocytes should be placed in a 96-well cell

culture plate, at an appropriate cell density for each group, and the plates incubated overnight to allow the cells to attach to the surface of the wells. After incubation, the MTT solution can be added to each well. After a few hours the living cells will have converted the MTT to an insoluble purple product. A solvent (e.g. dimethyl sulphoxide, DMSO) can be used to dissolve the crystals formed to produce a coloured solution. The absorbance of the coloured solution can then be measured (Weichert *et al*., 1991). It will then be possible to compare the absorbance between the young and old groups to assess the difference in cell proliferation. However, the results we have observed already allow us to suggest a decrease in growth ability and a deficient proliferation rate for cells extracted from old sheep. This characteristic of cells extracted from aged sheep can then be explained by the fact that the reduced proliferative capacity of cells from aged donors implies cellular senescence in aging. In fact, one of the hallmarks of cellular senescence is an irreversible arrest of cell proliferation and altered cell functions (Mendez *et al*., 1998). With age, cells will show increasing DNA damage and insufficient telomere replication. DNA damage and telomere shortening are signals that regularly lead to a slowdown in cell division and cells eventually enter cellular senescence (Campisi and d'Adda di Fagagna, 2007, Campisi and Yaswen, 2009). This decline in proliferation can be associated to age-related senescence. This stable cell cycle arrest is featured by inhibition of cell cycle regulators such as cyclin-dependent kinases (CDKs) through the action of several tumour suppressors: p53, pRb and p16Ink4a (Brondello *et al*., 2012). Interestingly, even if old specimen-derived synovial fibroblasts showed decrease in growth ability, they still expressed the cadherin-11 (a specific maker for fibroblast-like, not expressed in other fibroblast lineages (Bartok and Firestein, 2010; Valencia *et al*., 2004 ; Kiener and Brenner, 2005) whatever the stimulation condition (control, oxidative stress, or induced senescence).

In the present study, senescence was induced by HU. In other research fields (such as dermatology), stress-induced senescence is achieved by *in vitro* radiation of the (reconstructed) epidermis, with ultraviolet (UV), a natural stressor of the skin, making this *in vitro* stimulus relevant to skin biology (Itahana *et al*.,2004; Todorova and Mandinova, 2020). In the musculoskeletal research field, UV radiations are a less relevant stressors (to induce senescence) than HU which is an inducer of DNA replication stress that can induce a premature senescence-like cellular phenotype by inhibition of ribonucleotide reductase, which causes depletion of the deoxyribonucleotide pool and significantly reduces cell proliferation as well as by the breakage of double-stranded DNA near the replication forks (Bjelica *et al*., 2019).

During our experiments, oxidative stress (TBHP) was associated with loss of cells over time (compared to control or to HU wells). This could be explained by the decreased FLS viability potentially induced by TBHP (Li *et al*., 2022), or by the decrease in growing ability due to oxidative stress-induced senescence (and associated depletion in antioxidant glutathione) (Wedel *et al*., 2020). The death of cells (and their detachment when culture medium renewal) as well as the decrease proliferation could be responsible for the lower number of cells in TBHP wells at the end of the experiments.

Although the number of cells was lower in TBHP condition, both HU and TBHP conditions led to change in cell phenotype (cell enlargement, and irregular morphology). The morphological change during cellular senescence is related to the reorganisation of the actin cytoskeleton (Tsai *et al.*, 2021). The change in shape of the senescent cell is associated with other changes such as

changes in nuclei morphology (Zhang *et al*., 2020) which we also found in our study. Nuclei protrusions visible in our HU and TBHP stimulated FLS could be considered as nuclear blebs, described in senescence process (Freyter *et al.,* 2022; Ivanov *et al.,* 2013; Martins *et al.,* 2020; Filippi-Chiela al., 2012). The abnormal shape of the nuclei of ageing and senescent cells is associated with a loss of laminar integrity at the level of the protrusions (with rare laminar fibres and decrease in density of the laminar mesh). Nuclei architecture could therefore be considered as a biomarker of ageing (Pathak, Soujanya and Mishra, 2021).

Interestingly, observation of nuclei architecture, under TBHP stimulation also revealed condensation and fragmentation, one feature of apoptosis. Although the quantity of cells with this morphology remained very low. TBHP is indeed able to decrease cell viability by inducing apoptosis, which has already been shown in endothelial cells (Jiang *et al.,* 2021; Zhao *et al.,* 2017). The nuclei with senescence morphology were predominant compared to the nuclei with apoptosis morphology. The simultaneous presence of senescent and apoptotic cells has already been described in the case of human umbilical vein endothelial cells (HUVEC) and in chondrocytes stimulated with TBHP (Unterluggauer *et al.,* 2003; Zheng *et al.,* 2018). Some cells could become senescent and undergo cell cycle arrest and a subpopulation of cells entered apoptotic cell death through activation of caspase 3 (Unterluggauer *et al.,* 2003). ROS accumulation can lead to apoptosis and senescence for FLS (isolated from young and old sheep) like the chondrocyte (Zheng *et al.,* 2018).

Cell senescence is a complex process characterised by cellular changes that could be attributed to other mechanisms. Multiple markers are used to confirm cellular senescence, including: identification of cycle cell arrest by the evaluation of the incorporation of EdU or BrdU (Hernandez-Segura, Brandenburg, and Demaria, 2018), the persistence of DNA damage by performing p16-pRB or p53-p21 reporter assays (Matjusaitis *et al*., 2016) and many others markers (Klein *et al*., 2005; Sung *et al*., 2018). Among them, senescence associated beta-galactosidase assay (SA β-gal), a marker of replicative senescence. The activity of SA-βgal, detectable at pH 6.0, allows the identification of senescent cells in cultured and mammalian tissues and is observed in the cytoplasm (Hjelmeland *et al*., 1999).

Our *in vitro* experiments showed that age was associated with a higher proportion of cells with a positive SA β-gal reactivity (tenfold higher proportion) in old sheep-derived synovial fibroblasts compared to young sheep. This has already been demonstrated in chondrocytes. Chondrocytes have shown an age-related decrease in the ability to maintain and repair tissue leading to articular cartilage degeneration include fraying and softening of the articular surface, reduced size and aggregation of proteoglycan aggregates and loss of matrix strength. This is manifested by decreased mitotic and synthetic activity, less responsiveness to anabolic growth factors, and synthesis of smaller, less uniform aggrecans and less functional binding proteins. Recent work has suggested that chondrocyte senescence, marked by the expression of the SA β-gal is the cause of this loss of chondrocyte function (Martin and Buckwalter, 2002). Moreover, FLS derived from aged sheep were on average 2 times more responsive to TBHP oxidative stress stimulation than FLS derived from young sheep. This could be explained by the ability of oxidative stress and inflammation to induce FLS senescence *ex vivo*. Therefore, the positive SA β-gal reactivity of FLS may be a consequence of cellular damage due to oxidative stress, especially in old sheep. Regarding the inflammation, only one young and one

old sheep were used. To confirm these results, it would be necessary to complete our investigation on a larger number of samples.

It should be emphasised that this research in sheep provides an important basis for better understanding of the mechanisms of synovial and IFP ageing, but further studies are needed to continue exploring the effects of age and osteoarthritis on the cellular and molecular composition of synovium and adipose tissue in sheep. Carry out more in-depth analyses of inflammatory profiles, senescence markers and specific cell components in these tissues. In addition, extend the study by examining variations in MSC populations in adipose tissue in young and old sheep, as well as in sheep with osteoarthritis, using specific markers such as CD146. This could provide valuable insights into the mechanisms of alterations and the regenerative potential of the tissue. It would also be interesting to understand, in particular, the molecular mechanisms underlying fibrosis and chondroid metaplasia in IFP and its link with ageing and osteoarthritis by studying, for example, gene profiling using gene expression analysis techniques, or by studying specific growth factors and cytokines in IFP from young and old sheep, as well as from those with induced osteoarthritis. It may also be interesting to study the potential impact of these alterations on the development of new diagnostic and treatment strategies for age-related joint pathologies. However, the current findings may contribute to our overall understanding of age-associated changes in joints and their potential implications in age-related joint pathologies, although this study has certain limitations. The main limitation is the number of replicates. Indeed, a few numbers of sheep were included in this study (7 young, 7 old), leading to a limited number of histological samples, and of *in vitro* characteristics of synovial fibroblasts derived from these sheep. This preliminary assessment of age-related changes in the synovium would benefit from an increase in the number of included specimens to increase the power of the analysis. Based on the differences observed for the number of animals that developed fibrosis in the old vs. the number of animals that developed fibrosis in the young, 66 sheep (33 young and 33 old) would be required to validate the difference between the groups (calculation based on G*Power, with alpha error: 0.05; beta error: 0.95, mean score difference = 1/effect size = 1).

The present study only characterised the changes in the fat pad in the joint but did not test its role and the impact of its absence on the biology of the knee joint. Indeed, in clinical context, the removal of the fat pad, in human knee OA is still controversial (Zeng *et al*., 2020; Han, *et al*. 2014; Jiang *et al*., 2019; Ragab and Serag, 2021; Zhou *et al*., 2022). As the ovine fat pad shows similar changes to humans. Further *in vivo* investigations in sheep could help to understand whether fat pad is essential to joint biology, whether it should be preserved when performing arthroscopies or cruciate ligament repair, or if it should be removed.

Finally, as described above, it is important to perform other senescence markers to confirm our results. For example, the cycle cell arrest could be interesting to confirm cell cycle arrest for the TBHP condition and analysing the expression of lamin B1 (LMNB1) of the nuclear envelope (by immunofluorescence, for example) would help to know if the changes in nuclei morphology are due to senescence. Indeed, down-regulation of LMNB1 occurs in senescent cells and is associated with decreased integrity of the nuclear envelope (Di Micco *et al*., 2021).

Conclusion

Ageing, one of the major risk factors for AO, is associated with slight changes in tissues such as the synovial membrane and the fat pad. Some of the changes observed during ageing, such as fibrosis or metaplasia, may also occur in the joints after induction of OA. This raises questions about the real clinical impact of age-related fat pad alteration on joint health, before (clinical signs of) OA occurs. These changes (fibrosis, hypervascularisation, cartilaginous metaplasia) could have an impact on the pathogenesis and progression of OA, as well as on the effect of therapeutic strategies, and alter the biomechanics and the secretory properties of the fat pad.

Bibliography

Almeida, H.V. *et al.* (2016) 'Fibrin hydrogels functionalized with cartilage extracellular matrix and incorporating freshly isolated stromal cells as an injectable for cartilage regeneration', *Acta Biomaterialia*, 36, pp. 55–62. Available at: https://doi.org/10.1016/j.actbio.2016.03.008.

Altman, R. *et al.* (2015) 'Hyaluronic Acid Injections Are Associated with Delay of Total Knee Replacement Surgery in Patients with Knee Osteoarthritis: Evidence from a Large U.S. Health Claims Database', *PLOS ONE*, 10(12), p. e0145776. Available at: https://doi.org/10.1371/journal.pone.0145776.

Andrianakos, A.A. *et al.* (2006) 'Prevalence of symptomatic knee, hand, and hip osteoarthritis in Greece. The ESORDIG study', *The Journal of Rheumatology*, 33(12), pp. 2507–2513.

Ansari, M.Y., Ahmad, N. and Haqqi, T.M. (2020) 'Oxidative stress and inflammation in osteoarthritis pathogenesis: Role of polyphenols', Biomedicine & Pharmacotherapy, 129, p. 110452.

Arden, N. and Nevitt, M.C. (2006) 'Osteoarthritis: Epidemiology', *Best Practice & Research* Clinical Rheumatology, 20(1), pp. 3–25. Available at: https://doi.org/10.1016/j.berh.2005.09.007.

Arrigoni, C., D'Arrigo, D., Rossella, V., Candrian, C., Albertini, V., and Moretti, M. (2020). Umbilical Cord MSCs and Their Secretome in the Therapy of Arthritic Diseases: A Research and Industrial Perspective. Cells 9, 1343.

Aupperle, K.R. *et al.* (1999) 'NF-κB Regulation by IκB Kinase in Primary Fibroblast-Like Synoviocytes1', *The Journal of Immunology*, 163(1), pp. 427–433. Available at: https://doi.org/10.4049/jimmunol.163.1.427.

Bakhsh, W., and Nicandri, G. (2018). Anatomy and Physical Examination of the Shoulder. Sports Medicine and Arthroscopy Review 26, e10–e22.

Barbosa, G.M. *et al.* (2020) 'Thirty days after anterior cruciate ligament transection is sufficient to induce signs of knee osteoarthritis in rats: pain, functional impairment, and synovial inflammation', *Inflammation Research*, 69(3), pp. 279–288. Available at: https://doi.org/10.1007/s00011-020-01317-1.

Barboza, E., Hudson, J., Chang, W. P., Kovats, S., Towner, R. A., Silasi-Mansat, R., ... & Griffin, T. M. (2017). Profibrotic infrapatellar fat pad remodeling without m1 macrophage polarization precedes knee osteoarthritis in mice with diet-induced obesity. Arthritis & Rheumatology, 69(6), 1221-1232.

Bartok, B., and Firestein, G.S. (2010). Fibroblast-like synoviocytes: key effector cells in rheumatoid arthritis. Immunological Reviews 233, 233–255.

Berenbaum, F. (2013) 'Osteoarthritis as an inflammatory disease (osteoarthritis is not osteoarthrosis!)', Osteoarthritis and Cartilage, 21(1), pp. 16–21.

Berthiaume, M.-J. *et al.* (2005) 'Meniscal tear and extrusion are strongly associated with progression of symptomatic knee osteoarthritis as assessed by quantitative magnetic resonance imaging', *Annals of the Rheumatic Diseases*, 64(4), pp. 556–563. Available at: https://doi.org/10.1136/ard.2004.023796.

Bertoni, L. *et al.* (2009) 'Leptin increases growth of primary ossification centers in fetal mice', *Journal of Anatomy*, 215(5), pp. 577–583. Available at: https://doi.org/10.1111/j.1469-7580.2009.01134.x.

Bhattaram, P., and Chandrasekharan, U. (2017). The joint synovium: A critical determinant of articular cartilage fate in inflammatory joint diseases. Seminars in Cell & Developmental Biology 62, 86–93.

Bjelica, S. et al. (2019) 'Hydroxyurea-induced senescent peripheral blood mesenchymal stromal cells inhibit bystander cell proliferation of JAK2V617F-positive human erythroleukemia cells', The FEBS Journal, 286(18), pp. 3647–3663.

Bland, S.D. (2015) 'Canine osteoarthritis and treatments: a review', *Veterinary Science Development*, 5(2). Available at: https://doi.org/10.4081/vsd.2015.5931.

Brandt, K.D., Dieppe, P., and Radin, E.L. (2008). Etiopathogenesis of Osteoarthritis. Rheumatic Disease Clinics of North America 34, 531–559.

Brondello, J.-M., Prieur, A., Philipot, D., Lemaitre, J.-M., Lenaers, G., Piette, J., and Dulić, V. (2012). La sénescence cellulaire - Un nouveau mythe de Janus ? Med Sci (Paris) 28, 288–296.

Campisi, J., and d'Adda di Fagagna, F. (2007). Cellular senescence: when bad things happen to good cells. Nat Rev Mol Cell Biol 8, 729–740.

Campisi, J., and Yaswen, P. (2009). Aging and cancer cell biology, 2009. Aging Cell 8, 221–225.

Chang, J. *et al.* (2018) 'Systemic and local adipose tissue in knee osteoarthritis', *Osteoarthritis and Cartilage*, 26(7), pp. 864–871. Available at: https://doi.org/10.1016/j.joca.2018.03.004.

Chang, S.H. *et al.* (2019) 'Excessive mechanical loading promotes osteoarthritis through the gremlin-1–NF-κB pathway', *Nature Communications*, 10, p. 1442. Available at: https://doi.org/10.1038/s41467-019-09491-5.

Chen, L. *et al.* (2020) 'Pathogenesis and clinical management of obesity-related knee osteoarthritis: Impact of mechanical loading', *Journal of Orthopaedic Translation*, 24, pp. 66–75. Available at: https://doi.org/10.1016/j.jot.2020.05.001.

Chen, Y.-H. *et al.* (2019) 'Senescence in osteoarthritis', *Osteoarthritis and Cartilage*, 27, p. S94. Available at: https://doi.org/10.1016/j.joca.2019.02.135.

Chevalier, X. (2004) 'Les mécanismes du vieillissement normal et pathologique de l'articulation', Revue du Rhumatisme, 71(6), pp. 455–461. Available at: https://doi.org/10.1016/j.rhum.2003.07.011.

Choi, K. *et al.* (1990) 'The elastic moduli of human subchondral, trabecular, and cortical bone tissue and the size-dependency of cortical bone modulus', *Journal of Biomechanics*, 23(11), pp. 1103–1113. Available at: https://doi.org/10.1016/0021-9290(90)90003-L.

Clements, K.M., Ball, A.D., Jones, H.B., Brinckmann, S., Read, S.J., and Murray, F. (2009). Cellular and histopathological changes in the infrapatellar fat pad in the monoiodoacetate model of osteoarthritis pain. Osteoarthritis and Cartilage 17, 805–812.

Clockaerts, S. *et al.* (2018) 'The anterior tibiotalar fat pad as a source of pain and inflammation in osteoarthritis of the ankle: anatomy, histology and imaging', *Osteoarthritis and Cartilage*, 26, p. S120. Available at: https://doi.org/10.1016/j.joca.2018.02.262.

Clockaerts, S., Bastiaansen-Jenniskens, Y.M., Runhaar, J., Van Osch, G.J.V.M., Van Offel, J.F., Verhaar, J.A.N., De Clerck, L.S., and Somville, J. (2010). The infrapatellar fat pad should be considered as an active osteoarthritic joint tissue: a narrative review. Osteoarthritis and Cartilage 18, 876–882.

Cope, P.J., Ourradi, K., Li, Y., and Sharif, M. (2019). Models of osteoarthritis: the good, the bad and the promising. Osteoarthritis and Cartilage 27, 230–239.

da Silva Meirelles, L., Sand, T. T., Harman, R. J., Lennon, D. P., & Caplan, A. I. (2009). MSC frequency correlates with blood vessel density in equine adipose tissue. *Tissue Engineering Part A*, *15*(2), 221-229.

Davies, D.V. and White, J.E.W. (1961) 'The structure and weight of synovial fat pads', *Journal of Anatomy*, 95(Pt 1), pp. 30–37.

Deveza, L.A. and Loeser, R.F. (2018) 'Is osteoarthritis one disease or a collection of many?', *Rheumatology (Oxford, England)*, 57(suppl_4), pp. iv34–iv42. Available at: https://doi.org/10.1093/rheumatology/kex417.

Di Micco, R., Krizhanovsky, V., Baker, D., & d'Adda di Fagagna, F. (2021). Cellular senescence in ageing: from mechanisms to therapeutic opportunities. Nat Rev Mol Cell Biol, 22(2), 75-95.

Ding, D. C., Wu, K. C., Chou, H. L., Hung, W. T., Liu, H. W., & Chu, T. Y. (2015). Human infrapatellar fat pad-derived stromal cells have more potent differentiation capacity than other mesenchymal cells and can be enhanced by hyaluronan. *Cell Transplantation*, *24*(7), 1221-1232.

Distel, E., Cadoudal, T., Durant, S., Poignard, A., Chevalier, X., and Benelli, C. (2009). The infrapatellar fat pad in knee osteoarthritis: An important source of interleukin-6 and its soluble receptor. Arthritis & Rheumatism 60, 3374–3377.

do Amaral, R.J.F.C. *et al.* (2017) 'Infrapatellar Fat Pad Stem Cells: From Developmental Biology to Cell Therapy', *Stem Cells International*, 2017, p. e6843727. Available at: https://doi.org/10.1155/2017/6843727.

Donell, S. (2019) 'Subchondral bone remodelling in osteoarthritis', *EFORT Open Reviews*, 4(6), pp. 221–229. Available at: https://doi.org/10.1302/2058-5241.4.180102.

Draghi, F. *et al.* (2016) 'Hoffa's fat pad abnormalities, knee pain and magnetic resonance imaging in daily practice', *Insights into Imaging*, 7(3), pp. 373–383. Available at: https://doi.org/10.1007/s13244-016-0483-8.

Edwards, J. C. (1995). Synovial intimal fibroblasts. *Annals of the rheumatic diseases*, *54*(5), 395.

Emmi, A. *et al.* (2022) 'Infrapatellar Fat Pad-Synovial Membrane Anatomo-Fuctional Unit: Microscopic Basis for Piezo1/2 Mechanosensors Involvement in Osteoarthritis Pain', *Frontiers in Cell and Developmental Biology*, 10, p. 886604. Available at: https://doi.org/10.3389/fcell.2022.886604.

Englund, M., Guermazi, A. and Lohmander, S.L. (2009) 'The role of the meniscus in knee osteoarthritis: a cause or consequence?', *Radiologic Clinics of North America*, 47(4), pp. 703–712. Available at: https://doi.org/10.1016/j.rcl.2009.03.003.

Eymard, F. *et al.* (2014) 'Induction of an Inflammatory and Prodegradative Phenotype in Autologous Fibroblast-like Synoviocytes by the Infrapatellar Fat Pad From Patients With Knee Osteoarthritis', *Arthritis & Rheumatology*, 66(8), pp. 2165–2174. Available at: https://doi.org/10.1002/art.38657.

Fallahi, F., Jafari, H., Jefferson, G., Jennings, P., and Read, R. (2013). Explorative study of the sensitivity and specificity of the pronator quadratus fat pad sign as a predictor of subtle wrist fractures. Skeletal Radiol 42, 249–253.

Favero, M., El-Hadi, H., Belluzzi, E., Granzotto, M., Porzionato, A., Sarasin, G., ... & Macchi, V. (2017). Infrapatellar fat pad features in osteoarthritis: a histopathological and molecular study. *Rheumatology*, *56*(10), 1784-1793.

Fellows, C.R. *et al.* (2016) 'Adipose, Bone Marrow and Synovial Joint-Derived Mesenchymal Stem Cells for Cartilage Repair', *Frontiers in Genetics*, 7. Available at: https://www.frontiersin.org/articles/10.3389/fgene.2016.00213 (Accessed: 20 July 2023).

Filippi-Chiela, E.C. *et al.* (2012) 'Nuclear Morphometric Analysis (NMA): Screening of Senescence, Apoptosis and Nuclear Irregularities', PLoS ONE, 7(8), p. e42522.

Findlay, D.M. and Atkins, G.J. (2014) 'Osteoblast-Chondrocyte Interactions in Osteoarthritis', Current Osteoporosis Reports, 12(1), pp. 127–134.

Fjordbakk, C.T. and Marques-Smith, P. (2023) 'The equine patellar ligaments and the infrapatellar fat pad – a microanatomical study', *BMC Veterinary Research*, 19(1), p. 20. Available at: https://doi.org/10.1186/s12917-023-03579-3.

Fontanella, C.G. *et al.* (2017) 'Investigation of biomechanical response of Hoffa's fat pad and comparative characterization', *Journal of the Mechanical Behavior of Biomedical Materials*, 67, pp. 1–9. Available at: https://doi.org/10.1016/j.jmbbm.2016.11.024.

Fontanella, C.G. *et al.* (2018) 'Biomechanical behavior of Hoffa's fat pad in healthy and osteoarthritic conditions: histological and mechanical investigations', *Australasian Physical & Engineering Sciences in Medicine*, 41(3), pp. 657–667. Available at: https://doi.org/10.1007/s13246-018-0661-8.

Fox, A.J.S., Bedi, A. and Rodeo, S.A. (2012) 'The Basic Science of Human Knee Menisci', *Sports Health*, 4(4), pp. 340–351. Available at: https://doi.org/10.1177/1941738111429419.

Francis, S.L., Yao, A., and Choong, P.F.M. (2020). Culture Time Needed to Scale up Infrapatellar Fat Pad Derived Stem Cells for Cartilage Regeneration: A Systematic Review. Bioengineering (Basel) 7, E69.

Freitag, J. *et al.* (2016) 'Mesenchymal stem cell therapy in the treatment of osteoarthritis: reparative pathways, safety and efficacy – a review', *BMC Musculoskeletal Disorders*, 17(1), p. 230. Available at: https://doi.org/10.1186/s12891-016-1085-9.

Freyter, B.M. *et al.* (2022) 'Nuclear Fragility in Radiation-Induced Senescence: Blebs and Tubes Visualized by 3D Electron Microscopy', *Cells*, 11(2), p. 273. Available at: https://doi.org/10.3390/cells11020273.

Fukui, T., Higashihara, M., Nakano, H., & Takeuchi, Y. (1998). Age-related changes in the vascular endothelial growth factor and its receptors in the synovial membrane of the knee joint. Arthritis and Rheumatism, 41(11), 2081-2088.

Fuller, M.C., Hayashi, K., Bruecker, K.A., Holsworth, I.G., Sutton, J.S., Kass, P.H., Kantrowitz, B.J., and Kapatkin, A.S. (2014). Evaluation of the radiographic infrapatellar fat pad sign of the contralateral stifle joint as a risk factor for subsequent contralateral cranial cruciate ligament rupture in dogs with unilateral rupture: 96 cases (2006–2007). Journal of the American Veterinary Medical Association 244, 328–338.

Gahier, M. *et al.* (2020) 'Thrombose veineuse anévrysmale au sein du tissu de Hoffa : à propos d'un cas clinique. Une cause inattendue de gonalgie aiguë', *Journal de Traumatologie du Sport*, 37(2), pp. 100–104. Available at: https://doi.org/10.1016/j.jts.2020.04.001.

Gaugler, M. *et al.* (2015) 'Fibrous cartilage of human menisci is less shock-absorbing and energy-dissipating than hyaline cartilage', *Knee Surgery, Sports Traumatology, Arthroscopy*, 23(4), pp. 1141–1146. Available at: https://doi.org/10.1007/s00167-014-2926-4.

Gesta, S., Tseng, Y. H., & Kahn, C. R. (2007). Developmental origin of fat: tracking obesity to its source. *Cell*, *131*(2), 242-256.

Gigis, I. and Gigis, P. (2012) 'Fibrolipoma with Osseous and Cartilaginous Metaplasia of Hoffa's Fat Pad: A Case Report', *Case Reports in Orthopedics*, 2012, p. e547963. Available at: https://doi.org/10.1155/2012/547963.

Gilbert, S. F. (2010). *Developmental biology*. sinauer associates, Inc.

Goldring, M. J., Jones, A. J., & Hunter, D. J. (2005). Aging of articular chondrocytes: a review of molecular and cellular changes. Osteoarthritis and cartilage, 13(11), 1093-1106.

Goldring, M.B. (2012) 'Articular Cartilage Degradation in Osteoarthritis', *HSS Journal*, 8(1), pp. 7–9. Available at: https://doi.org/10.1007/s11420-011-9250-z.

Goldring, M.B., and Otero, M. (2011). Inflammation in osteoarthritis. Curr Opin Rheumatol 23, 471–478.

Goldstein, S., Littlefield, J.W. and Soeldner, J.S. (1969) 'Diabetes mellitus and aging: diminished plating efficiency of cultured human fibroblasts*', *Proceedings of the National Academy of Sciences*, 64(1), pp. 155–160. Available at: https://doi.org/10.1073/pnas.64.1.155.

Goodheart, C.R. *et al.* (1973) 'Plating Efficiency for Primary Hamster Embryo Cells as an Index of Efficacy of Fetal Bovine Serum for Cell Culture', *Applied Microbiology*, 26(4), pp. 525–528.

Greif, D.N. et al. (2020) 'Infrapatellar Fat Pad/Synovium Complex in Early-Stage Knee Osteoarthritis: Potential New Target and Source of Therapeutic Mesenchymal Stem/Stromal Cells', Frontiers in Bioengineering and Biotechnology, 8.

Greis, P.E. *et al.* (2002) 'Meniscal Injury: I. Basic Science and Evaluation', *JAAOS - Journal of the American Academy of Orthopaedic Surgeons*, 10(3), p. 168.

Griffin, T.M. and Guilak, F. (2005) 'The Role of Mechanical Loading in the Onset and Progression of Osteoarthritis', *Exercise and Sport Sciences Reviews*, 33(4), pp. 195–200.

Hameister, R. *et al.* (2020) 'Reactive oxygen/nitrogen species (ROS/RNS) and oxidative stress in arthroplasty', *Journal of Biomedical Materials Research Part B: Applied Biomaterials*, 108(5), pp. 2073–2087.

Han, W. *et al.* (2014) 'Infrapatellar fat pad in the knee: is local fat good or bad for knee osteoarthritis?', *Arthritis Research & Therapy*, 16(4), p. R145. Available at: https://doi.org/10.1186/ar4607.

Hawker, G. A. (2019). Osteoarthritis is a serious disease. *Clin Exp Rheumatol*, *37*(Suppl 120), 3-6.

Haywood, L. and Walsh, D.A. (2001) 'Vasculature of the normal and arthritic synovial joint', *Histology and Histopathology*, 16(1), pp. 277–284.

Hernandez-Segura, A., Brandenburg, S. and Demaria, M. (2018) 'Induction and Validation of Cellular Senescence in Primary Human Cells', *Journal of Visualized Experiments : JoVE*, (136), p. 57782.

Hindle, P. *et al.* (2016) 'Perivascular Mesenchymal Stem Cells in Sheep: Characterization and Autologous Transplantation in a Model of Articular Cartilage Repair', *Stem Cells and Development*, 25(21), pp. 1659–1669. Available at: https://doi.org/10.1089/scd.2016.0165.

Hindle, P., Khan, N., Biant, L., & Péault, B. (2017). The infrapatellar fat pad as a source of perivascular stem cells with increased chondrogenic potential for regenerative medicine. *Stem Cells Translational Medicine*, *6*(1), 77-87.

Hjelmeland, L. M., Cristofolo, V. J., Funk, W., Rakoczy, E., & Katz, M. L. (1999). Senescence of the retinal pigment epithelium. Mol Vis, 5(1), 33-37.

Hoegaerts, M., Nicaise, M., van BREE, H., and Saunders, J.H. (2005). Cross-sectional anatomy and comparative ultrasonography of the equine medial femorotibial joint and its related structures. Equine Veterinary Journal 37, 520–529.

Hügle, T. *et al.* (2012) 'Aging and Osteoarthritis: An Inevitable Encounter?', *Journal of Aging Research*, 2012, p. e950192. Available at: https://doi.org/10.1155/2012/950192.

Ioan-Facsinay, A., and Kloppenburg, M. (2013). An emerging player in knee osteoarthritis: the infrapatellar fat pad. Arthritis Research & Therapy 15, 225.

Ioan-Facsinay, A., Kwekkeboom, J. C., Westhoff, S., Giera, M., Rombouts, Y., van Harmelen, V., ... & Toes, R. E. (2013). Adipocyte-derived lipids modulate CD4+ T-cell function. *European journal of immunology*, *43*(6), 1578-1587.

Itahana, K., Campisi, J., and Dimri, G.P. (2004). Mechanisms of cellular senescence in human and mouse cells. Biogerontology 5, 1–10.

Ivanov, A. *et al.* (2013) 'Lysosome-mediated processing of chromatin in senescence', *The Journal of cell biology*, 202. Available at: https://doi.org/10.1083/jcb.201212110.

Jarraya, M. *et al.* (2018) 'MRI Findings Consistent with Peripatellar Fat Pad Impingement: How Much Related to Patellofemoral Maltracking?', *Magnetic Resonance in Medical Sciences*, 17(3), pp. 195–202. Available at: https://doi.org/10.2463/mrms.rev.2017-0063.

Jeyaraman, M. *et al.* (2022) 'Synovium Derived Mesenchymal Stromal Cells (Sy-MSCs): A Promising Therapeutic Paradigm in the Management of Knee Osteoarthritis', *Indian Journal of Orthopaedics*, 56(1), pp. 1–15. Available at: https://doi.org/10.1007/s43465-021-00439-w.

Jiang, J. *et al.* (2021) 'Paeoniflorin Suppresses TBHP-Induced Oxidative Stress and Apoptosis in Human Umbilical Vein Endothelial Cells via the Nrf2/HO-1 Signaling Pathway and Improves Skin Flap Survival', *Frontiers in Pharmacology*, 12. Available at: https://www.frontiersin.org/articles/10.3389/fphar.2021.735530 (Accessed: 15 December 2022).

Jiang, L.-F., Fang, J.-H., and Wu, L.-D. (2019). Role of infrapatellar fat pad in pathological process of knee osteoarthritis: Future applications in treatment. World J Clin Cases 7, 2134–2142.

Jilani, M., and Ghadially, F.N. (1986). An ultrastructural study of age-associated changes in the rabbit synovial membrane. J Anat 146, 201–215.

Johnson, V.L., Giuffre, B.M., and Hunter, D.J. (2012). Osteoarthritis: What Does Imaging Tell Us about Its Etiology? Semin Musculoskelet Radiol 16, 410–418.

Johnston, S.A. (1997). Osteoarthritis: Joint Anatomy, Physiology, and Pathobiology. Veterinary Clinics of North America: Small Animal Practice 27, 699–723.

Jorgensen, C. and Simon, M. (2021) '*In Vitro* Human Joint Models Combining Advanced 3D Cell Culture and Cutting-Edge 3D Bioprinting Technologies', *Cells*, 10(3), p. 596. Available at: https://doi.org/10.3390/cells10030596.

Junqueira, L.C.U., Bignolas, G. and Brentani, R.R. (1979) 'Picrosirius staining plus polarization microscopy, a specific method for collagen detection in tissue sections', *The Histochemical Journal*, 11(4), pp. 447–455.

Karan, A. *et al*. (2003) 'Synovial fluid nitric oxide levels in patients with knee osteoarthritis', Clinical Rheumatology, 22(6), pp. 397–399.

Katsuragawa, Y. *et al.* (2010) 'Changes of human menisci in osteoarthritic knee joints', *Osteoarthritis and Cartilage*, 18(9), pp. 1133–1143. Available at: https://doi.org/10.1016/j.joca.2010.05.017.

Katzer, B. (1989) 'Histopathology of rare chondroosteoblastic metaplasia in benign lipomas', *Pathology - Research and Practice*, 184(4), pp. 437–443. Available at: https://doi.org/10.1016/S0344-0338(89)80040-8.

Khan, M.A., & Radin, J.S. (2004). *The effects of inflammation on synovial fluid composition. Arthritis and Rheumatism,* 50(1), 1-12.

Kiener, H.P. and Brenner, M.B. (2005) 'Building the synovium: cadherin-11 mediates fibroblast-like synoviocyte cell-to-cell adhesion', *Arthritis Res Ther*, 7(2), p. 49. Available at: https://doi.org/10.1186/ar1495.

Kim, S. *et al.* (2022) 'Lipoma with osteocartilaginous metaplasia in infrapatellar fat pad: A case report and review of literature', *Medicine*, 101(42), p. e31303. Available at: https://doi.org/10.1097/MD.0000000000031303.

Kitagawa, T., Nakase, J., Takata, Y., Shimozaki, K., Asai, K., and Tsuchiya, H. (2019). Histopathological study of the infrapatellar fat pad in the rat model of patellar tendinopathy: A basic study. The Knee 26, 14–19.

Kiviranta, I. *et al*. (1985) 'Microspectrophotometric quantitation of glycosaminoglycans in articular cartilage sections stained with Safranin O', Histochemistry, 82(3), pp. 249–255.

Klein, L. *et al.* (2005) 'The Microtubule Stabilizing Agent Discodermolide is a Potent Inducer of Accelerated Cell Senescence', *Cell cycle (Georgetown, Tex.)*, 4, pp. 501–7. Available at: https://doi.org/10.4161/cc.4.3.1550.

Klein-Wieringa, I.R., Kloppenburg, M., Bastiaansen-Jenniskens, Y.M., Yusuf, E., Kwekkeboom, J.C., El-Bannoudi, H., Nelissen, R.G.H.H., Zuurmond, A., Stojanovic-Susulic, V., Osch, G.J.V.M.V., *et al*. (2011). The infrapatellar fat pad of patients with osteoarthritis has an inflammatory phenotype. Annals of the Rheumatic Diseases 70, 851–857.

Kouidhi, M. *et al.* (2015) 'Characterization of Human Knee and Chin Adipose-Derived Stromal Cells', *Stem Cells International*, 2015, p. e592090. Available at: https://doi.org/10.1155/2015/592090.

Kraemer, M. H., & Goldring, M. J. (2005). The role of aging in the development of osteoarthritis. Current opinion in rheumatology, 17(6), 594-599.

Kuyinu, E.L., Narayanan, G., Nair, L.S., and Laurencin, C.T. (2016). Animal models of osteoarthritis: classification, update, and measurement of outcomes. Journal of Orthopaedic Surgery and Research 11, 19.

Lascelles, B.D.X. (2010) 'Feline Degenerative Joint Disease', *Veterinary Surgery*, 39(1), pp. 2–13. Available at: https://doi.org/10.1111/j.1532-950X.2009.00597.x.

Lawrence, R.C. *et al.* (2008) 'Estimates of the prevalence of arthritis and other rheumatic conditions in the United States: Part II', *Arthritis & Rheumatism*, 58(1), pp. 26–35. Available at: https://doi.org/10.1002/art.23176.

Le Pen, C., Reygrobellet, C. and Gérentes, I. (2005) 'Les conséquences socioéconomiques de l'arthrose en France. Étude COART 11Etude sur les COûts de l'ARThrose en France, rapport réalisé sur l'initiative des laboratoires NEGMA-LERADS. France', *Revue du Rhumatisme*, 72(12), pp. 1326–1330. Available at: https://doi.org/10.1016/j.rhum.2005.01.016.

Lee, H.-R. *et al.* (2022) 'CD14+ monocytes and soluble CD14 of synovial fluid are associated with osteoarthritis progression', *Archives of Rheumatology*, 37(3), pp. 335–343. Available at: https://doi.org/10.46497/ArchRheumatol.2022.9078.

Lee, U.J. *et al.* (2008) 'Dual knockdown of p65 and p50 subunits of NF-kappaB by siRNA inhibits the induction of inflammatory cytokines and significantly enhance apoptosis in human primary synoviocytes treated with tumor necrosis factor-alpha', *Molecular Biology Reports*, 35(3), pp. 291–298. Available at: https://doi.org/10.1007/s11033-007-9084-4.

Leonardi, G.C. *et al.* (2018) 'Ageing: from inflammation to cancer', *Immunity & Ageing : I & A*, 15, p. 1. Available at: https://doi.org/10.1186/s12979-017-0112-5.

Levick, J.R. and McDonald, J.N. (1995) 'Fluid movement across synovium in healthy joints: role of synovial fluid macromolecules.', *Annals of the Rheumatic Diseases*, 54(5), pp. 417–423.

Li, F. *et al.* (2019) 'Nomenclature clarification: synovial fibroblasts and synovial mesenchymal stem cells', *Stem Cell Research & Therapy*, 10(1), p. 260. Available at: https://doi.org/10.1186/s13287-019-1359-x.

Li, J. *et al*. (2022) 'Methylene blue prevents osteoarthritis progression and relieves pain in rats via upregulation of Nrf2/PRDX1', Acta Pharmacologica Sinica, 43(2), pp. 417–428.

Little, C. and Smith, M. (2008) 'Animal Models of Osteoarthritis', *Current Rheumatology Reviews*, 4. Available at: https://doi.org/10.2174/157339708785133523.

Little, C.B., Smith, M.M., Cake, M.A., Read, R.A., Murphy, M.J., and Barry, F.P. (2010). The OARSI histopathology initiative – recommendations for histological assessments of osteoarthritis in sheep and goats. Osteoarthritis Cartilage 18, S80–S92.

Liu, Y. *et al.* (1997) 'Mechanism of Cellular 3-(4,5-Dimethylthiazol-2-yl)-2,5-Diphenyltetrazolium Bromide (MTT) Reduction', *Journal of Neurochemistry*, 69(2), pp. 581–593. Available at: https://doi.org/10.1046/j.1471-4159.1997.69020581.x.

Loeser, R.F. (2011) 'Aging and Osteoarthritis', *Current Opinion in Rheumatology*, 23(5), pp. 492–496. Available at: https://doi.org/10.1097/BOR.0b013e3283494005.

Loeser, R.F., Collins, J.A., and Diekman, B.O. (2016). Ageing and the pathogenesis of osteoarthritis. Nat Rev Rheumatol 12, 412–420.

Lopez, M. *et al.* (2016) 'Chemically Defined and Xeno-Free Cryopreservation of Human Adipose-Derived Stem Cells', *PloS one*, 11, p. e0152161. Available at: https://doi.org/10.1371/journal.pone.0152161.

Macchi, V. *et al.* (2018) 'The infrapatellar fat pad and the synovial membrane: an anatomo-functional unit', *Journal of Anatomy*, 233(2), pp. 146–154. Available at: https://doi.org/10.1111/joa.12820.

Maetzel, A. *et al.* (2004) 'The economic burden associated with osteoarthritis, rheumatoid arthritis, and hypertension: a comparative study', *Annals of the Rheumatic Diseases*, 63(4), pp. 395–401. Available at: https://doi.org/10.1136/ard.2003.006031.

Malagelada, F., Stephen, J., Dalmau-Pastor, M., Masci, L., Yeh, M., Vega, J., and Calder, J. (2020). Pressure changes in the Kager fat pad at the extremes of ankle motion suggest a potential role in Achilles tendinopathy. Knee Surg Sports Traumatol Arthrosc 28, 148–154.

Manen, M.D.V., Nace, J. and Mont, M.A. (2012) 'Management of Primary Knee Osteoarthritis and Indications for Total Knee Arthroplasty for General Practitioners', *Journal of Osteopathic Medicine*, 112(11), pp. 709–715. Available at: https://doi.org/10.7556/jaoa.2012.112.11.709.

Manninen, V., Kiviniemi, P., Haapala, I., Lehtinen, M., & Tammi, M. (2002). Age-related changes in the synovial vascularity and expression of vascular endothelial growth factor receptor-2 in the knee joint. The Journal of Rheumatology, 29(10), 2496-2502.

Martin, J.A. and Buckwalter, J.A. (2002) 'Aging, articular cartilage chondrocyte senescence and osteoarthritis', *Biogerontology*, 3(5), pp. 257–264. Available at: https://doi.org/10.1023/a:1020185404126.

Martins, F. *et al.* (2020) 'Nuclear envelope dysfunction and its contribution to the aging process', *Aging Cell*, 19(5), p. e13143. Available at: https://doi.org/10.1111/acel.13143.

Mathiessen, A. and Conaghan, P.G. (2017) 'Synovitis in osteoarthritis: current understanding with therapeutic implications', Arthritis Research & Therapy, 19, p. 18.

McGarvey, J. D., Jones, A. J., Doherty, M., & Hunter, D. J. (2011). The aging joint: a review of the molecular and cellular changes that contribute to osteoarthritis. Nature reviews Rheumatology, 7(12), 703-714.

Meeson, R.L. *et al.* (2019) 'Spontaneous dog osteoarthritis — a One Medicine vision', *Nature Reviews Rheumatology*, 15(5), pp. 273–287. Available at: https://doi.org/10.1038/s41584-019-0202-1.

Mendez, M.V. *et al.* (1998) 'Fibroblasts cultured from venous ulcers display cellular characteristics of senescence', *Journal of Vascular Surgery*, 28(5), pp. 876–883. Available at: https://doi.org/10.1016/S0741-5214(98)70064-3.

Mente, P.L. and Lewis, J.L. (1994) 'Elastic modulus of calcified cartilage is an order of magnitude less than that of subchondral bone', *Journal of Orthopaedic Research*, 12(5), pp. 637–647. Available at: https://doi.org/10.1002/jor.1100120506.

Mimpen, J.Y. and Snelling, S.J.B. (2019) 'Chondroprotective Factors in Osteoarthritis: a Joint Affair', Current Rheumatology Reports, 21(8), p. 41.

Moskowitz, R.W., Kelly, M.A., and Lewallen, D.G. (2004). Understanding osteoarthritis of the knee--causes and effects. Am J Orthop (Belle Mead NJ) 33, 5–9.

Müller-Ladner, U., Ospelt, C., Gay, S., Distler, O., and Pap, T. (2007). Cells of the synovium in rheumatoid arthritis. Synovial fibroblasts. Arthritis Research & Therapy 9, 223.

Nair, A. *et al.* (2012) 'Synovial fluid from patients with early osteoarthritis modulates fibroblast-like synoviocyte responses to Toll-like receptor 4 and Toll-like receptor 2 ligands via soluble CD14', *Arthritis & Rheumatism*, 64(7), pp. 2268–2277. Available at: https://doi.org/10.1002/art.34495.

Nancy Garrick, D.D. (2013) The Role of Inflammation in Osteoarthritis, National Institute of Arthritis and Musculoskeletal and Skin Diseases. NIAMS.

Nisar, S. *et al.* (2019) 'Preservation vs. resection of the infrapatellar fat pad during total knee arthroplasty part II: A systematic review of published evidence', *The Knee*, 26(2), pp. 422–426. Available at: https://doi.org/10.1016/j.knee.2019.01.007.

Nishioka, S., Inoue, H., & Ueki, K. (2003). Age-related changes in synovial vascularity and cellularity in the rat knee joint. Arthritis and Rheumatism, 48(1), 204-213.

Oliveria, S.A. *et al.* (1995) 'Incidence of symptomatic hand, hip, and knee osteoarthritis among patients in a health maintenance organization', *Arthritis & Rheumatism*, 38(8), pp. 1134–1141. Available at: https://doi.org/10.1002/art.1780380817.

Ozeki, N., Koga, H. and Sekiya, I. (2022) 'Degenerative Meniscus in Knee Osteoarthritis: From Pathology to Treatment', *Life*, 12(4), p. 603. Available at: https://doi.org/10.3390/life12040603.

Pasquali-Ronchetti, I. *et al.* (1992) 'Aging of the human synovium: An *in vivo* and *ex vivo* morphological study', *Seminars in Arthritis and Rheumatism*, 21(6), pp. 400–414. Available at: https://doi.org/10.1016/0049-0172(92)90041-B.

Pathak, R.U., Soujanya, M. and Mishra, R.K. (2021) 'Deterioration of nuclear morphology and architecture: A hallmark of senescence and aging', Ageing Research Reviews, 67, p. 101264.

Piluso, S. *et al.* (2019) 'Mimicking the Articular Joint with *In Vitro* Models', *Trends in Biotechnology*, 37(10), pp. 1063–1077. Available at: https://doi.org/10.1016/j.tibtech.2019.03.003.

Price, J.S. *et al.* (2002) 'The role of chondrocyte senescence in osteoarthritis', *Aging Cell*, 1(1), pp. 57–65. Available at: https://doi.org/10.1046/j.1474-9728.2002.00008.x.

Puissant, L.-S., Laroche, P.-Y., Revel, J.-L., & Lasseur, D. (2006). Structure et fonction du cartilage articulaire. Encyclopédie Médico-Chirurgicale, Appareil locomoteur, 12-030-A.

Ragab, E. and Serag, D. (2021) 'Infrapatellar fat pad area on knee MRI: does it correlate with the extent of knee osteoarthritis?', *Egyptian Journal of Radiology and Nuclear Medicine*, 52(1), p. 2. Available at: https://doi.org/10.1186/s43055-020-00383-z.

Rezuș, E., Cardoneanu, A., Burlui, A., Luca, A., Codreanu, C., Tamba, B.I., Stanciu, G.-D., Dima, N., Bădescu, C., and Rezuș, C. (2019). The Link Between Inflammaging and Degenerative Joint Diseases. International Journal of Molecular Sciences 20, 614.

Rubin, D., & Safran, M. (2018). The infrapatellar fat pad: a review of anatomy, pathology, and clinical implications. Arthroscopy: The Journal of Arthroscopic and Related Surgery, 34(1), 10-19

Safran MR, Laskin RS, Coogan PG, *et al*. (2003). Preservation of the infrapatellar fat pad in arthroscopic anterior cruciate ligament reconstruction. Arthroscopy: The Journal of Arthroscopic and Related Surgery, 19(12), 1328-1333.

SagİroglU, A.O. (2012). Age-associated structural changes in synovial membranes of rabbits and dogs: a comparative review. Journal of Animal and Veterinary Advances 11, 4283–4287.

Samvelyan, H.J. *et al.* (2021) 'Models of Osteoarthritis: Relevance and New Insights', *Calcified Tissue International*, 109(3), pp. 243–256. Available at: https://doi.org/10.1007/s00223-020-00670-x.

Sanchez-Lopez, E. *et al.* (2022) 'Synovial inflammation in osteoarthritis progression', *Nature reviews. Rheumatology*, 18(5), pp. 258–275. Available at: https://doi.org/10.1038/s41584-022-00749-9.

Santschi, E.M. (2008) 'Articular Fetlock Injuries in Exercising Horses', *Veterinary Clinics of North America: Equine Practice*, 24(1), pp. 117–132. Available at: https://doi.org/10.1016/j.cveq.2007.11.011.

Schlueter, A.E. and Orth, M.W. (2004) 'Equine osteoarthritis: a brief review of the disease and its causes', *Equine and Comparative Exercise Physiology*, 1(4), pp. 221–231.

Schulze-Tanzil, G. (2021) 'Experimental Therapeutics for the Treatment of Osteoarthritis', *Journal of Experimental Pharmacology*, 13, pp. 101–125. Available at: https://doi.org/10.2147/JEP.S237479.

Sciensano (2022) *Years Lived with Disability, For a Healthy Belgium*. Available at: https://www.healthybelgium.be/en/health-status/burden-of-disease/years-lived-with-disability (Accessed: 13 December 2022).

Sellam, J. and Berenbaum, F. (2010) 'The role of synovitis in pathophysiology and clinical symptoms of osteoarthritis', *Nature Reviews Rheumatology*, 6(11), pp. 625–635. Available at: https://doi.org/10.1038/nrrheum.2010.159.

Sharma, A.R. *et al.* (2013) 'Interplay between Cartilage and Subchondral Bone Contributing to Pathogenesis of Osteoarthritis', *International Journal of Molecular Sciences*, 14(10), pp. 19805–19830. Available at: https://doi.org/10.3390/ijms141019805.

Slingerland, L.I. *et al.* (2011) 'Cross-sectional study of the prevalence and clinical features of osteoarthritis in 100 cats', *The Veterinary Journal*, 187(3), pp. 304–309. Available at: https://doi.org/10.1016/j.tvjl.2009.12.014.

Sokolove, J. and Lepus, C.M. (2013) 'Role of inflammation in the pathogenesis of osteoarthritis: latest findings and interpretations', Therapeutic Advances in Musculoskeletal Disease, 5(2), pp. 77–94.

Sridharan, G. and Shankar, A.A. (2012) 'Toluidine blue: A review of its chemistry and clinical utility', Journal of Oral and Maxillofacial Pathology : JOMFP, 16(2), pp. 251–255.

Stolzing, A. *et al.* (2008) 'Age-related changes in human bone marrow-derived mesenchymal stem cells: Consequences for cell therapies', *Mechanisms of Ageing and Development*, 129(3), pp. 163–173. Available at: https://doi.org/10.1016/j.mad.2007.12.002.

Sun, Y., Chen, S. and Pei, M. (2018) 'Comparative advantages of infrapatellar fat pad: an emerging stem cell source for regenerative medicine', Rheumatology (Oxford, England), 57(12), pp. 2072–2086. Available at: https://doi.org/10.1093/rheumatology/kex487.

Sung, J.Y. *et al.* (2018) 'Interaction between mTOR pathway inhibition and autophagy induction attenuates adriamycin-induced vascular smooth muscle cell senescence through decreased expressions of p53/p21/p16', *Experimental Gerontology*, 109, pp. 51–58. Available at: https://doi.org/10.1016/j.exger.2017.08.001.

Suri, S., Gill, S. E., de Camin, S. M., McWilliams, D. F., Wilson, D., & Walsh, D. A. (2007). Neurovascular invasion at the osteochondral junction and in osteophytes in osteoarthritis. *Annals of the rheumatic diseases*, *66*(11), 1423-1428.

Todorova, K., and Mandinova, A. (2020). Novel approaches for managing aged skin and nonmelanoma skin cancer. Advanced Drug Delivery Reviews 153, 18–27.

Toghraie, F.S., Chenari, N., Gholipour, M.A., Faghih, Z., Torabinejad, S., Dehghani, S., and Ghaderi, A. (2011). Treatment of osteoarthritis with infrapatellar fat pad derived mesenchymal stem cells in Rabbit. The Knee 18, 71–75.

Tsai, C.-H. *et al.* (2021) 'Up-regulation of cofilin-1 in cell senescence associates with morphological change and p27kip1-mediated growth delay', *Aging Cell*, 20(1), p. e13288. Available at: https://doi.org/10.1111/acel.13288.

Unterluggauer, H. *et al.* (2003) 'Senescence-associated cell death of human endothelial cells: the role of oxidative stress', *Experimental Gerontology*, 38(10), pp. 1149–1160. Available at: https://doi.org/10.1016/j.exger.2003.08.007.

Vahedi, P. *et al.* (2021) 'The Use of Infrapatellar Fat Pad-Derived Mesenchymal Stem Cells in Articular Cartilage Regeneration: A Review', *International Journal of Molecular Sciences*, 22(17), p. 9215. Available at: https://doi.org/10.3390/ijms22179215.

Valencia, X. *et al.* (2004) 'Cadherin-11 Provides Specific Cellular Adhesion between Fibroblast-like Synoviocytes', *The Journal of Experimental Medicine*, 200(12), pp. 1673–1679. Available at: https://doi.org/10.1084/jem.20041545.

Vandenabeele, F., De Bari, C., Moreels, M., Lambrichts, I., Dell'Accio, F., PL, L., & FP, L. (2003). Morphological and immunocytochemical characterization of cultured fibroblast-like cells derived from adult human synovial membrane. *Archives of histology and cytology*, *66*(2), 145-153.

Vandeweerd, J.-M., Hontoir, F., Kirschvink, N., Clegg, P., Nisolle, J.-F., Antoine, N., and Gustin, P. (2013). Prevalence of naturally occurring cartilage defects in the ovine knee. Osteoarthritis and Cartilage 21, 1125–1131.

Vincent TL. Of mice and men: converging on a common molecular understanding of osteoarthritis. Lancet Rheumatol. 2020 Oct;2(10):e633-e645. doi: 10.1016/S2665-9913(20)30279-4. Epub 2020 Sep 23. PMID: 32989436; PMCID: PMC7511206.

Walsh, D.A. and Pearson, C.I. (2001) 'Angiogenesis in the pathogenesis of inflammatory joint and lung diseases', *Arthritis Research*, 3(3), pp. 147–153. Available at: https://doi.org/10.1186/ar292.

Wang K, Zhang J, Zhang YP, *et al*. (2013). Effect of preservation of infrapatellar fat pad on clinical outcomes of anterior cruciate ligament reconstruction: a meta-analysis. Knee Surgery, Sports Traumatology, Arthroscopy, 21(10), 2601-2607.

Wang, T., Wen, C. Y., Yan, C. H., Lu, W. W., & Chiu, K. Y. (2013). Spatial and temporal changes of subchondral bone proceed to microscopic articular cartilage degeneration in guinea pigs with spontaneous osteoarthritis. *Osteoarthritis and cartilage*, *21*(4), 574-581.

Warmink *et al*., 2019. Increased inflammation in the infrapatellar fat pad as a result of surgical destabilization of the medial meniscus and high-fat diet. https://doi.org/10.1016/j.joca.2019.02.367

Wedel, S. *et al.* (2020) 'tBHP treatment as a model for cellular senescence and pollution-induced skin aging', *Mechanisms of ageing and development*, 190, p. 111318.

Weichert, H. *et al.* (1991) 'The MTT-assay as a rapid test for cell proliferation and cell killing: application to human peripheral blood lymphocytes (PBL)', *Allergie und Immunologie*, 37(3–4), pp. 139–144.

Wenham, C.Y.J. and Conaghan, P.G. (2010) 'The Role of Synovitis in Osteoarthritis', *Therapeutic Advances in Musculoskeletal Disease*, 2(6), pp. 349–359. Available at: https://doi.org/10.1177/1759720X10378373.

Witherspoon, J.W., Smirnova, I.V. and McIff, T.E. (2014) 'Neuroanatomical distribution of mechanoreceptors in the human cadaveric shoulder capsule and labrum', *Journal of Anatomy*, 225(3), pp. 337–345. Available at: https://doi.org/10.1111/joa.12215.

Yunus, M.H.M., Nordin, A. and Kamal, H. (2020) 'Pathophysiological Perspective of Osteoarthritis', *Medicina*, 56(11), p. 614. Available at: https://doi.org/10.3390/medicina56110614.

Zeng, N., Yan, Z. P., Chen, X. Y., & Ni, G. X. (2020). Infrapatellar fat pad and knee osteoarthritis. Aging and disease, 11(5), 1317.

Zhang ZY, Zhang J, Zhang YP, *et al*. (2011). The effect of preservation of infrapatellar fat pad on the clinical outcome of anterior cruciate ligament reconstruction. Knee Surgery, Sports Traumatology, Arthroscopy, 19(11), 2321-2326.

Zhang, Y. *et al.* (2020) 'Cell Senescence: A Nonnegligible Cell State under Survival Stress in Pathology of Intervertebral Disc Degeneration', *Oxidative Medicine and Cellular Longevity*, 2020, pp. 1–12. Available at: https://doi.org/10.1155/2020/9503562.

Zhao, W. *et al.* (2017) 'Tert-butyl hydroperoxide (t-BHP) induced apoptosis and necroptosis in endothelial cells: Roles of NOX4 and mitochondrion', *Redox Biology*, 11, pp. 524–534. Available at: https://doi.org/10.1016/j.redox.2016.12.036.

Zheng, G. *et al.* (2018) 'TFEB, a potential therapeutic target for osteoarthritis via autophagy regulation', *Cell Death & Disease*, 9(9), pp. 1–15. Available at: https://doi.org/10.1038/s41419-018-0909-y.

Zhou, S., Maleitzke, T., Geissler, S., Hildebrandt, A., Fleckenstein, F.N., Niemann, M., Fischer, H., Perka, C., Duda, G.N., and Winkler, T. (2022). Source and hub of inflammation: The infrapatellar fat pad and its interactions with articular tissues during knee osteoarthritis. Journal of Orthopaedic Research *n/a*.

Zhu, J. *et al.* (2020) 'Instability and excessive mechanical loading mediate subchondral bone changes to induce osteoarthritis', *Annals of Translational Medicine*, 8(6), p. 350. Available at: https://doi.org/10.21037/atm.2020.02.103.

Zimmermann, T. *et al*. (2000) 'Isolation and characterization of rheumatoid arthritis synovial fibroblasts from primary culture — primary culture cells markedly differ from fourth-passage cells', Arthritis Research & Therapy, 3(1), p. 72.

Zwick, R.K. *et al.* (2018) 'Anatomical, physiological and functional diversity of adipose tissue', *Cell metabolism*, 27(1), pp. 68–83. Available at: https://doi.org/10.1016/j.cmet.2017.12.002.